CODIGEM

CORPORACIÓN DE DESARROLLO E INVESTIGACIÓN GEOLÓGICO-MINERO-METALÚRGICA

MINISTERIO DE ENERGÍA Y MINAS

DFID

DEPARTMENT FOR INTERNATIONAL DEVELOPMENT

BGS 1835

BRITISH GEOLOGICAL SURVEY

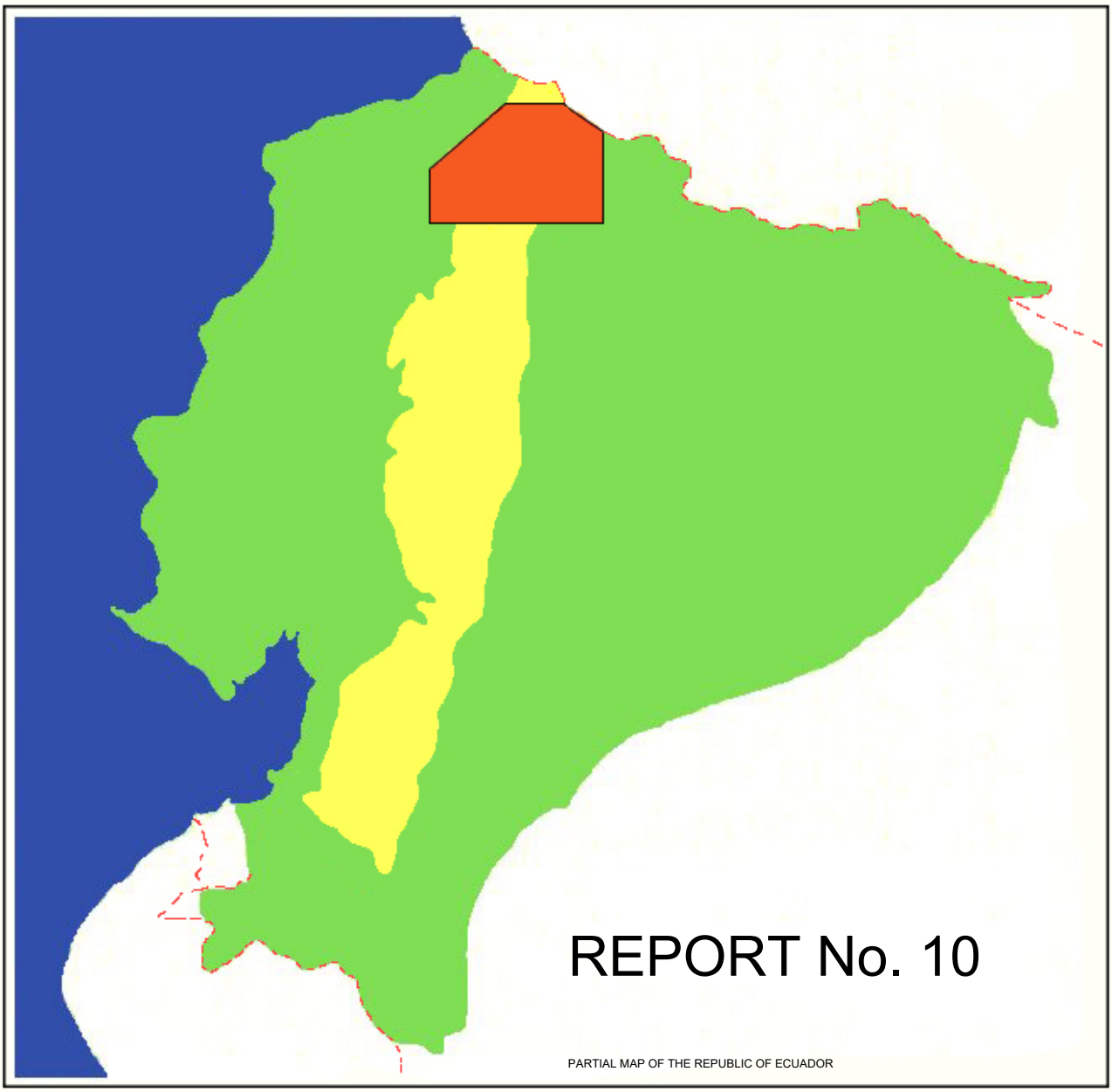

REPORT No. 10

PARTIAL MAP OF THE REPUBLIC OF ECUADOR

WORLD BANK MINING DEVELOPMENT AND ENVIRONMENTAL CONTROL PROJECT

GEOLOGICAL INFORMATION MAPPING PROGRAMME (WESTERN CORDILLERA)

PATRI MATRIQUE

MINING DEVELOPMENT AND ENVIRONMENTAL CONTROL PROJECT

GEOLOGICAL INFORMATION MAPPING PROGRAMME

Report Number 10

GEOLOGY OF THE WESTERN CORDILLERA OF ECUADOR BETWEEN 0°00' AND 1°00'N

Martin Boland

Luis Pilatasig

Elías Ibadango

William McCourt

John Aspden

Richard Hughes

Bernardo Beate

CODIGEM-BRITISH GEOLOGICAL SURVEY

Quito-Ecuador

2000

Stalyn Paucar

2024 edition

Reference

Boland, M., Pilatasig, L., Ibadango, E., McCourt, W., Aspden, J., Hughes, R., & Beate, B. (2000). *Geology of the Western Cordillera of Ecuador between 0°00' and 1°00'N* (Stalyn Paucar, Ed., 2024). Report Number 10. Geological Information Mapping Programme. BGS-CODIGEM/MEM.

CONTENTS

FIGURES

PLATES

APPENDICES

1. INTRODUCTION

1.1 Background

This report describes the findings of the geological reconnaissance mapping project carried out between 0° and 1°N as part of the Geological Information Mapping Programme (GIMP) Western Cordillera of Ecuador (Figure 1), subcomponent 3.3 of the Mining Development and Environmental Control Technical Assistance Project (PRODEMINCA). This multi-national project, co-funded by the World Bank, the Governments of Ecuador, Sweden and the United Kingdom (Department for International Development), has as one of its primary aims the production of an accurate and internally consistent geological database for the Western Cordillera. Geological investigations were undertaken jointly by geologists of the British Geological Survey (BGS), the Corporación de Desarrollo e Investigación Geológico-Minero-Metalúrgica (CODIGEM) and national consultants of PRODEMINCA.

Fieldwork was undertaken between September 1995 and December 1999 over an area of approximately 12000 km^2, with altitudes ranging from less than 200 m to over 5200 m ASL. Mapping was carried out by seven geologists: Drs. M. P. Boland, W. J. McCourt, J. A. Aspden and R. A. Hughes of the British Geological Survey; Ing. L. F. Pilatasig of CODIGEM; and Ings. C. E. Ibadango and B. Beate of PRODEMINCA. Ing. B. Beate's work focused mainly on the Quaternary volcanics which outcrop in the eastern part of the map area, and this work is described separately in Appendix 1.

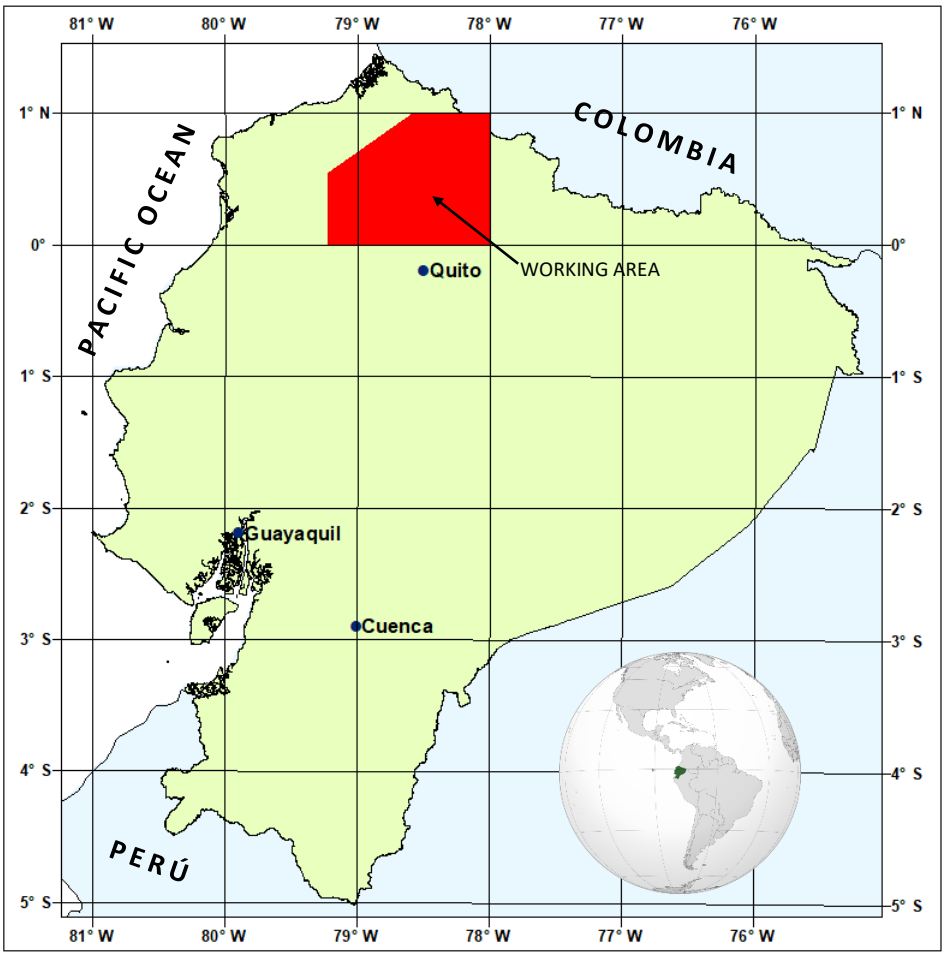

Figure 1. Location of study area

1.2 Geological framework of Ecuador

Geographically and geomorphologically, Ecuador is divided into three main units: a central Andean region, the "Sierra", separating the Amazon Basin or "Oriente" in the east, from the Coastal Plain or "Costa" in the west. The Oriente is an extensive sedimentary basin, including a platform carbonate sequence, overlying an older cratonic basement which together have been intruded by large granitoid batholiths mainly along the structurally complex sub-Andean zone of folding and thrusting that separates the Oriente from the Sierra. The Andean Sierra comprises two mountain chains separated by a central graben. The Cordillera Real to the east is dominated by linear belts of metamorphic rocks, intruded by Early Mesozoic granitoids of both S- and I-type, capped along much of its length by Cenozoic volcanics. The Cordillera Occidental to the west of the graben is dominated by Late Mesozoic to Early Cenozoic basaltic volcanic and volcaniclastic rocks, representing at least in part accreted oceanic terranes, and clastic turbidites. These sequences are intruded by Mid-Late Tertiary granitoids and overlain by post-Eocene, continental margin, mainly acid to intermediate, calc-alkaline volcanics. The Interandean Depression or central intermontane graben is an important extensional structure bounded for much of its length by active faults and comprises extensive Tertiary to Recent sedimentary and volcanic sequences. The Costa comprises the whole region west of the Andes and represents a Late Cretaceous to Cenozoic fore-arc basin, or series of basins, underlain by basic oceanic crust locally exposed in the hills of the Coastal Range.

1.3 Previous geological studies

Wolf (1892) produced the first map and comprehensive geological/geographical synthesis of Ecuador which remained the standard reference work until those of Sauer (1957, 1965), which included and complemented the earlier work by Tschopp (1948, 1953) based mainly on confidential studies of the sedimentary basins of Ecuador for the oil industry. Further systematic studies of the sedimentary basins were carried out by the French Petroleum Institute (IFP, e.g. Faucher et al., 1968) that led to the publication of a 1:1000000 scale national geological map in 1969 (Servicio Nacional de Geología y Minas) and the first geodynamic synthesis by Faucher and Savoyat (1973). During the period 1968-1980, systematic mapping by geologists of the Dirección General de Geología y Minas (DGGM) and the Institute of Geological Sciences (IGS), now the British Geological Survey (BGS), under a bilateral Technical Cooperation Project between the Governments of Ecuador and the United Kingdom resulted in the publication of various 1:100000 regional geological maps and a new 1:1000000 national map and explanatory bulletin (Baldock and Longo, 1982; Baldock, 1982). Related publications on the geology and stratigraphy of Ecuador were those of Kennerley (1980), Bristow and Hoffstetter (1977), Bristow (1981) and Henderson (1977, 1979). Further albeit more specialised regional studies include among others, Sigal (1968), Goossens (1972), Goossens and Rose (1973), Feininger (1977, 1978) and DGGM (1980).

A second BGS-DGGM/INEMIN/CODIGEM technical cooperation project from 1986-1993 concentrated in the Cordillera Real produced detailed reports and maps on the geology and mineral potential of the metamorphic basement (Litherland et al., 1994; Aspden et al., 1995; BGS-CODIGEM, 1994a, b) in addition to a new 1:1000000 scale national geological map and accompanying tectono-metallogenic map at the same scale (Litherland et al., 1993a, b). The latter authors incorporated data from numerous sources in their National Geological Map of Ecuador, covering university theses, reports of international missions to Ecuador (Misión Belga, Misión Francesa, Misión Japonesa) and studies by governmental institutions such as INEMIN/CODIGEM and INECEL.

1.4 Access and climate

Access to the area is variable, with the density of roads generally decreasing towards the west. Two principal roads cross the Cordillera: the Calacalí-San Miguel de Los Bancos road in the south of the area and the Ibarra-San Lorenzo road in the north. Good sections are exposed on these roads as well as a number of others such as those between Otavalo-Selva Alegre, Tulcán-Maldonado and those around Pacto (Figure 2). In the extreme western parts of the map area the starting points for traverses were accessed by canoe along the Cayapas, Santiago and Canandé rivers, while access to the area to the west of the Cordillera Toisán, was by helicopter. Traverses of up to 25 days duration were undertaken by up to 3 geological field parties working independently to achieve maximum coverage.

Topographic base maps at 1:50000 are available for 50% of the area and of the 8 full or partial 1:100000 maps required only 3 published maps exist (Otavalo, Ibarra and Rosa Zarate). Those areas for which published topographic maps did not exist 1:50000 scale base maps, showing the principal rivers, were produced by the project from aerial photographs and satellite imagery (Figure 3).

The climate is highly variable over the area, but generally it is only possible to work in the summer months from (late) May to December, particularly in the high páramo and to the west of the Cordillera Toisán.

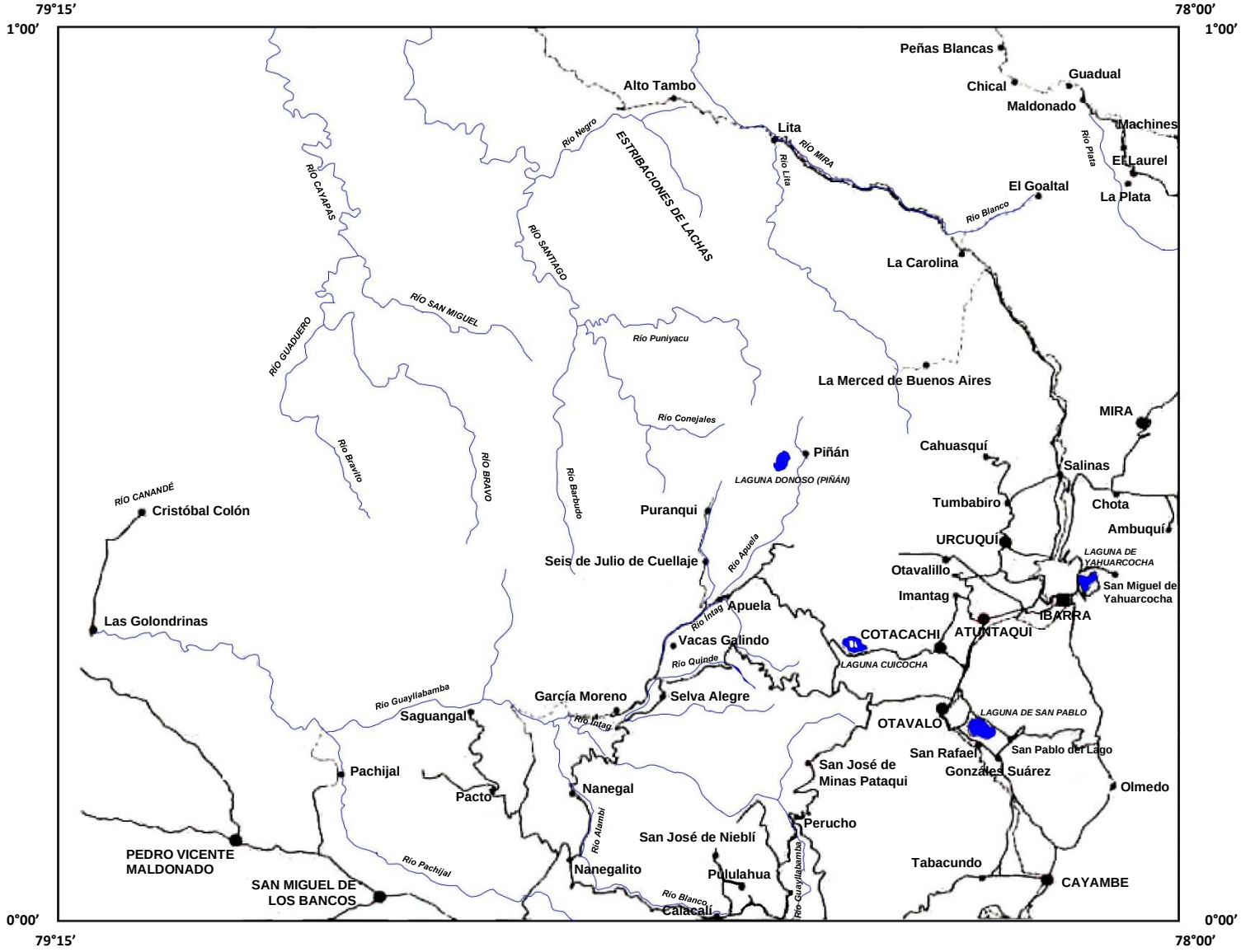

Figure 2. Map showing the principal towns, roads and rivers in the area mapped between 0°-1°N

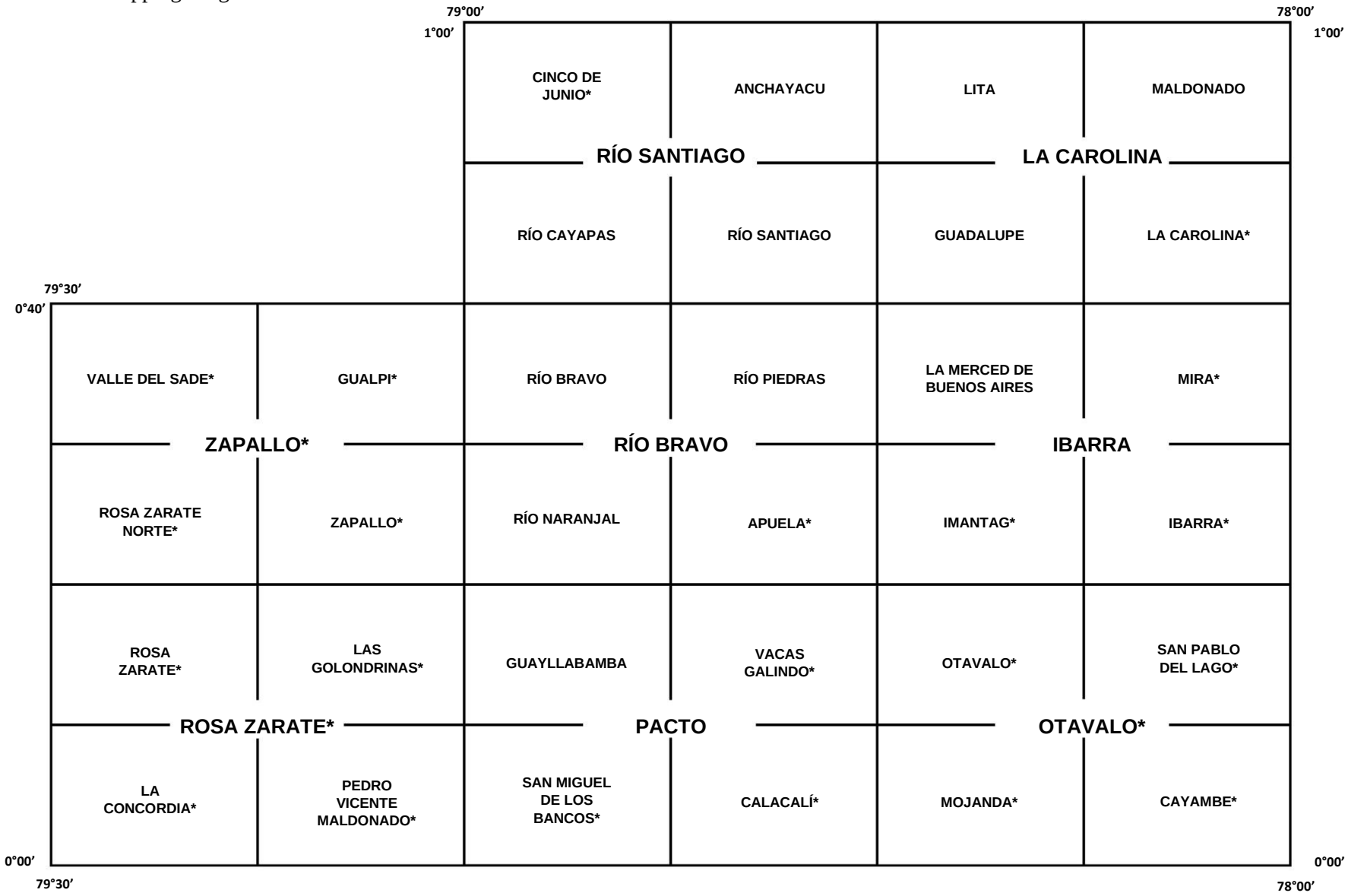

Figure 3. Topographic maps at 1:50000 and 1:100000 scale used in present study. Maps starred with an asterix are published by IGM, while those without were produced by the Misión Británica from Landsat Images and aerial photographs

2. GEOLOGY OF THE WESTERN CORDILLERA OF ECUADOR

2.1 Tectonic setting

The Andes form a morphologically continuous mountain range more than 7000 km long located along the active Pacific margin of South America and bounded to the west by a deep oceanic trench that extends uninterrupted from Patagonia to Colombia. The Ecuadorian part of this margin is today characterised by the essentially orthogonal subduction of the Nazca Plate beneath continental South America. In detail, young oceanic crust (<20 Ma) produced by the Nazca-Cocos spreading centre at the Galápagos Rift Zone is being subducted in the Ecuadorian trench at an angle of 25°-35° (Rea and Malfait, 1974; Lonsdale, 1978). The Andean Range can be conveniently divided into three segments: the Southern, Central and Northern Andes (Gansser, 1973; Sillitoe, 1974). The Western Cordillera of Ecuador forms part of the Northern Andes segment, that is characterised by the presence of allochthonous terranes, including ophiolitic/oceanic fragments (Feininger and Bristow, 1980; McCourt et al., 1984; Megard and Lebrat, 1987) that have been accreted to the margin of South America since the Middle Cretaceous (Egüez, 1986; Van Thournout, 1991).

2.2 Stratigraphic summary

Since the earliest studies of Wolf (1892) it has been recognised that the geology of the Western Cordillera and the more westerly Coastal Range is characterised by “rocas porfídicas y rocas verdes”. Tschopp (1948) was the first to introduce formal stratigraphic names to these sequences with the introduction of the term “Piñón Formation” for the basic volcanic sequences of the Costa, while retaining Wolf’s descriptive term for the basic volcanics of the Sierra. Sauer (1965) followed Tschopp in using the name Piñón Formation for the basic rocks of the Costa, and resurrected the term Cayo Formation (cf. Olsson, 1942), for the overlying Late Cretaceous marine, volcano-sedimentary sequence, while for the basic rocks of the Cordillera he used the term “Formación Diabásica-Porfirítica”. Sauer also re-introduced the term Yunguilla Formation, originally used by Thalmann (1946), for a sequence of marine sediments of mainly Maastrichtian age from the Quito-Nono-Nanegal area of the western Cordillera. Systematic mapping by geologists of the IFP (Institut Français du Pétrole) in the mid-sixties resulted in the first attempts at correlating the stratigraphy of the Costa and the Western Cordillera and the name Piñón Formation was used in both areas for the Cretaceous “oceanic” basement comprising diabase and rocas verdes. The name Cayo Formation was retained for the overlying volcano-sedimentary sequence on the coast and the term “Cayo de la Sierra” was introduced for its supposed age equivalent in the Western Cordillera. In addition, two more formations were described, the previously mentioned Yunguilla Formation of Maastrichtian to Paleocene age, confirmed by micropalaeontological studies in the Nono area northwest of Quito (Sigal, 1968) and a conformably overlying sequence of volcanic conglomerates, sandstones, greywackes and green-purple shales, the “Cayo Rumi Formation” of assigned Paleocene age. Goossens and Rose (1973) meanwhile proposed that both the Piñón and Diabásica-Porfirítica Formations be renamed the Basic Igneous Complex and suggested a correlation with similar rocks from Costa Rica, Panamá and Western Colombia on petrographic grounds.

Subsequent stratigraphic nomenclature in the Western Cordillera was influenced by the mapping of the IGS/DGGM geologists and in particular the tectono-stratigraphic interpretation of Henderson (1979) who proposed that the basic volcanics of the Cordillera and the Costa were different both in age and origin. In the early maps both Formación Piñón and/or Complejo Ígneo-Básico were used for the Costa rocks and Formación Piñón in the Sierra. From 1976 onwards, however, new names were introduced following an interpretation of the oceanic volcanics of the Western Cordillera as an island arc based on a combination of lithological and geochemical evidence. The name Piñón was retained but restricted to the basaltic ocean floor volcanics of the Costa, while the name Macuchi Formation was created for the rocas verdes of the Western Cordillera, consisting mainly of basaltic to andesitic rocks, a high percentage of which had been reworked. Thus, the Macuchi as defined by Henderson was predominantly sedimentary in origin comprising turbiditic volcanic sandstones and siltstones, with lesser amounts of breccia, tuff and lava and essentially included all of the volcanic and volcanoclastic "rocas verdes" of the Western Cordillera. The (?)overlying Late Cretaceous sediments, the formerly named "Cayo de la Sierra", were also considered to be part of the Macuchi Formation and renamed the "Chontal Member". In addition, the conglomeratic Cayo Rumi Formation on the Alóag-Santo Domingo road, was renamed the Silante Formation and reinterpreted to directly overlie the Macuchi volcanoclastics, yet was itself considered to be overlain by the Yunguilla "flysch" Formation of assigned Maastrichtian to Paleocene age. On this evidence therefore the Macuchi Formation is Late Cretaceous or older. Further south however, to the east of Quevedo-La Maná. Early Eocene fossils were reported from the Macuchi Formation and andesitic sills within the sequence yielded Middle Eocene K-Ar ages. In addition, Eocene fossils were recorded from the overlying "Yunguilla-type" flysch sequence. Thus (the top of) the Macuchi Formation and by inference the overlying flysch unit were interpreted to be strongly diachronous and attributed a (Late) Cretaceous to Eocene age along the length of the Cordillera. Almost simultaneously with Henderson's re-interpretation of the Western Cordillera geology, Kehrer and Van der Kaaden (1979) subdivided the "Piñón de la Sierra" (or Macuchi) rocks of the Alóag-Santo Domingo road section into three units. The Toachi Unit, considered equivalent to the coastal Piñón Formation; the Pilatón Unit, equated with the "Formación Cayo de la Sierra" (the Chontal Member of Henderson) and the distinctive probably younger, Tandapi Beds.

This nomenclature was resurrected by Egüez (1986) whose work in the central part of the Western Cordillera was fundamental to understanding and partly resolving the Macuchi-Yunguilla dilemma introduced by Henderson (1979, 1981). Egüez (1986) demonstrated the presence of two lithologically similar, but different age, flysch sequences that had previously been mapped as a single unit, namely the Yunguilla Formation. To the east of Quevedo the Macuchi volcanics are regionally overlain by the Unacota Limestone of early Middle Eocene age, which itself passes upwards into a sandy quartzose turbiditic sedimentary sequence of Middle to Late Eocene age that Egüez named the Apagua Formation. The flysch sequence of the Quito-Nono area however is different comprising a muddy turbiditic sequence with intercalated limestones of Late Cretaceous to possibly Early Paleocene age, the Yunguilla Formation. The recognition of a younger flysch sequence resolves much of the earlier confusion and makes the introduction of diachronous formations unnecessary. In addition, the Silante-Yunguilla contact was re-interpreted by Egüez, and the relative age relations reversed, that is, the Silante overlies, in apparent conformable contact, the Yunguilla Formation. However, the age of the Silante is poorly understood and remains problematic. It is clearly post-Maastrichtian in age in that it overlies and contains reworked fossils from the Yunguilla Formation (Savoyat et al., 1970) and following Egüez (1986) the Silante overlies the Macuchi, suggesting an Eocene or younger age. Van Thournout (1991) however preferred a Paleocene age for the Silante due to its position "on top" of the Yunguilla and its unproven contact relationships with the Macuchi Formation.

Egüez restricts the term Macuchi (s.s.) to a volcanic-volcanosedimentary unit of Early to Middle Eocene age, with Kuroko style massive sulphide mineralisation at the type locality of the Macuchi mine east of La Maná, and also recognises the presence of oceanic floor basalts in the Western Cordillera. He suggests the name Toachi Unit for these and equates them with the Piñón Formation of the Costa and for the associated siliceous sediments, the former Cayo de la Sierra, he proposes the name Pilatón Unit. In contrast Santos and Ramírez (1986), although reaching similar conclusions concerning the stratigraphy, particularly the presence of an Eocene flysch unit which they named the Apagua Formation, and underlining the complexities and inadequacies of Henderson’s interpretation, proposed to reintroduce the old stratigraphic nomenclature “Piñón de la Sierra” and “Cayo de la Sierra” for the older sequences. About the same time Lebrat (1985) on purely geochemical grounds showed that the Macuchi Formation of Henderson was made up of three distinct types of “basalts”: tholeiitic island-arc basalts, oceanic MORB and calc-alkaline arc basalts. The MORB material was correlated with the coastal Piñón Formation and the calc-alkaline volcanics were mistakenly correlated with the Cretaceous Celica Formation of southern Ecuador, when in fact they are part of the Oligocene Saraguro volcanics. The island-arc volcanics define the type Macuchi of the Western Cordillera. Similarly, Van Thournout et al. (1992) recognised the presence of three major volcanic sequences in the (North) Western Cordillera, an Early Cretaceous sequence of MORB basalts and overlying arc tholeiites, a mainly Eocene sequence of island-arc, tholeiitic to calc-alkaline, basalts and a (Mid-to) Late Oligocene sequence of calc-alkaline volcanics of predominantly andesitic-dacitic composition. The first and second sequences correlating with the “Piñón/Toachi” and Macuchi Formations respectively of Egüez (1986) and Lebrat (1985), while the third he termed the San Juan de Lachas unit. Finally, Litherland et al. (1993a) on the 1:1000000 National Map of Ecuador, divided the pre-Oligocene volcanics of the Western Cordillera into a Paleo-Eocene island-arc sequence, the Macuchi Unit and a pre-Senonian ophiolitic (MORB) sequence, for which they re-introduced the name “Piñón de la Sierra”.

In addition to the ensimatic volcanics of the Piñón and Macuchi Formations there are at least five calc-alkaline, continental-margin volcanic arc sequences present in the Western Cordillera: the Late Cretaceous Celica Formation of Southern Ecuador; a latest Cretaceous to Early Tertiary composite arc, the Sacapalca Group; an Oligocene to earliest Miocene arc typified by the Saraguro Group andesitic to rhyolitic pyroclastic deposits; the Miocene volcanics and volcanoclastics of the Pisayambo Volcanics and the Plio-Pleistocene to Recent sequences that locally extend into the intermontane graben, for example the Turi and Sicalpa Formations (Baldock, 1982; Litherland et al., 1993a). All of these volcanic sequences are in general poorly defined and dated, and accordingly may contain the volcanic products of more than one phase of activity as presently mapped.

3. LITHOSTRATIGRAPHY

3.1 Introduction

The following sections describe the main lithostratigraphical units mapped in the present study area (Figure 4). Where appropriate the stratigraphical nomenclature established by previous workers e.g. Egüez (1986), Van Thournout (1991), Litherland et al. (1993a). Hughes and Bermúdez (1997) and McCourt et al. (1997) have been followed. Details of the metamorphic rocks exposed in the east, in the Chota valley, are given in Appendix 1.

3.2 Pallatanga Unit (K_{Pa})

3.2.1 Distribution

The Pallatanga Unit, which was defined by McCourt et al. (1997), occurs along the eastern margin of the cordillera in a number of fault bounded lenses, the best exposures of which are seen along the Salinas-San Lorenzo road [8197-00616, 8147-00738], the Otavalo-Selva Alegre road to the west of Quebrada La Portada [7845-00287], and at Isopamba [7719-00038] to the west of Calacalí.

3.2.2 Age

The age of the Pallatanga Unit is not well established; however, Reynaud et al. (1999) reference a Sm/Nd internal isochron age of 123 ± 13 Ma from an amphibole-bearing gabbro of the San Juan peridotites, located to the west of Quito. Lebrat et al. (1987) have interpreted these peridotites and the Pallatanga Unit as each representing different fragments of a dismembered ophiolite, while Cosma et al. (1998) interpret both units to represent fragments of an ocean plateau. These authors also correlate the Pallatanga Unit with the Piñón Formation of the Guayaquil area which is overlain by the Cenomanian-Turonian age Calentura Formation.

In this study, a sequence of red mudstones intercalated with pillow basalts on the Otavalo-Selva Alegre road [7845-00287] yielded a Santonian-early Campanian age (ca. 86-75 Ma) (Wilkinson, 1998b, Appendix 2). However, the tectonised nature of the contacts make it unclear as to whether the mudstones represent original interbeds or a tectonically interleaved overlying sequence.

3.2.3 Facies

The Pallatanga Unit consists of a sequence of dark green mafic rocks, typically including pillow basalts and hyaloclastites, with in places intercalated sediments (Plate 1). The volcanic rocks are generally fine-grained with aphanitic textures, though in some sections e.g. Calacalí [7706-00010] they are vesicular. In general, the outcrops are heavily tectonised, with the development of brittle fractures and joints, often with quartz or calcite fills. In thin section the basalts are generally heavily altered with replacement by chlorite, calcite and epidote. Fresher samples preserve phenocrysts of olivine, pyroxene and feldspar while spherulitic textures indicative of devitrified glass are also seen.

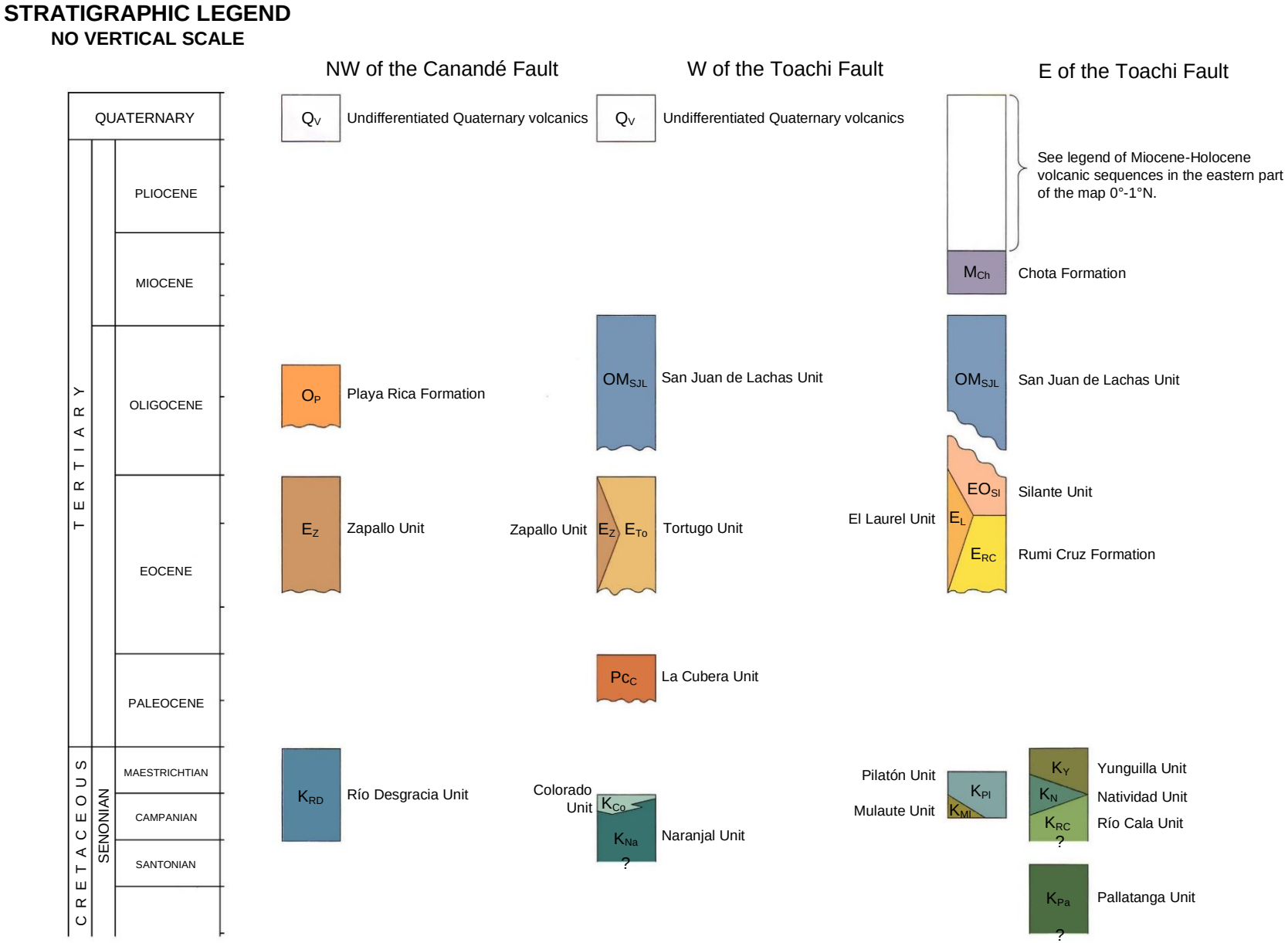

Figure 4. Stratigraphic relationships of the major units

Plate 1. Pillow basalts of the Pallatanga Unit, Salinas-Lita road [8197-00616]

Seven samples have been analysed for whole rock geochemistry, six of which have included analysis of rare earth elements (Appendix 3). The samples plot as both alkalic and sub-alkalic basalts, with samples M5-125 and M5-205a switching between fields suggesting a transitional nature (Figures 5 and 6). On the discrimination diagram of Miyashiro (1974) all samples are tholeiitic (Figure 7), while on the AFM diagram of Irvine and Baragar (1971) samples M5-124 and 125 plot as calc-alkaline while the others plot within the tholeiitic field (Figure 8). A plot of alkali index versus alumina shows all the samples to be tholeiitic. On the nomenclature diagram of Le Maitre (1989) the samples fall within the basaltic-tephrite/basanite field (Figure 9).

On the tectonic environment discrimination diagrams of Pearce and Cann (1973) the samples plot mainly in the ocean floor basalt field (Fig. 10), however again with samples M5-124 and 125 tending towards the calc-alkaline field.

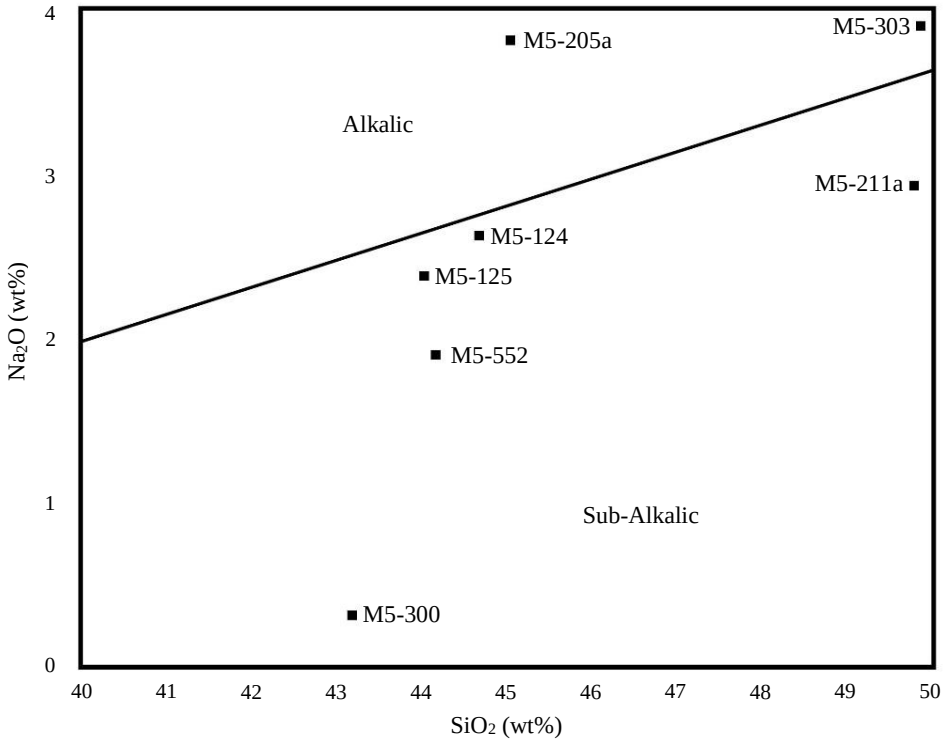

Figure 5. Plot of Pallatanga Unit samples on the basalt discrimination diagram of Middlemost (1975)

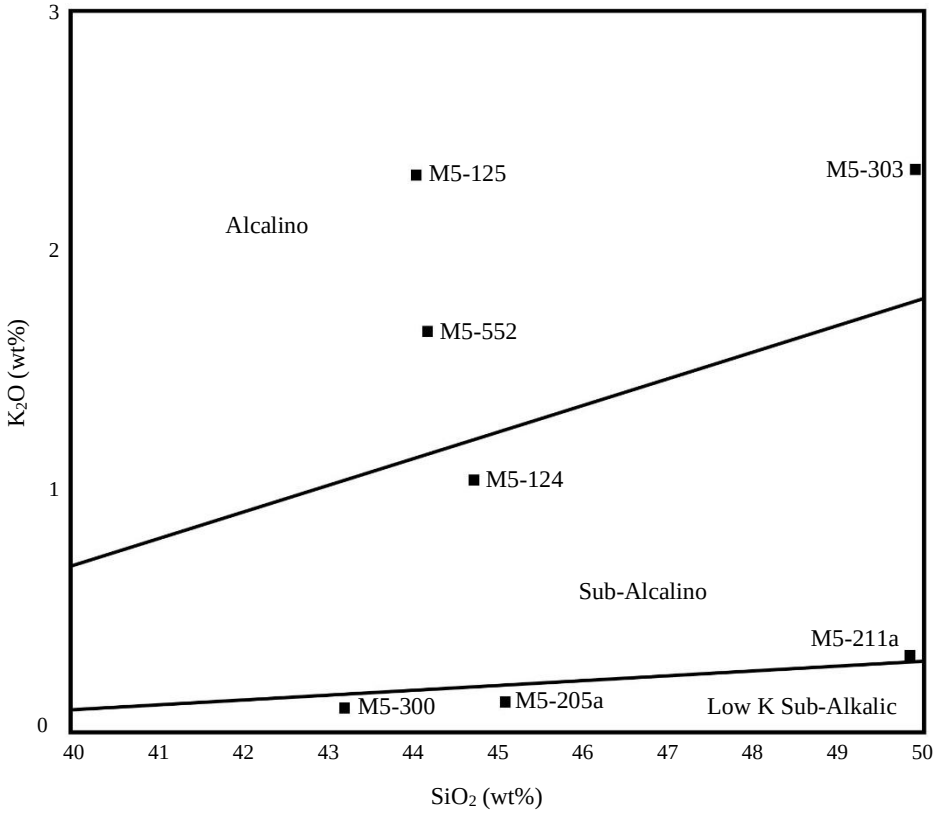

Figure 6. Plot of Pallatanga Unit samples on the basalt discrimination diagram of Gill (1981)

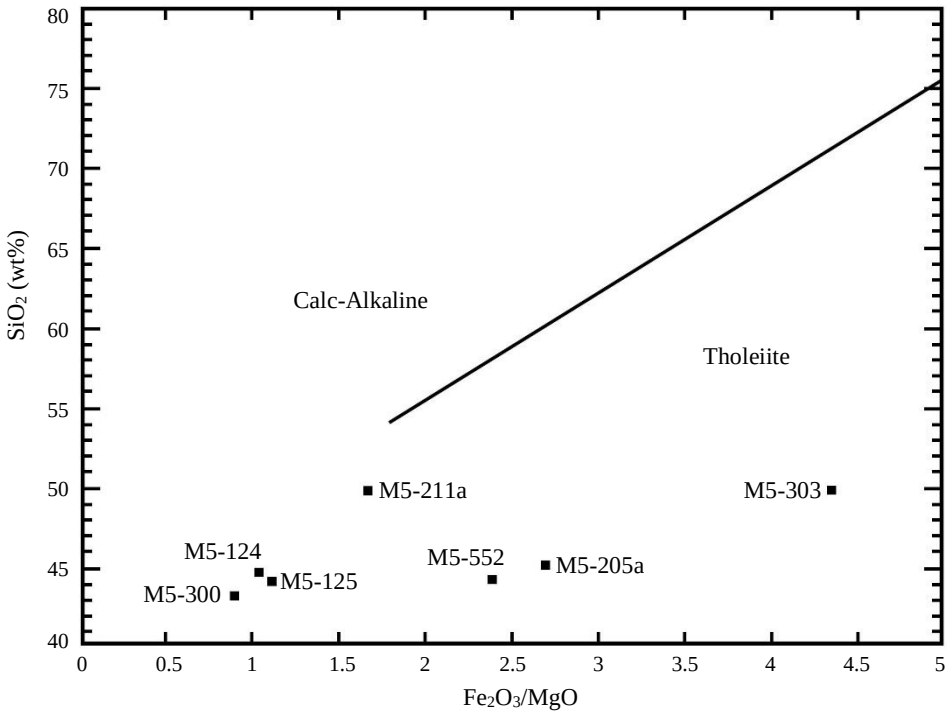

Figure 7. Plot of Pallatanga Unit samples on the basalt discrimination diagram of Miyashiro (1974)

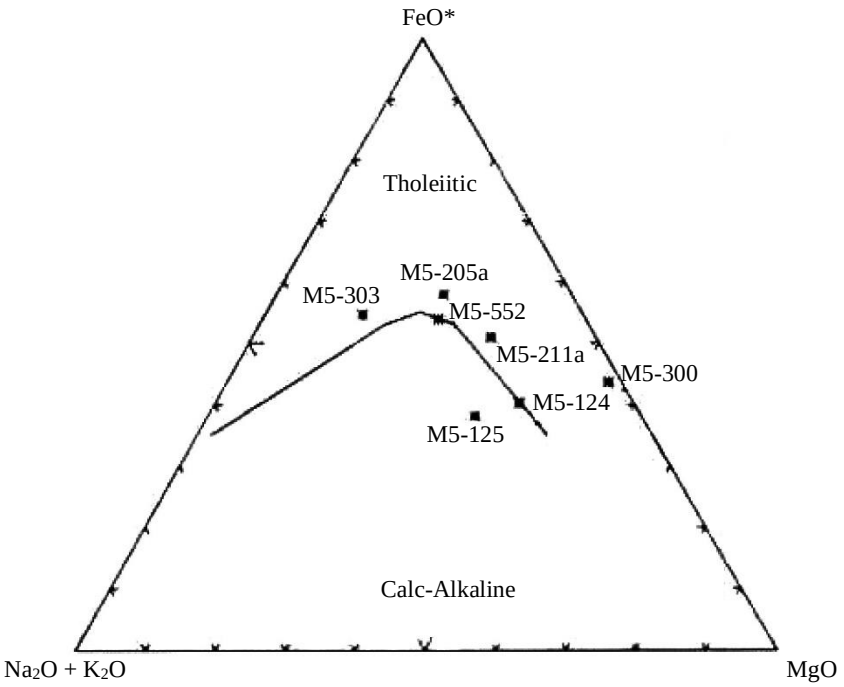

Figure 8. Plot of Pallatanga Unit samples on the basalt discrimination diagram of Irvine and Baragar (1971)

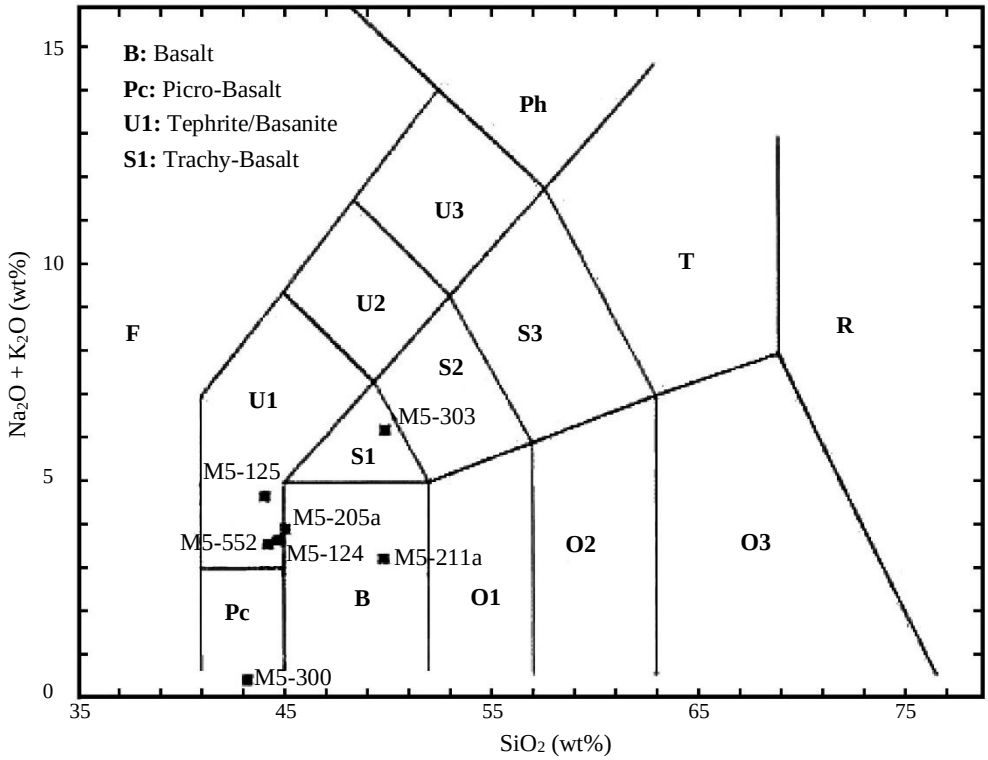

Figure 9. Plot of Pallatanga Unit samples on the rock classification diagram of Le Maitre (1989)

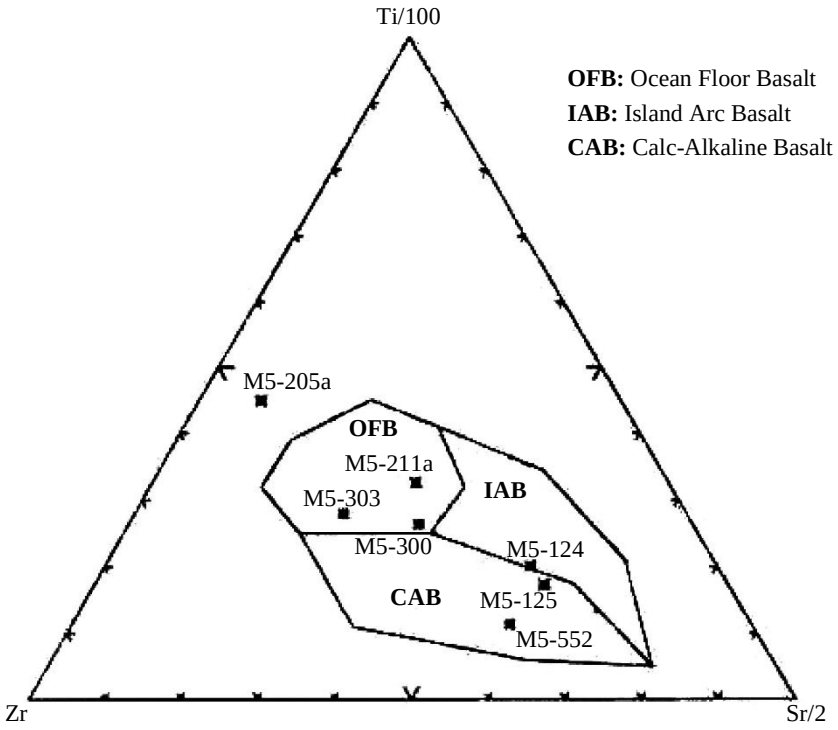

Figure 10. Plot of Pallatanga Unit samples on the tectonic environment discrimination diagram of Pearce and Cann (1973)

Plots of rare earth elements (REE) normalised against chondrite in general show light rare earth depleted to flat patterns, patterns which are indicative of typical N-MORB (Fig. 11). REE concentrations are between ×3 and ×30 chondrite, reflecting either varying degrees of partial melting or fractional crystallisation. A number of the samples show enrichment in lanthanum and cerium in relation to the other light rare elements (LREE) giving a "dish shaped" appearance to the curves, however overall, they maintain a LREE depleted pattern. This lanthanum enrichment means that the standard La/Yb chondrite normalised ratio shows two samples (M5-205a and M5-303) to be enriched in light rare earths, and the range to be $0.7<(La/Yb)_{CN}<1.1$. However plotting praseodymium against ytterbium gives ratios of $0.5<(Pr/Yb)_{CN}<1.1$, with only sample M5-205a showing LREE enrichment. The flat rare earth patters, for example sample M5-205a, are similar to those of P-MORB. Zr/Nb ratios fall in the range 13-22, and are thus comparable to the ratios reported from Colombian Cretaceous basalts by Kerr et al. (1996). These authors interpreted the Colombian basalts with Zr/Nb ratios of 10-15 as being transitional between N-MORB (ratio ~32) and OIB (ratio ~5), and as being rather similar to Icelandic basalts (ratio ~10). Thus overall, the basalts do not appear to be simple MORB, but may instead reflect either a plume-influenced ocean ridge or an ocean plateau.

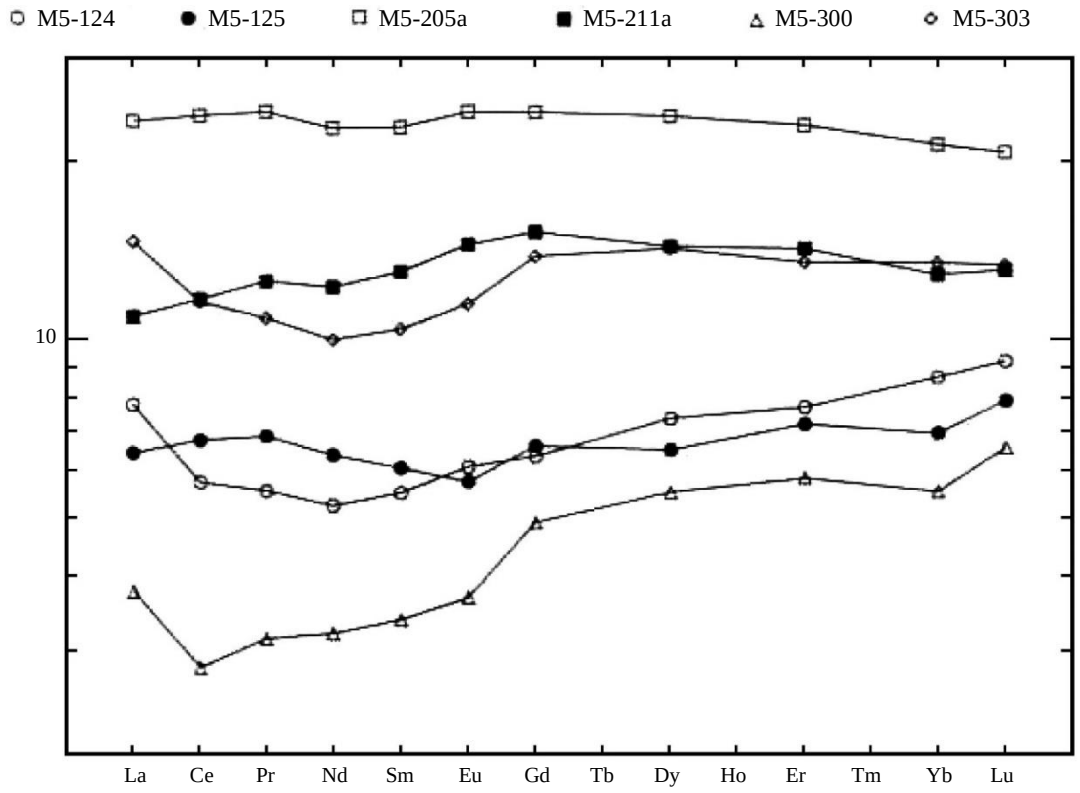

Figure 11. Rare earth element plot of samples from Pallatanga Unit

3.3 Río Cala Unit (K_{RC}) (Boland et al., 2000)

3.3.1 Distribution

This is a new unit defined in this report which outcrops between the Pallatanga and Natividad units. The best exposures are seen in the Urcutambo section of the Otavalo-Selva Alegre road, in the Río Cala above its confluence with the Quebrada Pucará [7856-00204] and in the Río Huarmiyacu [8033-00486] to the NNW of Imantag. Smaller outcrops are seen further north in the Río La Plata [8327-00883] and along the path from Tulcán-Chical [8328-00903].

3.3.2 Age

The age of the unit is unknown but its structural position and geochemical/petrographical characteristics suggest that it postdates the Pallatanga Unit and is either older than or contemporaneous with the Campanian-Maastrichtian Natividad Unit, for which it may have acted as a source (see below).

3.3.3 Facies

The Río Cala Unit consists predominantly of massive lavas and volcanoclastic rocks, though occasional lenses of sandstone occur within the sequence. The unit was first distinguished due to the presence of fresh pyroxene phenocrysts up to 1cm is size which are best seen on the Otavalo-Selva Alegre road between [7877-00277] and [7866-00302]. In thin section these rocks contain equant phenocrysts and fragments of both pyroxene and feldspar set in a vesicular, chloritised matrix.

Five samples of phenocryst-rich rocks were analysed for whole rock geochemistry, three of which include rare earths (Appendix 3). They are andesites to basaltic andesites (Figure 12), and plot mainly in the calc-alkaline field on both the AFM diagram of Irvine and Baragar (1971) (Figure 13) and on the plot of Miyashiro (1974) (Figure 14). On a variety of tectonic environment discrimination diagrams (Figures 15 and 16) the samples consistently plot as calc-alkaline basalts, while plots of trace elements show the steeply inclined negative slope from light to heavy rare earths indicative of a subduction zone related, intraoceanic or continental margin volcanic arc (Figure 17). The plot of the ratio Zr/Y versus Zr (Pearce and Norry, 1979), modified by Pearce (1983) can be used to discriminate between arc basalts developed in an island-arc setting and those from an active continental margin, the latter having both higher Zr/Y and Zr values. On the Pearce and Norry (1979) diagram (Figure 18) all samples fall within the continental arc basalt field which is defined by Zr/Y ratios >3. Comparison of the data with geochemical analyses from the Pallatanga Unit shows that some samples of non-porphyritic lavas, which had been mapped in the field during this study as Pallatanga Unit, in fact show greater affinities with the Río Cala Unit. The inability to differentiate between the two units in the absence of either whole rock geochemistry data or the distinctive pyroxene phenocryst rich facies means that the Río Cala Unit may in fact be more extensive than currently recognised, both within the current map area and further to the south.

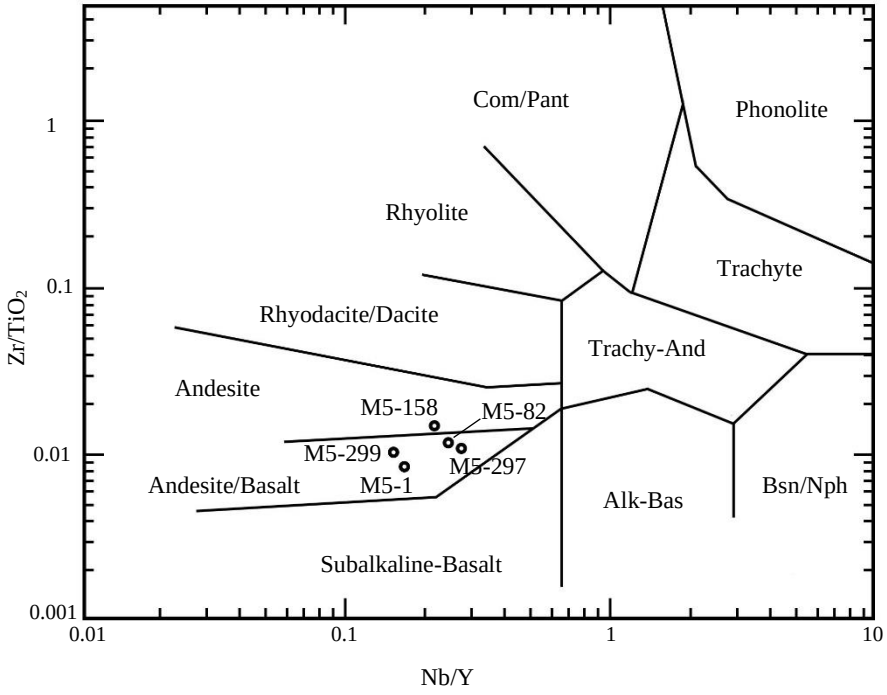

Figure 12. Plot of Río Cala Unit samples on the rock-classification diagram of Winchester and Floyd (1977)

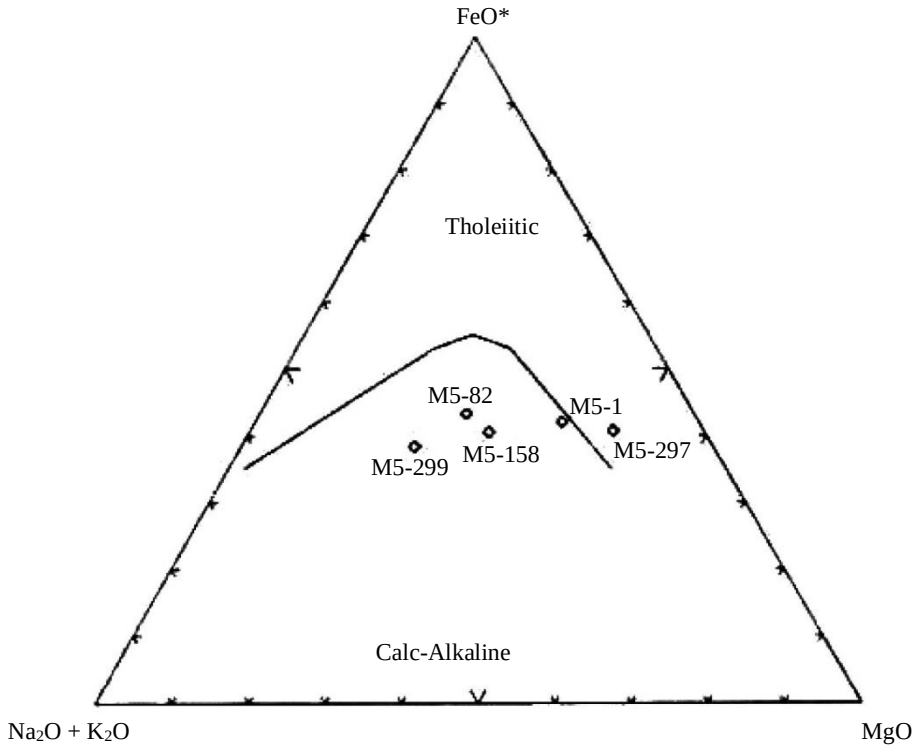

Figure 13. Plot of Río Cala Unit samples on the basalt discrimination diagram of Irvine and Baragar (1971)

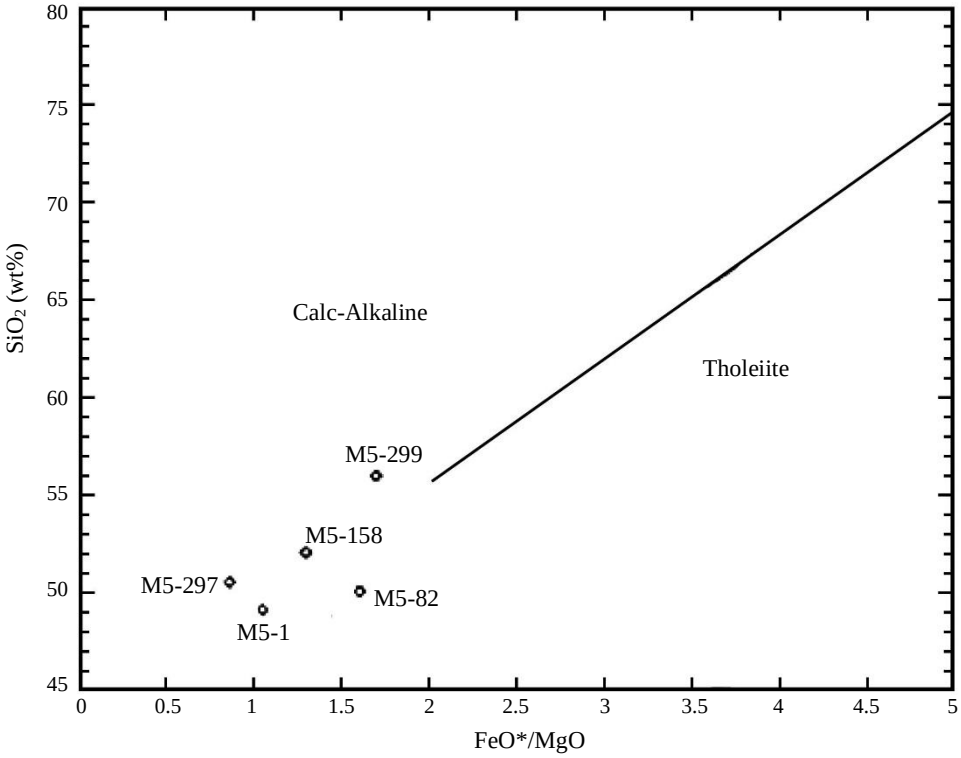

Figure 14. Plot of Río Cala Unit samples on the basalt discrimination diagram of Miyashiro (1974)

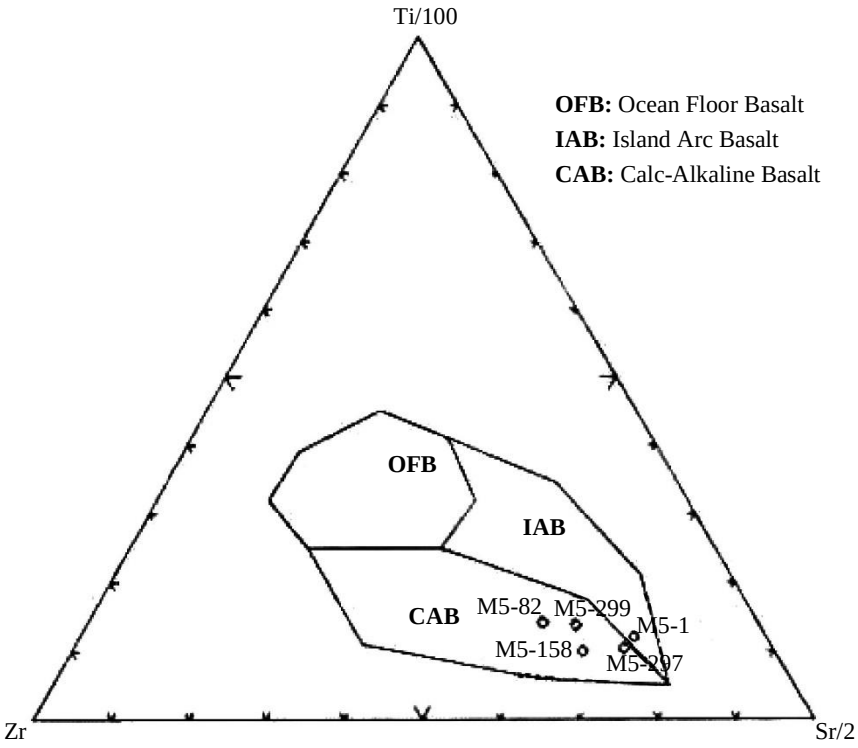

Figure 15. Plot of Río Cala Unit samples on the tectonic environment discrimination diagram of Pearce and Cann (1973)

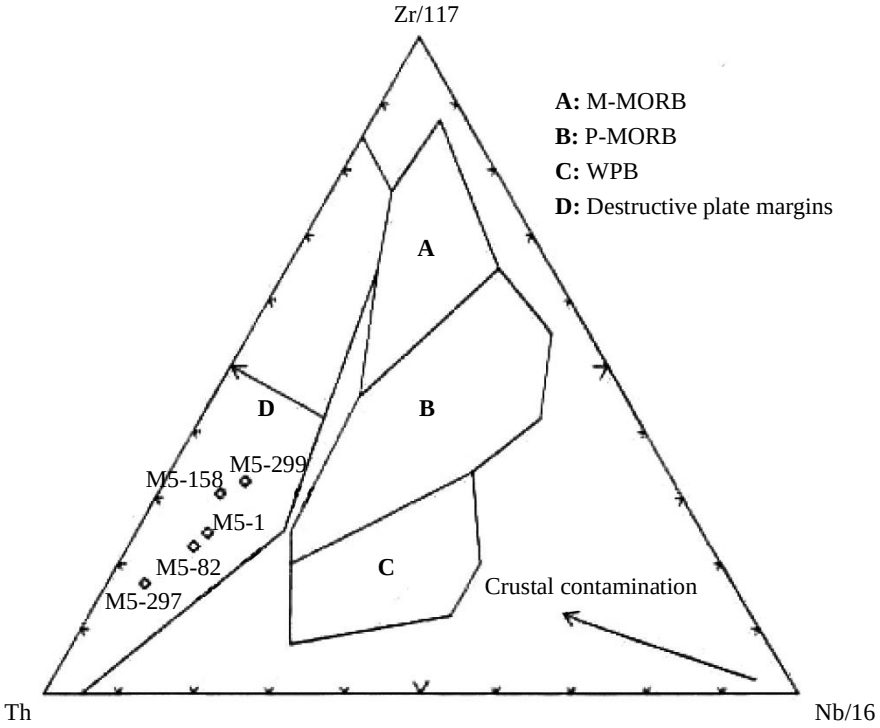

Figure 16. Plot of Río Cala Unit samples on the tectonic environment discrimination diagram of Wood (1980)

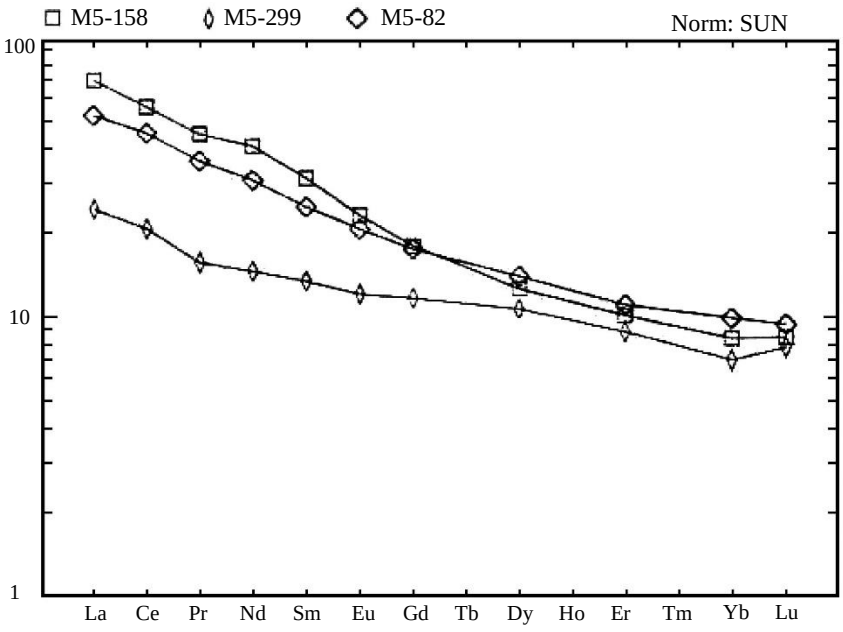

Figure 17. Rare earth element plot of samples from the Río Cala Unit

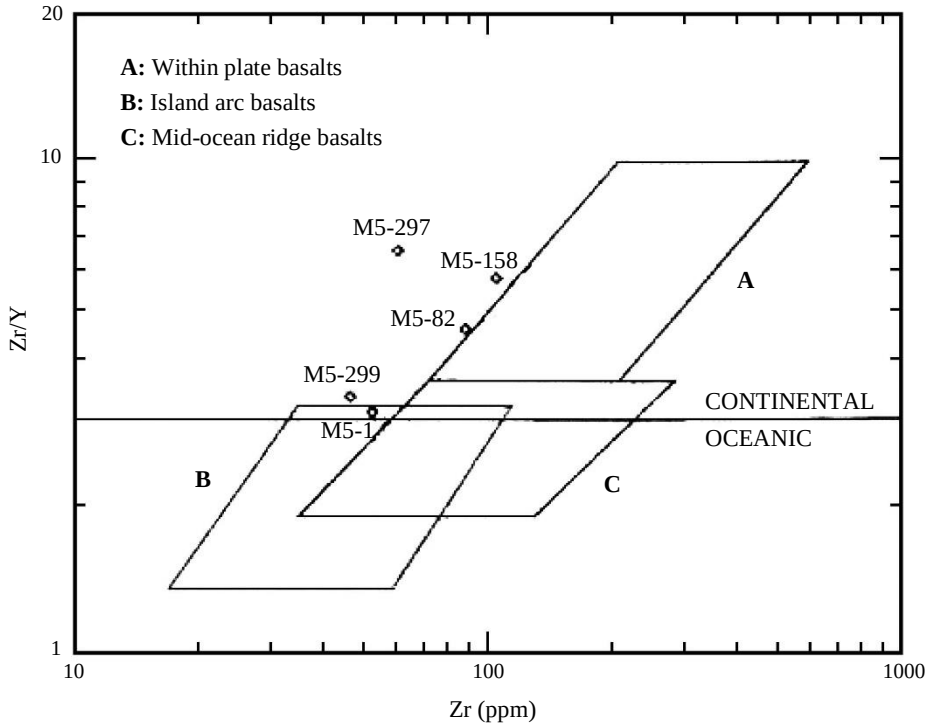

Figure 18. Plot of Río Cala Unit samples on the tectonic environment discrimination diagram of Pearce (1983)

3.4 Natividad Unit (K_N) (Boland et al., 2000)

3.4.1 Distribution

This new unit defined in this report, comprises a sequence of sedimentary rock which occurs mainly to the east of, and in faulted contact with, the igneous rocks of the Pallatanga and Río Cala units. The type section is on the Otavalo-Selva Alegre road, around the Quebrada Natividad [7860-00300], while extensive outcrops are also seen in the Río Guayllabamba to the west of Perucho [7832-00151] and on the Salinas-Lita road [8187-00645].

3.4.2 Age

Five samples collected from the Otavalo-Selva Alegre and Salinas-Lita roads have yielded ages of Campanian-Maastrichtian (65-83 Ma) based on foraminifera faunas which include *Hedbergella monmouthensis, Osangularia navarroana,* and *Osangularia cordieriana* (Wilkinson, 1998c).

3.4.3 Facies

The Natividad Unit consists of an indurated and variably tectonised sequence of sandstones, mudstones and cherts, predominantly grey-greenish to black in colour, but including some red and green mudstones, cherts and intercalated lavas. The sequence is thin to medium-bedded, though some sandstone beds up to 2 m in thickness occur (Plate 2).

Plate 2. Thin to medium bedded turbidites of the Natividad Unit, Otavalo-Selva Alegre road [7852-00296]

In thin section the sandstones from the Río Guayllabamba area contain subangular to subrounded clasts up to 1cm in size of feldspar phyric lavas set in a fine-grained quartz/chlorite/epidote matrix (thin section M5-165, Appendix 5). Sample M5-260 also contains euhedral pyroxenes and feldspars together with volcanic clasts and indicates an intermediate to basic volcanic source for these sediments. In places a penetrative cleavage is developed within the sequence and in thin section this is defined by green biotite, chlorite augens, deformed volcanic clasts and altered feldspar crystals.

Intercalated lavas, with non-faulted contacts, occur within the Natividad close to Hacienda Natividad [7860-00300] and further south on the Otavalo-Selva Alegre road [7840-00267]. The lavas at the latter locality consist of augite and feldspar phenocrysts within a matrix of fine-grained feldspar laths. The lavas are vesicular with chlorite and epidote vesicle fills. Lavas also occur within the Natividad sequence along the Salinas-Lita road though the nature of their contacts is unclear. The rare earth element geochemistry of a sample collected from one of these lavas [8193-00632] (M5-299, see Fig. 17, Appendix 3) shows its close affinity to the lavas of the Río Cala Unit which suggests that the marine, largely turbiditic sediments of the Natividad Unit were contemporaneous and closely associated with the Río Cala arc.

3.5 Mulaute Unit (K_{MI}) (Hughes and Bermúdez, 1997)

3.5.1 Distribution

This unit occurs in a wide belt in the southwestern part of the map, and represents the northward continuation of the sequence from which the unit was originally defined by Hughes and Bermúdez (1997). To the north the belt is crosscut by the Apuela Batholith and only a few outcrops of the Mulaute Unit are seen further northwards of the intrusion.

The unit is well exposed in a number of road and path sections which crosscut the entire sequence, in particular the traverses Pactoloma-Guayabillas-Mashpi [7400-00190], Pacto-Saguangal [7474-00224] and in the Río Guayllabamba from the settlement of San Roque to the Río Verde [7440-00257]. Further north the unit is exposed in a number of small outcrops in the Ríos Lita and Toctemi [7912-00757, 7895-00742].

3.5.2 Age

The age of this unit is not well established but it was interpreted by Hughes and Bermúdez (1997) as being of Late Cretaceous age. Samples collected from the present map area proved to be largely barren of foraminifera, though one sample yielded the *Stensioeina* cf. *excolata* which has previously been reported from Campanian age rocks in Mexico (Wilkinson, 1998b).

3.5.3 Facies

The Mulaute Unit is a sequence of sedimentary rocks which pass from breccias and coarse-grained sandstones in the east into thin bedded, dark-coloured siltstones and mudstones further west (Plate 3).

The western part of the sequence can be seen on the road from Pactoloma to Mashpi [7410-00176] and La Victoria-Saguangal [7474-00224] where massive, green coloured sandstones and conglomerates are exposed. At 7410-00176 the microconglomerates contain rounded clasts of vesicular and porphyritic lavas, together with feldspar fragments, in a chloritised matrix, while elsewhere the clasts are dominated by black mudstones. The sandstones show evidence of brittle deformation with joint development and some fractures being slickensided.

The transition from the massive arenites to a mudstone-siltstone dominated sequence occurs over about 50 m on the La Delicia-Mashpi road [7406-00175]. Deep weathering of the sequence here may reflect the presence of a faulted contact. To the west of this contact the sequence is dominated by thin bedded, intensely cleaved mudstone, siltstones and cherty sandstones, however massive, green-coloured sandstones similar to those which dominate the facies to the east do occur intercalated within the sequence. The cleavage trends NE-SW and dips steeply to the SE, often at a higher angle than S_O.

A strongly deformed breccia is seen at 7400-00190 (Plate 3) where trains of orientated clasts of cherts, black mudstone and green sandstones occur within a mylonitised matrix. Clast orientation indicates a dextral sense of displacement in the zone. The zone of "slaty cleavage" development has a cross zone width of approximately 8 km, and is still present at its western, apparently, faulted contact, with the Tortugo Unit (see below).

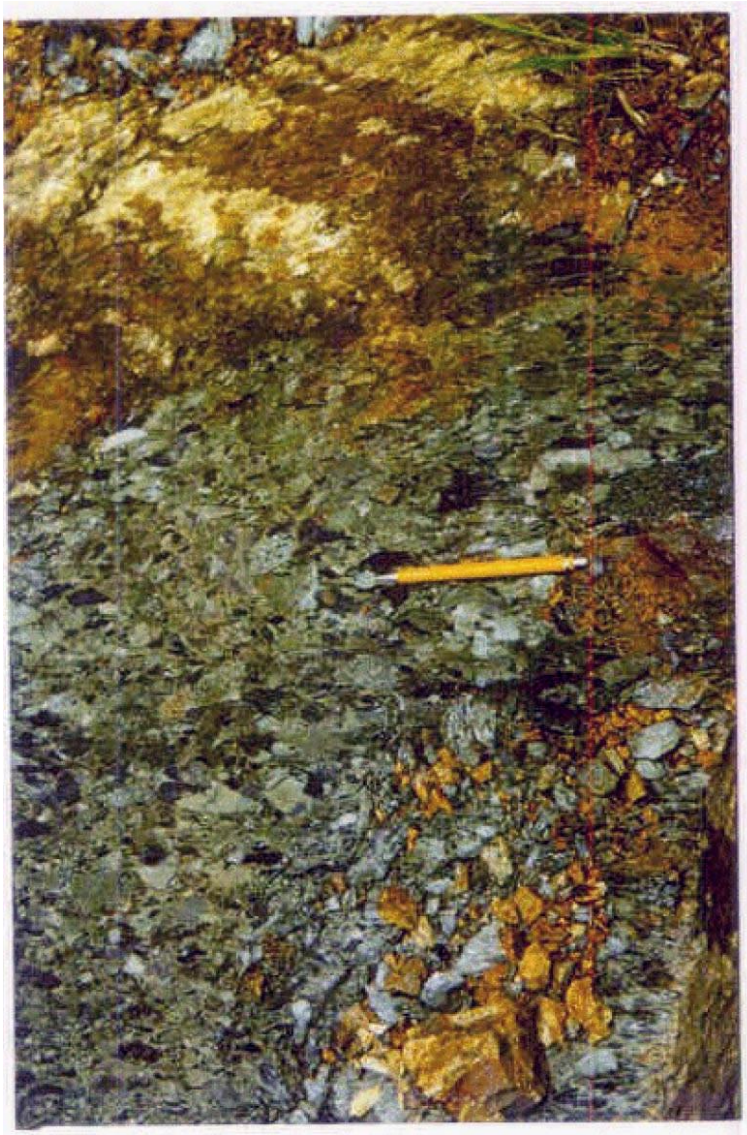

Plate 3. Deformed breccias of the Mulaute Unit, Pacto-Mashpi road [7400-00190]

The depositional environment of the Mulaute sediments is interpreted as being a submarine turbidite fan, with the massive breccias representing mass flow processes and the fine-grained siltstones and mudstones reflecting deposition in the more distal parts of the fan environment. Petrographically, the sediments consist of feldspar-phyric igneous clasts, occasionally vesicular, with both phenocrysts and matrix being extensively sericitised and suggests an effusive volcanic source for the material. The occurrence of amphibole and K-feldspar interpreted by Hughes and Bermúdez (1997) as suggesting an acidic/calc-alkaline compositional source was not seen in the current study area.

3.6 Pilatón Unit (K_{Pl}) Egüez, 1986)

3.6.1 Distribution

This report follows the approach taken by Hughes and Bermúdez (1997) and uses the terminology of Egüez (1986) and Van Thournout (1991) for these rocks formerly known as the 'Formación Cayo de la Sierra'. The unit outcrops extensively in both road and river sections around Pacto, with excellent sections being seen on the road from Pacto to Gualea [7500-00145], and from Pacto to El Paraíso [7480-00176]. Strongly deformed sediments of the Pilatón are exposed in a path which runs eastwards along the Río Guayllabamba from Playa Rica [7644-00206]. Further north the Pilatón Unit is seen adjacent to the Río Mira westwards from Tercer Paso to Collapí [8044-00862]. A faulted contact between the Pilatón and rocks of the Pallatanga Unit has been mapped at Tercer Paso, while the various contact relationships with other units such as the San Juan de Lachas, El Laurel, Mulaute and the Tortugo can be seen on the paths from Lita to Cristal [7931-00743] and which runs westwards from La Merced de Buenos Aires through El Corazón [7936-00679].

3.6.2 Age

Reynaud et al. (1999) reported a Turonian to Coniacian age for the Pilatón Unit based on inoceramid faunas, while a Senonian (Late Cretaceous) age is indicated by the foraminifera *Globotruncana* sp. *Guembelina* sp. and *Globigerina* sp. (Sigal, 1968). These faunas were collected from outcrops along the Alóag-Santo Domingo road section to the south of the current map area.

Three samples collected during the current study from sequences interpreted as being part of the Pilatón Unit yielded ages of Campanian-Eocene, Maestrichtian and Paleocene (Wilkinson, 1998a, b, c, Appendix 2). Although a high level of confidence cannot be attached to any of the determinations, the greatest degree of certainty is given to the Maestrichtian age obtained from the sequence on the Salinas-San Lorenzo road.

3.6.3 Facies

The unit consists of sedimentary rocks, ranging from breccias to black cherts, locally with a very strong volcanoclastic input. The sequences seen on the road sections around Pacto consist of massive, green fine to coarse grained sandstones with locally pale green cherty partings. Many of these outcrops show signs of hornfelsing probably reflecting their proximity to the Apuela Batholith. In thin section the sediments consist of a fine-grained quartz/chlorite/epidote rich matrix with larger fragments of feldspar and igneous clasts. A weak pervasive cleavage is developed through much of the sequence, and in places a stronger penetrative cleavage is developed within sandstones and breccias e.g. Río Chirape [7501-00169] and Río Guayllabamba [7688-00192] (Plate 4). Thin section M5-050 shows a strong shear zone fabric defined by chlorite and quartz augening feldspar grains. Some actinolite and green-brown biotite also occur within the slide, the former possibly representing the remnants of now chloritised grains while the latter does appear to be defining the fabric. In places weak dextral S-C fabrics are developed.

Plate 4. Deformed sediments of the Pilatón Unit, close to the Río Guayllabamba [7688-00192]

On the Salinas-Lita road [8118-00781] the Pilatón Unit is dominated by massive, green coloured, siliceous, volcanoclastic sediments, containing a mix of subrounded clasts of purple and grey coloured, porphyritic lavas together with green, fine grained sediments. The matrix is rich in plagioclase and pyroxene grains. Interbeds of finer grained material occur, grading from coarse grained sandstones, up to 2 m in thickness, to 5 cm thick mudstone units (Plate 5). A variety of sedimentary structures including graded beds and flame structures are seen. Units up to 10 m in thickness of parallel laminated sandstones with clast rich bases occur. This section is dominated by volcanoclastic sediments with subordinate cherty horizons, which differs from the sequences to the south that consist predominantly of well bedded, siliceous sediments with occasional interbeds of volcanic dominated material. In thin section the clasts are dominated by feldspar phyric lavas, though clasts of augite phyric lavas are also seen [8036-00807]. The breccia matrix is composed of fine-grained quartz/chlorite/epidote and is therefore similar in composition to the sandstones seen to the south.

Thin bedded, black-grey cherts-rich sequences (up to 500 m in thickness) are particularly common within the northern part of the sequence and are well-exposed along the Maldonado road section [8269-00973].

Structurally the sequence is folded by open flexures though tight, upright, isoclinal folds are seen within the more cherty sequences [8271-00980]. A ductile deformation fabric is locally developed, e.g. Salinas-Lita road [8111-00794], with weakly developed S-C fabrics indicating a dextral movement sense.

Plate 5. Medium to thick bedded sandstones and cherts of the Pilatón Unit, Salinas-Lita road [8107-00798]

The turbidites of the Pilatón Unit were deposited in the proximal to medial parts of a submarine fan setting. The sediments most likely were sourced from an effusive volcanic centre of basic to intermediate composition. Hughes and Bermúdez (1997) interpreted the lack of airfall material within the sediments and the need for considerable topography to develop large turbidite fans, as being indicative of a submarine island arc source. The apparent intercalation of green, massive arenites, similar to those assigned to the Pilatón Unit in the Pacto area, with mudstones and siltstones of the Mulaute Unit e.g. as seen to the west of La Delicia at [7401-00190], suggests that the two units may in fact be contemporaneous, possibly representing a lateral facies transition. However further evidence relating to the age and petrographic composition of these units is required to resolve this question. The apparent northward transition in the Pilatón Unit to a coarser, breccia dominated sequence may also reflect closer proximity to the sediment source if the sequences are time equivalents.

3.7 Yunguilla Unit (K_Y) (Thalmann, 1946)

3.7.1 Distribution

The Yunguilla Unit, which was defined by Thalmann (1946) from the sections around Alambi [7950-9993], outcrops in a number of lenses, predominantly in the south of the map area. Its contacts with rocks of the Pallatanga and Natividad units are faulted, while further to the south Hughes and Bermúdez (1997) report that the contact between the Yunguilla and the Silante is unfaulted. The principal exposures of the unit occur in the south of the map area along the Calacalí-Nanegalito road and also in the Río Guayllabamba between Los Reales and Entables de Chespi [7776-00144]. Further north the Yunguilla Unit is only recorded from a number of isolated outcrops on the Salinas-Lita road, close to the Río Amarillo [8183-00654]. A thickness of at least 2000 m is reported from the type area which lies just south of the current map area [765-9993] (Thalmann, 1946; Bristow and Hoffstetter, 1977).

3.7.2 Age

The age of the Yunguilla Unit was given as Danian (earliest Paleocene) by Savoyat et al. (1970) and by Faucher et al. (1971) based on foraminifera collected from the type section around Alambi. However, a reassessment of the faunal lists by Dr. Ian Wilkinson of the British Geological Survey concluded that they indicated an age no younger than Maastrichtian, while Hughes and Bermúdez (1997) also report a Campanian-Maastrichtian age attributed to Dr. Etienne Jaillard of the Institut Dolomieu, Grenoble, France.

Age determinations were made for five separate localities in the current map areas, three samples yielding Campanian-Maastrichtian ages and the other two a Campanian age based on the occurrences of *Bolivinoides decoratus*, *Osangularia "cordieriana"* and *Globigerinelloides volutus* (Wilkinson, 1998a, b, c, Appendix 2). These results confirm the Late Cretaceous age of the unit but suggest a probable Campanian age for the initiation of Yunguilla deposition.

Plate 6. Folded mudstones and siltstones of the Yunguilla Unit [8183-00656]

3.7.3 Facies

The Yunguilla Unit consists predominantly of black to grey, thin bedded, locally calcareous, mudstones and siltstones. In the Los Reales to Los Entables de Chespi section [7776-00144] a westward transition occurs with medium to thick bedded sandstones comprising a higher percentage of the sequence. A weak cleavage is developed within the mudstones and upright, close, symmetric folds are developed (Plate 6).

The sequence exposed on the Salinas-Lita road consists of black mudstones in faulted contact with both Pallatanga [8183-00656] and Natividad [8184-00654]. A cleavage, dipping gently to the NW, is developed in the mudstones at the contact with the Pallatanga, and numerous calcite and quartz filled fractures are also present.

The Yunguilla Unit was deposited in a submarine fan environment, the fine-grained nature of the sediments and the presence of carbonate-rich beds possibly indicating deposition in the more distal parts of the fan. Hughes and Bermúdez (1997) report the presence of both strained quartz, indicative of a metamorphic source, and volcanic glass shards within the Yunguilla sediments. The age evidence suggests that deposition of the Yunguilla may have been in part contemporaneous with the Natividad, though whether they represent lateral facies equivalents is unclear.

3.8 Naranjal Unit (K_{Na}) (Boland et al., 2000)

3.8.1 Distribution

This new unit comprises a sequence of pillow basalts, basaltic to andesitic lavas, high level intrusives and igneous breccias which occur to the west of the Toachi Fault and form the basement to the Cretaceous to Oligocene-age sediments and lavas seen in the western part of the map. The unit is named after the section seen in the Río Naranjal at the footbridge on the path between Salto de Tigre and Rumiñahui [7227-00293], where sediments intercalated within a sequence of pillow basalts have yielded a radiolaria fauna. The section here is largely inaccessible but spectacular exposures of the pillow basalts can be reached in the Río Guayllabamba at Salto de Tigre [7213-00260] (Plates 7 and 8). Further sections of the unit were seen on traverses carried out in the rivers which drain westwards off the Cordillera del Toisán including the San Carlos, Bravito, Tigre, Bravo, Barbudo and Rumiyacu. The unit is also well exposed in both the Salinas-Lita road and the Río Mira westward from the village of Cachaco [7895-00923].

3.8.2 Age

A radiolaria fauna was collected from a sequence of purple to grey coloured, siliceous mudstones which are interbedded within pillow basalts exposed in the Río Naranjal [7227-00293]. The index taxa present include *Amphipyndax pseudoconulus* (Campanian), *A. tylotus* (late Campanian-Maastrichtian), *Archaeodictyomira lamellicostata* (late Camp.-Paleocene), *Dictyomitra formosa* (Turonian-late Camp.), *D. kozlovae* (Coniacian-early Maast.) and *Xitus grandis* (Cenomanian-Paleocene). Based on the co-occurrence of the first three taxa a late Campanian-age is proposed (Hollis, 1999).

3.8.3 Facies

The sequence seen in the road and river sections along the Río Mira consists of both lavas and igneous breccias. The breccias seen in the rivers Mira and Lita to the west of Lita village consist of clasts up to 50 cm in size of plagioclase-phyric, sometimes vesicular, andesitic material in a matrix rich in euhedral plagioclase grains. Both the matrix and clasts are compositionally similar and probably reflect derivation from the same igneous source. In the Río Lita the clasts are rounded and may represent detached pillows. Although not seen in situ in this northern section boulders of pillow basalts were seen in the Río Verde [7953-00948]. The breccias have irregular contacts with massive igneous rocks which may represent high level intrusions within this volcanoclastic pile.

In thin section the clasts consist of euhedral augite and plagioclase phenocrysts in a fine-grained matrix of feldspar laths, with minor opaques and chlorite. The latter normally filling interstices between aggregates of euhedral pyroxenes and may represent altered glass. The clasts are occasionally vesicular with fills of chlorite, quartz and epidote group minerals. Many samples show extensive alteration with chlorite, epidote and calcite being the principal replacement minerals. Angular amphibole grains are present in a number of samples though whether this reflects original or secondary mineralogy is unclear. The latter is suggested by the presence of eight sided grains in M5-446, the amphibole replacing original pyroxene, a replacement that can be seen in M5-630 (Appendix 5).

Plate 7. Pillow basalts of the Naranjal Unit exposed in the Río Guayllabamba at Salto del Tigre [7213-00260]

Plate 8. Pillow basalts of the Naranjal Unit exposed in the Río Guayllabamba at Salto del Tigre [7213-00260]

Further south the Naranjal Unit is dominated by lavas and high level intrusives, with a small percentage of breccias and sediments within the sequence. The pillow lavas exposed in the Río Guayllabamba at Salto del Tigre and further north-east in the Río Naranjal have a cross strike width of 1.5 km, representing a possible thickness of 1km. The basalts are fine grained, and in thin section consist of millimetre sized feldspar phenocrysts and quartz/chlorite filled vesicles set in a matrix of feldspar laths, opaques and chlorite, submillimetre pyroxene grains form a small modal percentage of the rocks' mineralogy. In the Río Naranjal [7227-00293] a 10 m thick sequence of siliceous mudstones is intercalated within the pillow lavas, and these sediments have yielded the radiolarian fauna upon which the age of the unit is based.

To the west of the pillow basalts the Naranjal Unit consists of generally massive, fine grained green coloured, igneous rocks. In places a parting can be seen in these rocks, but whether this represents original lava flows or is some sort of 'pseudo-bedding' is unclear.

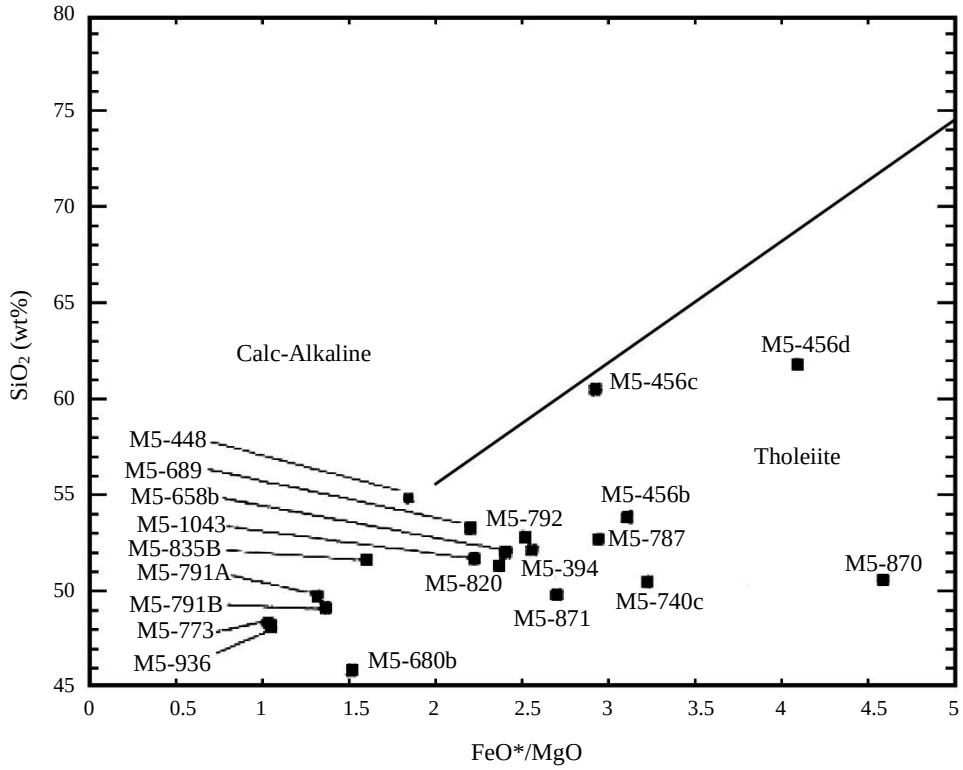

Figure 19. Plot of Naranjal Unit samples on the basalt discrimination diagram of Miyashiro (1974)

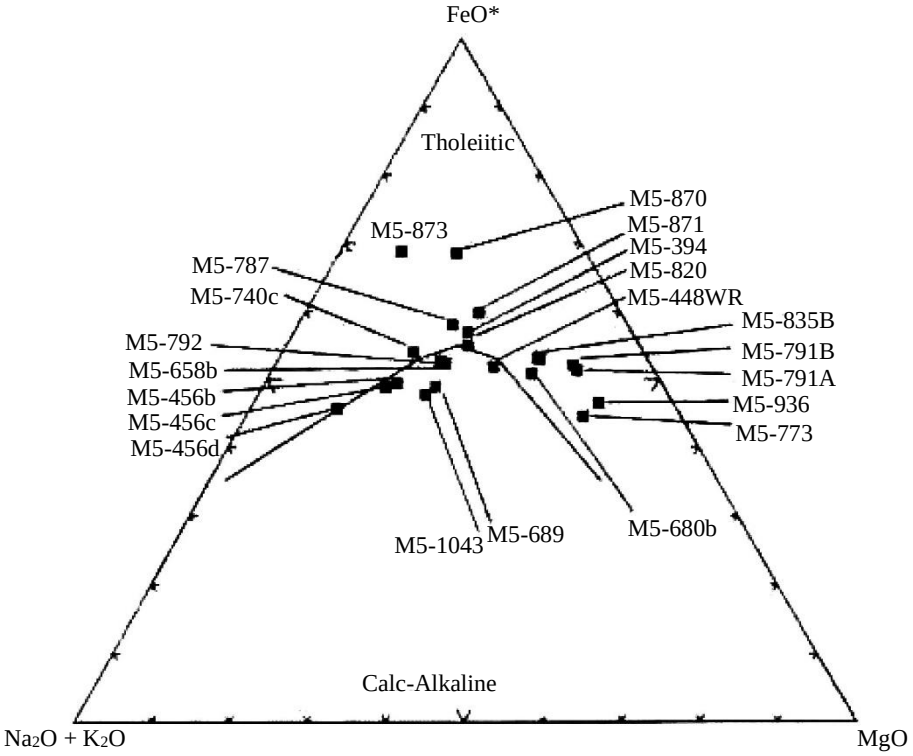

Figure 20. Plot of Naranjal Unit samples on the basalt discrimination diagram of Irvine and Baragar (1971)

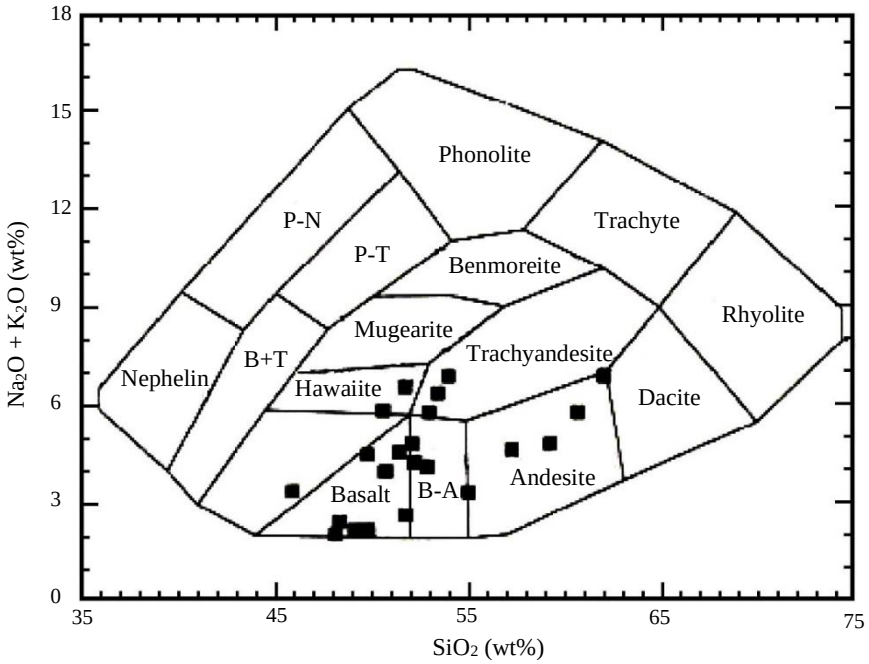

Figure 21. Plot of Naranjal Unit samples on the rock classification diagram of Cox et al. (1979)

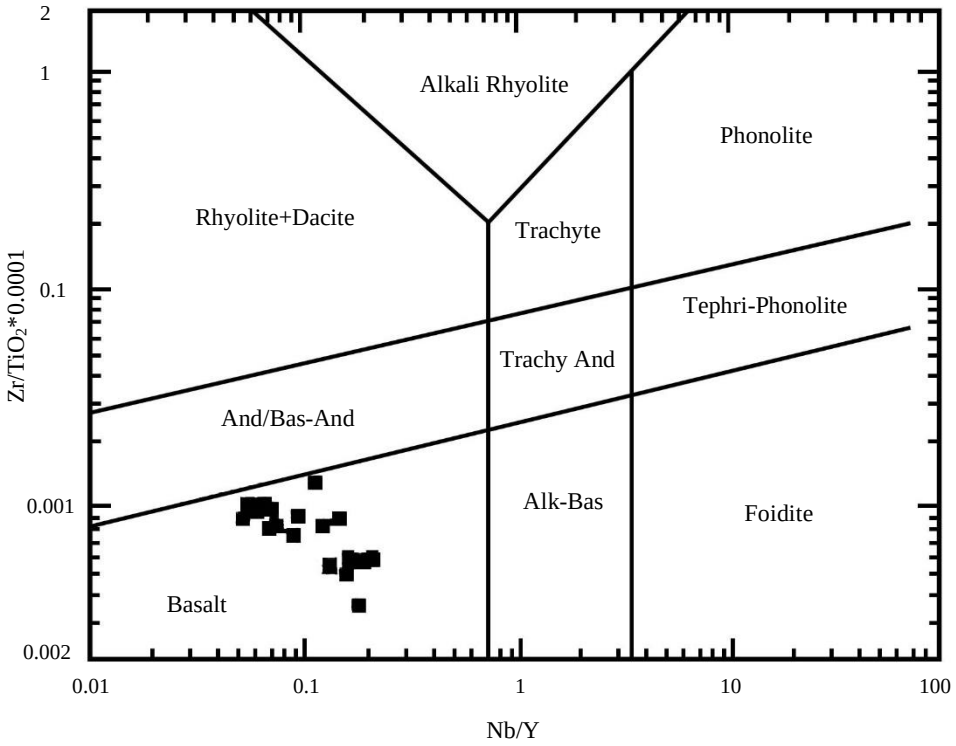

Figure 22. Plot of Naranjal Unit samples on the rock classification diagram of Winchester and Floyd (1977)

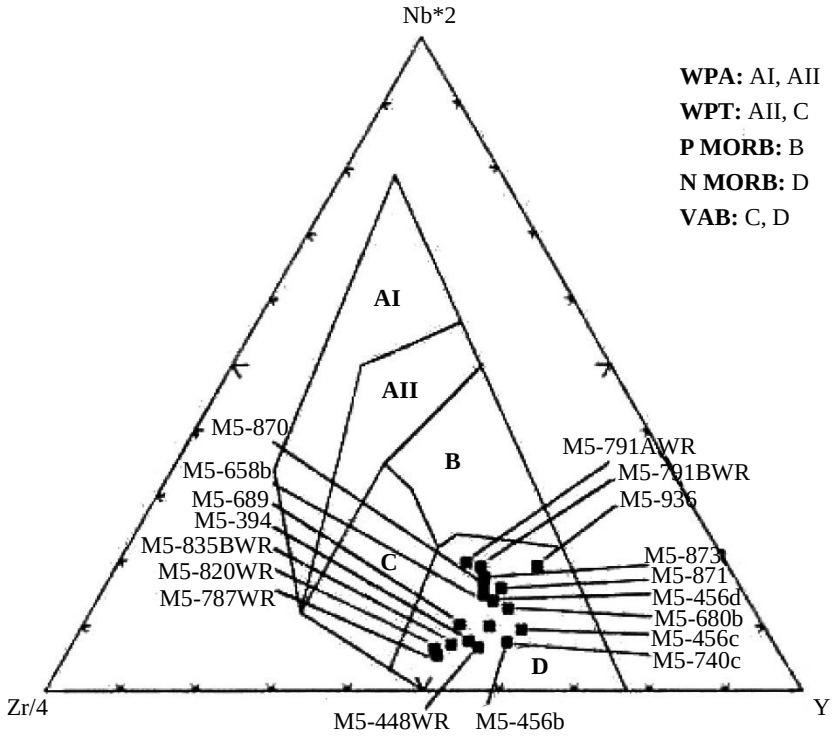

Figure 23. Plot of Naranjal Unit samples on the tectonic environment discrimination diagram of Meschede (1986)

Thirty-one samples have been analysed for whole rock geochemistry, 19 of which have included analysis of rare earth elements (Appendix 3). The samples generally plot as tholeiites on both the discrimination diagrams of Miyashiro (1974) and Irvine and Baragar (1971) (Figures 19 and 20), although some samples such as M5-1043 change fields from calc-alkaline to tholeiitic between the two diagrams. M5-448, which is an analysis of the breccias which outcrop at Lita [7794-00970], plot as calc-alkaline on both diagrams. The rocks plot predominantly as basalts on a range of classification diagrams (Cox et al., 1979; Winchester and Floyd, 1977), though some samples from the Lita area plot as andesites (Figures 21 and 22). MgO contents range from 3-9 wt%. The samples plot in the N-MORB/volcanic-arc field of the Meschede (1986) tectonic environment discrimination diagram (Figure 23), with the majority of the samples plotting in the island arc tholeiite field on the discrimination diagram of Mullen (1983) which can be used to distinguish between MORB and arc basalts (Figure 24). Some samples plot in the calc-alkaline basalt field on this latter diagram, including the andesites from the Lita area and the pillow basalts of Salto del Tigre.

On spidergram plots a number of samples show negative niobium anomalies indicative of igneous rocks generated in a subduction related environment (Figure 25). Other samples however show no depletion of niobium relative to lanthanum suggesting that the lavas of the Naranjal Unit may represent more than one tectonic environment. Rare earth element traces predominantly have negative slopes, while primitive mantle normalised La/Nd and Sm/Yb ratios range from 1-2, indicating light REE enrichment (Figure 26). However, samples M5-773 and M5-791 show the light REE depleted patterns of MORB basalts, indicating that MORB basalts occur within the sequence of predominantly arc-related tholeiites. These MORB basalts may represent the ocean floor to the Naranjal island arc, with the ocean floor and arc basalts becoming tectonically interleaved during accretion of the arc onto the continental margin.

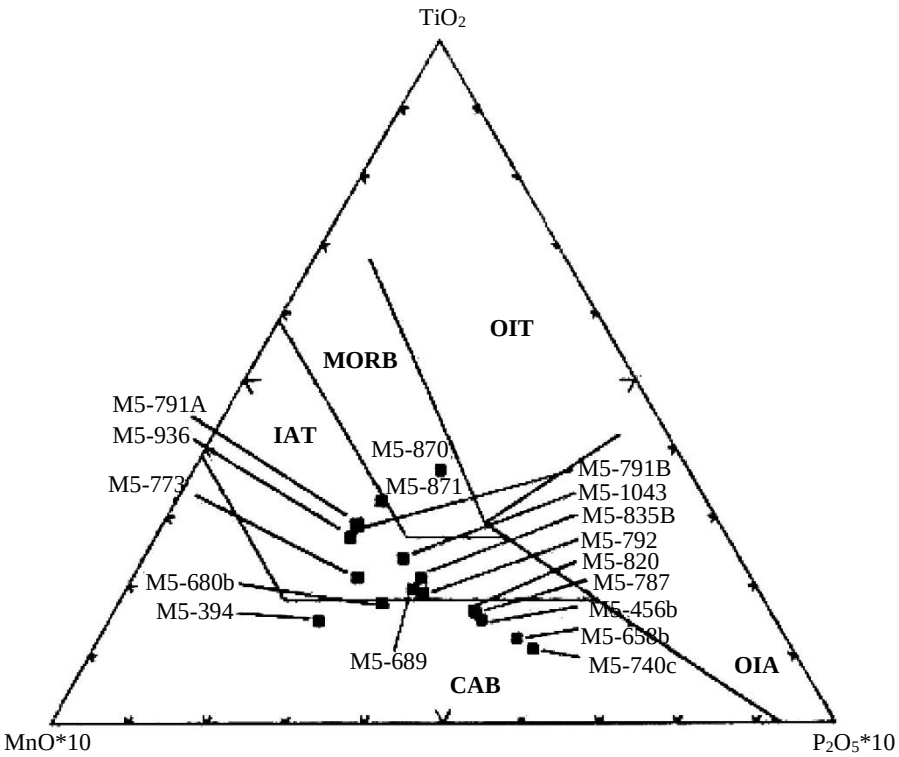

Figure 24. Plot of Naranjal Unit samples on the tectonic environment discrimination diagram of Mullen (1983)

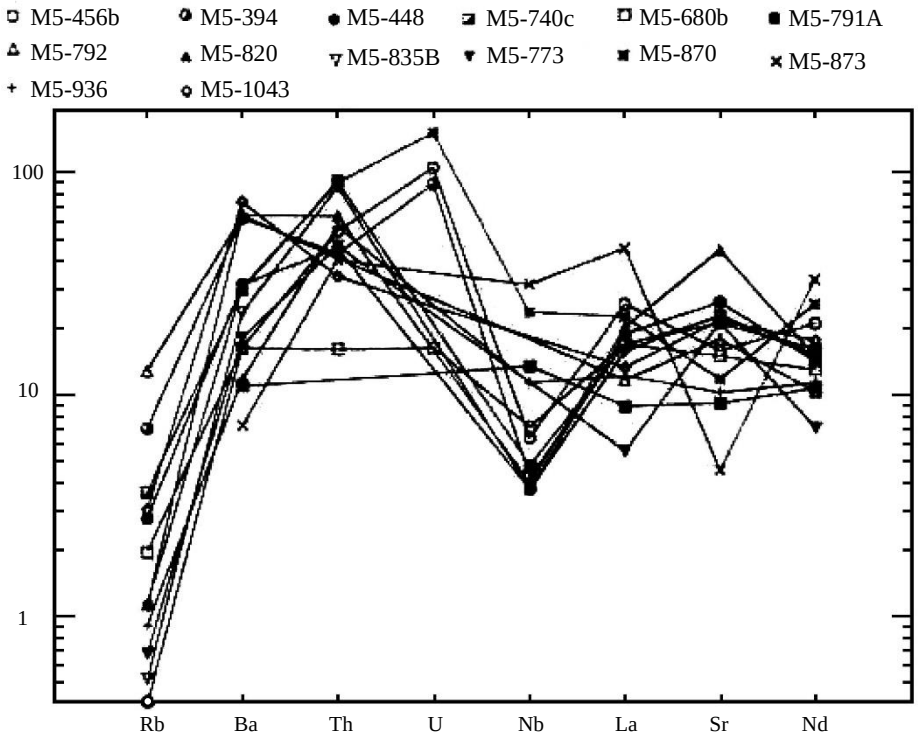

Figure 25. Spider diagram plot of samples from the Naranjal Unit

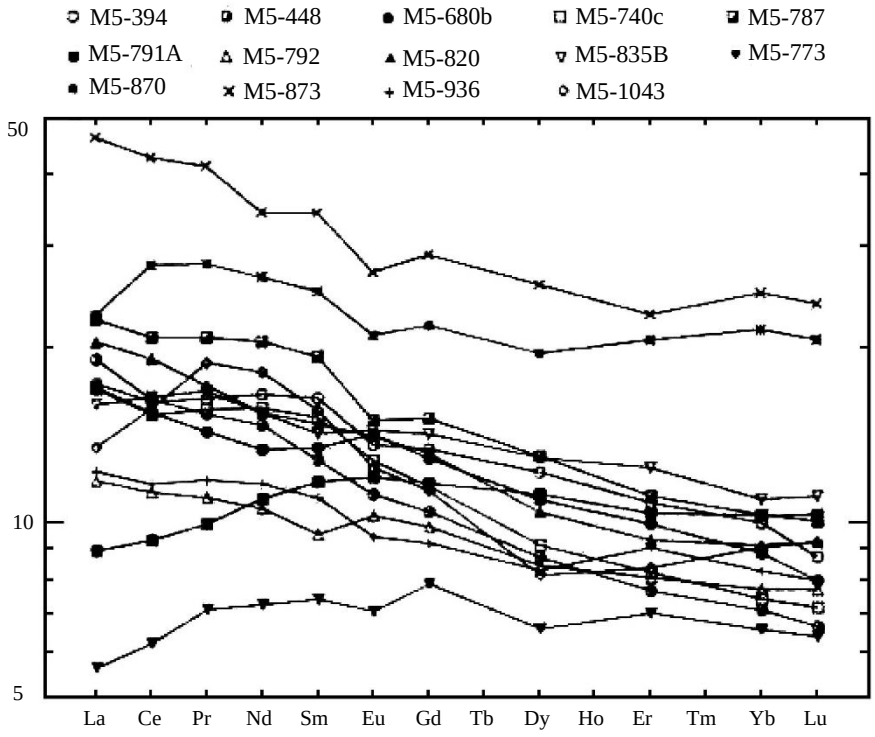

Figure 26. Rare earth element plot of samples from the Naranjal Unit

3.9 Colorado Unit (K_{Co}) (Boland et al., 2000)

3.9.1 Distribution

This new unit, which overlies the igneous rocks of the Naranjal Unit, is defined by the exposures of thin to medium bedded, fine grained sandstones and siltstones seen in the quebradas to the north of the Estero Colorado [7213-00336]. Further sections through the unit were mapped in the rivers, Salvador [7252-00495], Bravito [7303-00545], Bravo [7452-00617] and Barbudo [7564-00645]. The unit is also preserved as large roof pendants within the Santiago Batholith [7668-00894] while the most northerly section is exposed on the road between Lita and Alto Tambo [7765-00990].

3.9.2 Age

A Campanian age was determined based on the radiolaria fauna derived from a green-grey chert collected from the Río Barbudo section [7558-00626]. The fauna includes taxa assignable to the *Amphipyndax pseudoconulus-tylotus* complex and *Theocampe apicata-vanderhoofi* complex, both indicative of a Campanian-Maastrichtian age, but based on the presence of *Theocampe salilum* a Campanian age is preferred (Hollis, 1999a).

3.9.3 Facies

The type section for the unit is exposed to the north of the Estero Colorado [7213-00340] and consists of generally deeply weathered, buff coloured, thin to medium bedded, grey-green coloured, alternating siltstones and fine-grained sandstones, with both parallel and ripple laminated beds. In thin section the sandstones consist of a fine-grained quartz matrix with larger angular grains of feldspar and amphibole.

Similar sequences are seen in the rivers Salvador, Bravito and Bravo to the north with green-coloured siltstones, locally interbedded with fine grained sandstones. A transition between pillow basalts of the Naranjal Unit and gently dipping siltstones is seen in the Río Salvador [7268-00487], though whether this contact is an original sedimentary one in unclear.

Further north between the Río Barbudo and the Lita-Alto Tambo road [7762-00994] the Colorado Unit is coarser grained, with sandstones and microconglomerates becoming more prominent in the sequence. In the Río Negro [7682-00884] the unit is dominated by breccias containing subangular clasts, up to 5 cm in size, of dark coloured basaltic/andesitic, while at [7777-00987] the sequence again includes thin bedded siltstones and sandstones but with interbeds of massive, microconglomerates containing clasts of both vesicular lavas and fine-grained green mudstones. Petrographically these sediments contain subangular feldspar and amphibole fragments within a fine-grained quartz-chlorite matrix and are similar to the sediments seen adjacent to the Estero Colorado.

The Colorado Unit comprises a sequence of marine turbidites, probably deposited on the proximal to medial parts of a submarine fan. The presence of clasts of vesicular basaltic/andesitic lavas indicates derivation from an effusive, volcanic source. Radiolaria have shown the Colorado Unit and the lavas of the Naranjal Unit to be broadly contemporaneous in age and thus the simplest interpretation is that the Colorado Unit sediments were sourced from the Naranjal island arc. The absence of intercalated hyaloclastites and lavas may reflect the distal nature of the sediments or the cessation of Naranjal Unit volcanism prior to the deposition of the Colorado Unit.

3.10 Río Desgracia Unit (K_{RD}) (Boland et al., 2000)

3.10.1 Distribution

This new unit outcrops to the north of the Río Canandé northeastwards to the Río Bravito where it is overlapped by the Zapallo Unit. Its southern boundary is marked by the Canandé Fault [6957-00516], across which it is in tectonic contact with the Naranjal Unit, while its northern limit is marked by the onlap of the Zapallo Unit in the east and the Playa Rica Formation in the west. These northern contacts have been mapped principally using satellite imagery.

The principal section through the unit is exposed along the new road between Puerto Nuevo [6957-00516] and the caserío of Hoja Blanca [7010-00616]. Neither the road nor Hoja Blanca are shown on the published topographical 1:50000 maps so the unit is named after the Río Desgracia, along whose river valley the road initially runs. Further exposures were mapped along both the Río Canandé [7154-00547] and the Río Bravito [7276-00629].

3.10.2 Age

Two samples taken from mudstone beds within the sequence yielded diagnostic radiolaria. The first sample collected close to the Río Canandé contained *Phaseliforma subcarinata*, *Protoxiphotractus* sp., *Theocapsomma* sp., *Cryptamphorella conara*, *Amphipyndax tylotus* and *Dictyomitra andersoni* an assemblage correlated with the late Campanian-Maastrichtian *Amphipyndax tylotus* zone (Hollis, 2000, Appendix 2).

The second sample collected further west yielded a fauna of *Conocaryomma universa*, *Amphipyndax pseudoconulus*, *A. stocki*, *Dictyomitra kozlovae*, *D. multicostata* and *Lithocampe* sp., an assemblage correlated with the early to mid-Campanian *Amphipyndax pseudoconulus* zone (Hollis, 2000, Appendix 2).

3.10.3 Facies

This unit is a sedimentary sequence of predominantly coarse grained turbidites with intercalated lavas and dykes. A sequence of thick to very thick bedded turbidites is exposed in a river section beneath the bridge at [6983-00560] and includes massive conglomeratic T_A beds up to 5 m in thickness which contain rounded clasts of predominantly sedimentary, but also igneous, material. Individual units grade through graded sandstones, cross-bedded units into mudstones reflecting a T_{ABCD} turbidite sequence. Bedding dips steeply to the N and youngs in that direction. Downstream of the bridge the sequence changes to medium to thick bedded T_{ABC} units without the massive conglomerates.

Further south along the road at [6973-00546] a sequence of conglomerates consisting of subrounded clasts of igneous material occur which appear to grade into more massive igneous bodies. These igneous bodies are intercalated within the sedimentary sequence and thus probably represent coeval lava flows into the sedimentary basin. Thin sections of samples from both the igneous bodies and the clasts show that they consist of intergrowths of fine-grained augite and plagioclase, with minor ilmenite (see thin sections M5-1009, 1009B, 1012 and 1012A). Some replacement by chlorite has occurred but the rocks are generally quite fresh. The igneous clasts are generally finer grained and in places vesicular possibly reflecting a faster cooling rate and are set in quartz, feldspar, pyroxene and chlorite rich matrix.

The sequence seen along the Río Canandé [7055-00515] is finer grained, consisting of thin to medium bedded, grey coloured, calcareous mudstones to siltstones and is affected by brittle deformation with extensive calcite vein development.

The unit was deposited in a submarine turbidite environment and is believed to have been derived from a submarine volcanic source. The presence of massive, conglomeratic units suggests deposition within submarine channels, possibly on the proximal parts of the fan. The intercalated lavas also indicate deposition near to, and contemporaneous with, the volcanic source for the sediments. The transition to finer-grained, thinner bedded sediments seen within the younger part of the sequence adjacent to the Río Canandé may reflect reduction in the topography of the source region, either through erosion or cessation of volcanism and thus deposition in a lower energy regime. The relationship between the units Río Desgracia and Colorado is unclear, though both appear to be roughly contemporaneous, and were deposited in similar sedimentary environments and derived from volcanic sources.

3.11 La Cubera Unit (Pc_C) (Boland et al., 2000)

3.11.1 Distribution

The principal exposure of this newly defined unit is found in a roadstone quarry [7080-00125] to the west of Diez de Agosto on the Calacalí-La Independencia road, and it takes its name from the Estero Cubera which crosses the unit at this point. The unit forms a prominent feature, including the ridge termed El Cebu [7364-00359] between the Naranjal and Mandariyacu river valleys, and can be easily traced on the aerial photographs.

3.11.2 Age

Two samples collected in the roadstone quarry at Diez de Agosto yielded unequivocal Paleocene ages based on the radiolarian index species *Amphisphaera kina*, *Burella dumitricai* and *Burella granulata*. The coexistence of these Paleocene restricted species with the Late Paleocene-early Eocene index species *Axoprunum pierinae*, *Buryella pentadica*, *B. tetradica*, *Lamptonium fabaeformae pennatum* suggest that deposition continued into the Late Paleocene (Hollis, 2000, Appendix 2).

3.11.3 Facies

The sequence is dominated by thin bedded, pink-cream-grey cherts which in places pass into more massive sandstone units. In the quarry at Diez de Agosto bedding dips at 40° to the south, and includes at the base 70 m of rose to cream-coloured cherts with a bed thickness of between 10-20 cm. This sequence passes upwards into massive, dark-coloured sandstones. The other outcrops which were seen to the north [7364-00339] consist of generally thin bedded, silicified rocks with dips varying between 30°-70°.

The highly siliceous nature of these sediments suggests deposition in a basin isolated from significant inputs of clastic material, a situation most often associated with deep sea pelagic environments. However, similar environments can be created closer to land masses by the presence of significant seafloor topography which results in small isolated basins shielded from terrigenous inputs.

3.12 Rumi Cruz Formation (E_{RC}) (Hughes and Bermúdez, 1997, see also Egüez, 1986)

3.12.1 Distribution

The Formation is restricted in outcrop to the trigonometric point at Los Reales [7770-00120] to the east of the road between Calacalí and Infiernillo.

3.12.2 Age

The age of this unit, whose type section is to the south of the village of Apagua [7307-98932], is assumed to be of Late Eocene age because of its stratigraphical position above the Unacota Limestone of Middle to Late Eocene age (Hughes and Bermúdez, 1997). An Eocene age was determined for a sample collected at Los Reales based on the presence of the foraminifera *Epistomina eocenica* (Wilkinson 1998a, Appendix 2).

3.12.3 Facies

The sequence at Los Reales consists of coarse conglomerates unconformably overlying rocks of the Yunguilla Unit. The conglomerates contain clasts of grey-green volcanics, black and green mudstones and clasts of vein quartz. Hughes and Bermúdez (1997) have interpreted the deposits of the type area as reflecting deposition in a fan-delta environment, with mature clast material from fluvial/alluvial systems being redeposited by mass flow mechanism as laterally extensive sheets in relatively shallow water.

3.13 El Laurel Unit (E_L) (Van Thournout, 1991)

3.13.1 Distribution

This unit occurs in the northeast sector of the current study area, adjacent to the Colombian border [8250-00991]. It consists of fine-grained deposits, predominantly black shales with occasional siltstone and fine-grained sandstone intercalations. Limestones occur towards the top of the sequence and these are quarried at Selva Alegre and Hualchán [8092-00856]. The unit outcrops principally in two, fault bounded, NE-SW trending lenses which extend southwards 20 km from the Colombian border. A few isolated and much smaller lenses occur further SW along strike for example at [8039-00822].

3.13.2 Age

Van Thournout (op. cit.) assigns the El Laurel Unit an Eocene age which is followed here based largely on the ages of limestones present towards the top of the sequence. The limestones at Selva Alegre [7741-00313] were correlated by Baldock (1982) with the Unacota Formation and, thus by association, are Eocene in age, while the limestones around Hualchán [8092-00856] have yielded faunas interpreted as being of Middle Eocene to Lower Miocene (Durán, 1983), Middle Eocene to Upper Oligocene (Wernli, 1986) and Lower Oligocene to Lower Miocene (Butterlin, 1987).

3.13.3 Facies

The El Laurel Unit consists predominantly of a very uniform sequence of thin bedded, black to grey-coloured mudstones with occasional sandstone beds. The most complete sequence is seen on the road from Tufiño to Maldonado, which passes the caserío of El Laurel [8280-00925]. This section, which cuts through the two principal lenses of the El Laurel Unit, is dominated by thin bedded mudstones, locally with a "sooty" appearance. The sequence includes characteristic blue-grey coloured sandstone beds on the 1-5 cm scale, which together with the absence of cherts and lack of folding helps differentiate this unit in the field from the older black mudstone sequence of the Yunguilla Unit.

Access to the quarry at Hualchán [8091-00855] could not be obtained during the present study but Van Thournout (1991) describes the limestones as consisting of 50 m of biomicrites, showing biohermic characteristics and containing corals, gastropods and bivalves. The sequence at Selva Alegre comprises 150 m of limestones, intercalated with sandstones and shales, which have been largely recrystallised by the contact metamorphic effects of the Apuela Batholith and where in places small sulphide-bearing skarn horizons are seen.

The correlation of the Hualchán and Selva Alegre limestones with the Unacota Limestone suggests that the El Laurel unit is in part time equivalent to the Angamarca Group of Hughes and Bermúdez (1997) who report the occurrence of dark grey, thin bedded, sheared, siliceous silty mudstone and mudstone turbidites from the Apagua Formation which has also yielded a Middle to Late Eocene fauna (Egüez and Bourgois, 1986). These sediments are interpreted to represent deposition on the lower parts of a submarine fan, and the absence of coarser material in the El Laurel Unit may reflect a more distal position on the fan than of the age-equivalent sediments seen further south.

3.14 Silante Unit (EO_{Sl}) (DGGM, 1978)

3.14.1 Distribution

The sedimentary sequence of the Silante Unit occurs in a N-S belt bounded to the east by rocks of the Pallatanga, Natividad and Yunguilla Units and to the west by the Pilatón Unit. The unit extends from the southern boundary of the map northwards to the Río Mira. The principal section is seen on the Calacalí-Nanegalito road [7683-00856], while other sections were mapped on the roads to the north of Loma La Liberia [7730-00115, 7723-00089] and in the Río Mira at Tercer Paso [8147-00738].

3.14.2 Age

Two mudstone samples from the current map area have yielded age diagnostic foraminifera faunas for the Silante, a unit whose age was previously poorly constrained. One sample contained the forams *Bulimina secaensis*, *Globigerina angiporoides*, *Globorotalia munda*, a fauna which indicates the sample is no older than Middle or Late Eocene, and may in fact be early Oligocene in age. The second sample yielded a single specimen of *Neouvigerina chirana*, a species reported from Eocene-age rocks in both Ecuador and Perú (Wilkinson, 1998b, Appendix 2).

3.14.3 Facies

Hughes and Bermúdez (1997) report that the exposures between Calacalí and Nanegalito are more continuous and fresher than those in the type area which lies just south of the current map area [Quebrada Bomboli 7570-9950] and the following description of this section is taken from their report. They noted that three components of the sequence can be mapped in the section. To the east, at the contact with the Yunguilla Unit [7683-00009], is a sequence of unsorted, chaotic, matrix-supported breccias and conglomerates consisting of mainly feldspar-phyric igneous clasts in a feldspathic sandy matrix. Further west the middle component is a red bed sequence, consisting of red-brown siltstones, fine-grained sandstones and breccias, with probable pedogenic carbonate caliches at least at one horizon. The third component, which makes up most of the sequence, consists of "typical" Silante sandstones and comprises mostly lithic-rich quartz arenites which often contain abundant ferromagnesian minerals (pyroxenes and amphiboles) and magnetite-rich, probable placer horizons.

Within the sandstone-dominated unit along the Calacalí-Nanegalito road at [7646-00038] there is a 3 m sequence of yellow-buff coloured, parallel-laminated claystones containing well-preserved angiosperm leaves. These beds may be lacustrine, but are clearly of terrestrial origin. Along the same road at [7615-00029], tuffaceous sandstones containing flattened lithic clasts indicate contemporaneous, probably subaerial explosive volcanism.

The sequence exposed on the Otavalo-Selva Alegre road [7833-00302] shows a transition from a sequence of well bedded, fine grained sandstones, purple mudstones and conglomerates in the east into tuffs and volcanoclastic sandstones, rich in clasts of plagioclase phyric lavas, further west. The sequence is in faulted contact with both the Yunguilla to the east and the Pilatón to the west, the Silante Unit being highly tectonised towards these contacts.

A sequence of conglomerates in faulted contact with pillow basalts of the Pallatanga Unit and containing clasts of cherts, plagioclase-phyric lavas and "rocas verdes" is exposed by the bridge crossing the Río Mira at Tercer Paso [8147-00738]. These conglomerates were interpreted by Van Thournout (1991) as part of the Chota Formation, however, because of their more indurated nature and their oxidised matrix they are here considered to be part of the Silante Unit.

The depositional environment of the Silante Unit is characterised by Hughes and Bermúdez (1997), whose evidence of pedogenic horizons, extensive red bed development and the preservation of angiosperm leaf fossils within laminated lacustrine sediments are indicators of non-marine, continental sedimentation. However, the presence of foraminifera (see earlier) indicates that at least part of the Silante Unit was deposited in a brackish/estuarine or possibly fully marine environment. The high percentage of mass-flow deposits within the sequence may indicate deposition within alluvial fans, a sedimentary environment commonly associated with active, fault bounded valleys, such as those associated with the San Andreas fault in California. The Silante Unit contains numerous volcanic clasts of predominantly feldsparphyric andesites, and euhedral grains of feldspars, pyroxenes and amphiboles are common in the sediment matrix (Plate 9). The supposedly intercalated lavas of the "Tandapi Unit" (Kehrer and Van der Kaaden, 1979; Egüez, 1986) are calc-alkaline in composition and presumably were derived from the same source as the volcanic material in the sediments.

Plate 9. Conglomerates of the Silante Unit exposed in the Río Nieto [7720-00233]

3.15 Tortugo Unit (E_{To}) (Boland et al., 2000)

3.15.1 Distribution

This new unit of sedimentary rocks occurs to the west of the Toachi fault and outcrops have been recorded from the Río Guayllabamba and as far north as the Salinas-Lita road. The unit is defined from the area around the confluence of the ríos Tortugo and Cajones with the Río Guayllabamba [7272-00255], but also outcrops extensively in a number of river valleys which drain south into the Guayllabamba such as the Mandariyacu [7345-99322], the Verde Chico [7403-00314] and the Naranjal [7253-00289]. Further north the principal section through the unit is seen in the Río Lita, alongside the path that runs between Lita and the caserío of Cristal [7865-00816].

Along its eastern margin the Tortugo Unit is in faulted contact along the Toachi fault with the Mulaute Unit in the south and the Pilatón Unit further north. The Tortugo rocks overlie the Naranjal Unit with an apparent sedimentary contact, a window of Naranjal basement being exposed through this overlying cover in the Río Verde area, and the Tortugo Unit is in turn overlain by the San Juan de Lachas Unit. Finally, the unit limits the outcrop of the La Cubera Unit, both to the east and west, suggesting a possible thrust faulted relationship between the two sequences.

3.15.2 Age

A Middle to Late Eocene (50-35 Ma) age for the Tortugo Unit is indicated by planktonic foraminifera *Globigerinatheka index* and *Globigerina eocaenica*, together with the benthonics *Asterigerinoides crassaformis*, "*Anomalina*" *chirana* and *Lenticulina caroliniana* collected from the Tortugo Unit exposed in the Río Guayllabamba [7275-00236] (Wilkinson, 1998a, Appendix 2).

3.15.3 Facies

The outcrops in the Río Guayllabamba and its north-bank tributaries comprise massive coarse to medium grained sandstones, in places grain supported, with intercalated grey siltstones and mudstones up to 1 m in thickness. The grey-green coloured sediments are silicified. In thin section the sediments are rich in subrounded to subangular feldspars. Lithoclasts consist mainly of rhyolitic lavas showing flow banded textures of feldspar laths. Fragments of augite and amphibole are present but the rock composition is dominated by saussuritised feldspar grains and variable amounts of chlorite and epidote are present in the rock matrix.

A similar sequence exposed in the Río Lita, where it is crossed by the path from Lita to Cristal [7865-00816], comprises massive, silicified, light grey-coloured sandstones and interbedded siltstones containing rounded clasts of purple and green lavas. In the rivers Toctemi [7893-00794] and San Francisco [7842-00748] these sandstones are overlain by less silicified, amphibole rich sandstones of the San Juan de Lachas Unit.

The association of green-coloured, coarse grained, grain supported sandstones with mudstones up to 1 m in thickness suggests deposition in a marine environment, probably from gravity flows but also possibly in a deltaic environment. Petrographically the sediments indicate derivation from an active volcanic source, with fresh flow banded feldspar phyric lavas dominating the clast population and angular grains of feldspar, pyroxene and amphibole occurring in the sandstone matrix.

3.16 Zapallo Unit (E_Z) (Boland et al., 2000, see Bristow and Hoffstetter, 1977)

3.16.1 Distribution

This unit occurs in the west of the map area and marks the western limit of the Cretaceous age basement. The Zapallo Unit consists of the previously defined Zapallo and Santiago Formations. These are included in a single unit in this study because the two formations form a single prominent feature, seen in both the satellite images and aerial photographs, which was used to extrapolate the boundaries both northwards and southwards away from the area where the unit had been mapped. However, a boundary between the two formations could not be seen in the satellite images/aerial photographs, nor could the previously reported unconformity between the Zapallo and Santiago Formations (Bristow and Hoffstetter, 1977) be proven in the field.

The best sections through the unit were seen in a number of quebradas crossed by the path accessing the Río Bravo [7314-00678], and also the exposures seen further north along the Río San Miguel [7456-00733].

3.16.2 Age

The Zapallo Formation was defined by oil company geologists working on the Borbón Basin in the 1940’s and the information on the unit is summarised in the Stratigraphic Lexicon (Bristow and Hoffstetter, 1977). The unit contains an abundant microfauna, rich in foraminifera, which yield a consistent upper Middle Eocene to lower Upper Eocene age. The same work in the 1940s defined a formation termed the Santiago Formation, again described in the Stratigraphic Lexicon, which consists of a basal conglomeratic unit passing up into limestones and calcareous sandstone. The age of this formation was determined as Middle to Upper Eocene. The age of the Zapallo Unit is therefore Middle to Upper Eocene.

3.16.3 Facies

The marine Zapallo Unit consists of a generally massive, gently to moderately dipping, basal conglomeratic unit which passes upwards through massive sandstones into a sequence of thin bedded mudstones to fine-grained sandstones. The conglomerates consist of rounded clasts, up to 30 cm in diameter, of a highly, vesicular red-brown coloured lava within a coarse-grained, green coloured arenaceous matrix. In thin section the clasts contain feldspar and pyroxene phenocrysts and chlorite filled vesicles and compositionally they are very similar to the lavas of the Naranjal Unit which are exposed in the Río San Miguel at [7432-00744]. The unconformable relationship between the Zapallo Unit and the underlying basement is best defined in the Río San Miguel [7446-00739] where a consistent relationship can be seen between exposures of lavas of the Naranjal Unit in the river passing upwards along the valley sides into massive conglomerates.

The conglomerates pass westwards into a sequence of massive sandstones, similar in composition to the matrix of the conglomerate, and then into a thick sequence of thin bedded, highly weathered, buff-coloured mudstones to siltstones, which form the prominent dip scarps seen on the aerial photographs.

3.17 San Juan de Lachas Unit (OM_{SJL}) (Salazar, 1981)

3.17.1 Distribution

The unit was first defined by Salazar (1981) and its extent was subsequently further defined by the work of Van Thournout (1991). The unit, which consists of breccias and intercalated lavas and sediments, occurs principally in the north of the current map area, with outcrops occurring both to the north and south of the Río Mira [8052-00846 to 7968]. An isolated outcrop has been identified further south near the Río Guayllabamba largely based on Oligocene-age fission track ages (Appendix 4) (see below). Good sections can be seen on the roads both to the north and south of the Río Mira between La Carolina and Parambas [7987-00906] and also in the Río San Francisco [7825-00778]. The boundary between the San Juan de Lachas and underlying units is exposed in the paths between La Carolina and Urbina [8012-00836] and Cachaco and Getsemani [7943-00877] but elsewhere it has been largely mapped from aerial photographs.

3.17.2 Age

No fossil ages have been determined for this unit, but Van Thournout (1991) proposed an Oligocene age based on a single K-Ar determination of 32.6 Ma for a hornblende bearing dyke intruding a sequence of lavas and agglomerates of similar composition. Two samples collected during the present project of a hornblende-phyric unit, outcropping close to San Juan de Lachas [7948-00905, 8023-00875], yielded K-Ar ages of 36.3 ± 2 Ma and 19.8 ± 3.1 Ma respectively, while two samples of plagioclase-phyric crystal tuffs collected from the Río Guayllabamba [7319-00241, 7338-00253] yielded fission track ages of 23.5 ± 1.5 Ma and 24.5 ± 3.1 Ma (Appendix 4). Thus, the ages determined during the current project support an Oligocene to Early Miocene age range for the unit.

3.17.3 Facies

The San Juan de Lachas unit is characterised by massive, matrix-supported breccias with occasional interbeds of lavas and sandstones. The breccias contain subangular clasts of plagioclase-phyric, purple-red lavas in a greenish, feldspar-rich matrix [8075-00854]. The clasts, which are up to 5 cm in size, are generally andesitic in composition, with both feldspar and amphibole phenocrysts [see thin section M5-368] (Plate 10).

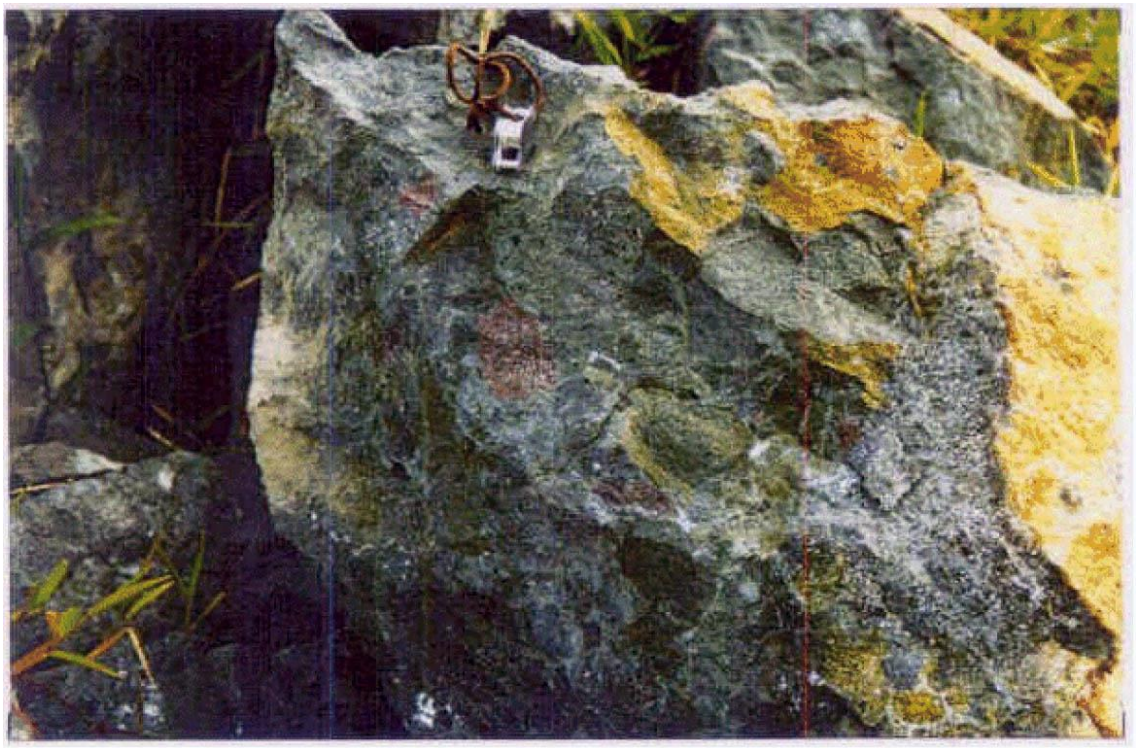

Plate 10. Feldspar-phyric rhyolitic clasts within breccias of the San Juan de Lachas Unit [8004-00907]

Interleaved plagioclase-phyric andesites are exposed along the Salinas-Lita road [7949-00905], and in thin section these consist of euhedral feldspars and aggregates of amphibole in a matrix of flow oriented feldspar laths. A few hundred metres further east along the road a hornblende-rich intrusive is exposed which has been dated at 36.23 ± 2.0 Ma. Although no clear cross-cutting relationship between the intrusive and country rock is seen, the compositional similarity between this and the lavas of the San Juan de Lachas Unit suggests that it is coeval and probably represents a high-level intrusive body. Van Thournout (1991) describes a much higher occurrence of hornblende rich andesitic lavas in the San Juan de Lachas area that were identified during the present study.

Siliceous sediments intercalated within the sequence are generally massive, and are compositionally identical to the matrix of the breccias. They consist of fine-grained quartz and chlorite and are often rich in calcite. The presence of rounded feldspar/amphibole rich clasts within the coarser clastic units [8010-00878] may suggest reworking.

The flat lying nature of the contact between the San Juan de Lachas and the underlying rocks is reflected in the topography, for example in the hill to the west of La Carolina [8052-00831]. This particular contact between the Pilatón and El Laurel units and overlying massive breccias of the San Juan de Lachas Unit is exposed along the path between La Carolina and Urbina [8045-00828].

The sequence exposed in the south near the Río Guayllabamba consists of purple-coloured, plagioclase phyric lavas and crystal tuffs with associated breccias and sandstones.

One sample, M5-334, from the San Juan de Lachas Unit was analysed for whole rock geochemistry (Appendix 3). The sample plots as being calc-alkaline in composition on the AFM diagram (Irvine and Baragar, 1971), and falls in the continental arc field on the Zr/Y versus Zr plot of Pearce (1983) and on the Zr-Th-Nb diagram of Wood (1980). This data supports the interpretation of Van Thournout (1991), who also correlated the San Juan de Lachas unit with the Tandapi lavas of Egüez (1986), thus suggesting that deposition of the Silante Unit was at least in part contemporaneous with this continental margin volcanism.

3.18 Playa Rica Formation (O_P) (Olsson, 1942)

3.18.1 Distribution

This formation, originally defined by Olsson (1942) occurs on the western edge of the map, its contact with the underlying Zapallo Unit being taken as the western limit of the study area. This contact has been mapped exclusively from the satellite imagery. Previous work reports that the unit lies unconformably on the Zapallo Unit and this is supported by an apparent overstepping relationship in the satellite imagery.

3.18.2 Age

The Formation is of Lower Oligocene to Lower Miocene age (Bristow and Hoffstetter, 1977).

3.18.3 Facies

Outcrops of flat lying, brown to black coloured shales, which correspond to previous descriptions of the Playa Rica Formation were seen along the Río Cayapas and Río San Miguel [e.g. 7332-00806], these localities have been used to fix the position of the boundary from the satellite image.

3.19 Chota Formation (M_{Ch}) (Bristow and Hoffstetter, 1977)

3.19.1 Distribution

The Chota Formation outcrops along the margins of the Chota River [8240-00550] and also as an outlier to the west of Estación Carchi [8185-00668], where exposures are seen on the Ibarra-San Lorenzo road. This Formation is described in the Stratigraphic Lexicon (Bristow and Hoffstetter, 1977) and also by Van Thournout (1991).

3.19.2 Age

Although a diagnostic fossil assemblage has not been reported from this Formation Van Thournout (op. cit.) assigns a Miocene age. Van Thournout also assigns the rocks outcropping to the west of Estación Carchi [8185-00668] to a unit he terms the Ponce Unit, which he interprets as representing the western continuation of the Chota Basin. In the present project however, these rocks are designated to the Chota Formation, to indicate their equivalence to the sequences to the east.

3.19.3 Facies

The principal section of this Formation is exposed on the Ibarra-San Lorenzo road [8185-00668 to 8173-00693] where a sequence of massive grey sandstones are in faulted contact with rocks of the Yunguilla Unit to the east. Van Thournout (op. cit.) reports unconformable contacts between the Chota Formation and the underlying “Cretaceous basement”, though these were not seen in the present study. Further west along the road the sequence is dominated by massive, matrix supported conglomerates with well-rounded clasts of shales, cherts and granitoids. Some of the granitoid clasts are weakly foliated. Intercalations of siltstone and claystone beds occur within the sequence.

The sequence, although bearing a superficial resemblance to the Silante, is distinguished on the basis of its less indurated matrix, different clast composition (presence of numerous granitoid clasts, absence of plagioclase phyric volcanic material) and absence of red-beds.

3.20 Miocene to Holocene deposits

Detailed mapping of the Miocene to Holocene volcanics which dominate the eastern part of the map area was carried out by Ing. Bernardo Beate. A description of these rocks, which include the major volcanic centres of Cayambe, Imbabura, Cuicocha and Pululahua (Plate 11), is given in Appendix 1.

Plate 11. Crater and dacitic domes of the Pululahua volcanic center in the distance with related ignimbrites flooring the valley in the middle and near ground

To the west of the area mapped by Ing. Beate little attempt has been made to subdivide the Quaternary deposits. The extent of these deposits has been mapped largely from aerial photographs and the compositional classes may have been assigned based on limited field observations.

3.20.1 Undifferentiated Quaternary volcanics

This classification includes all rocks of volcanic origin and apparently "young" age mapped in the western part of area. It includes dacitic and andesitic lavas, feldspar-phyric tuffs and volcanic ash and includes those deposits where no direct correlation has been possible with the detailed stratigraphy established for the volcanic sequences in the east.

3.20.2 Terrace and alluvial deposits

Holocene alluvium occurs along the courses of many river valleys and is the product of deposition from modern river systems. The term terrace deposits has been used where field observations show that a deposit has a mixed genetic origin, for example sediments deposited by both lahars and modern river systems. Extensive deposits of this type occur in association with the Río Guayllabamba and Río Apuela in the south of the map area and between the Río Mira and the Colombian border in the north.

A major alluvial deposit can be seen adjacent to San Miguel de Los Bancos [7345-00030], the deposit extending from 0.3°S northwards as far north as Cristobal Colón [7052-000508] where the alluvium marks the southern limit of the Cordillera Toisán. The terrace system represents the amalgamation of deposits related to several different rivers, including in the present map area the rivers Guayllabamba, Blanco and Jordán. The terrace deposits associated with one of these feeder rivers, the Río Apuela, are shown in Plate 12. The sediment carried by many of these rivers is sourced principally from the Quaternary volcanic centres located along the eastern margin of the Western Cordillera. Terrace deposits are reported as being up to 1000 m thick (BGS-CODIGEM, 1993).

Plate 12. 200 m thickness of stratified Terrace Deposits, Río Apuela

4. INTRUSIVE ROCKS

4.1 Santiago Batholith

The geological map of Ecuador (BGS-CODIGEM, 1993) shows two large batholiths occupying the western portion of the current map area. The batholiths were originally identified by the Belgian Mission, largely from aerial photographs, and were termed the Santiago and Cayapas batholiths after the river basins in which they occurred. The current field study has confirmed the existence of the Santiago Batholith and considerably refined the control on its extent. However, numerous traverses further to the south have shown that the Cayapas batholith does not exist in the form shown on the national geological map. Boulders of a hornblende-biotite granitoid, similar in composition to the Santiago Batholith, were found in the Río Tigre [7313-00633] suggesting that an intrusive of limited extent may exist in the headwaters of this river although this was never seen at outcrop.

The main Santiago Batholith forms a continuous intrusive body with an extent of approximately 30 km north-south and 10 km east-west, while a number of smaller related intrusions are seen in the Río Baboso [7839-00984] and at Cachaco [7912-00915]. The intrusion is medium to coarse-grained, granodioritic to tonalitic in composition, comprising quartz, K-feldspar, plagioclase, hornblende and biotite. The biotites show some replacement by chlorite. Hornfelsing of the country rock is seen adjacent to both the Baboso and Cachaco intrusions, the former intrude the Naranjal Unit and the latter the sediments of the Tortugo Unit.

Whole rock geochemical analysis has been carried out on three samples, two from the main Santiago Batholith and one from the related Cachaco pluton. On a plot of Rb versus Y+Nb the three samples plot in the volcanic arc field (Figure 27), while sample M5-441 plots in the calc-alkaline field on a Na_2O+K_2O vs. SiO_2 plot (Figure 28), and in the meta-aluminous field of Maniar and Piccoli (1989) (Figure 29). Calc-alkaline, meta-aluminous granitoids are normally associated with continental arcs. On a plot of Rb/Zr versus Nb, used by Brown et al. (1984) to distinguish arc maturity all the samples plot in the field of primitive island arcs and continental arcs. However, care must be used in interpreting this diagram as it was constructed for rocks with silica contents between weight 66-75%, while the Santiago Batholith and related bodies have SiO_2 contents of 54-59%.

Four samples from the main Santiago Batholith and one each from the related Baboso and Cachaco intrusions were dated by the K-Ar method (Appendix 4). The Santiago samples yielded a range of ages of 44.6 ± 2.2, 41.9 ± 2.1, 38.2 ± 1.9 and 35.8 ± 1.8, while the Baboso and Cachaco intrusions were dated respectively at 42.4 ± 2.1 and 34.7 ± 1.7 Ma. The K-Ar age derived for the Baboso intrusion is in good agreement with that of 42.3 ± 1.7 Ma previously published by Van Thournout (1991) and the range of ages, from Middle to Late Eocene, probably reflect the multiple phase nature of the intrusions, a suggestion that was first made by Van Thournout to explain the petrographical variations seen within the batholith.

In regional terms the Santiago Batholith and Baboso pluton appear to be older than the majority of I-type intrusives dated from further south in the Cordillera, for example the Río Hugshatambo granodiorite dated at 38.09 ± 0.39 Ma (Hughes and Bermúdez, 1997) or the 25.6 ± 0.3 Ma Echeandía granodiorite (McCourt et al., 1997) but are very similar in age to a suite of I-type granitoids mapped by McCourt et al. (1991) in SW Colombia.

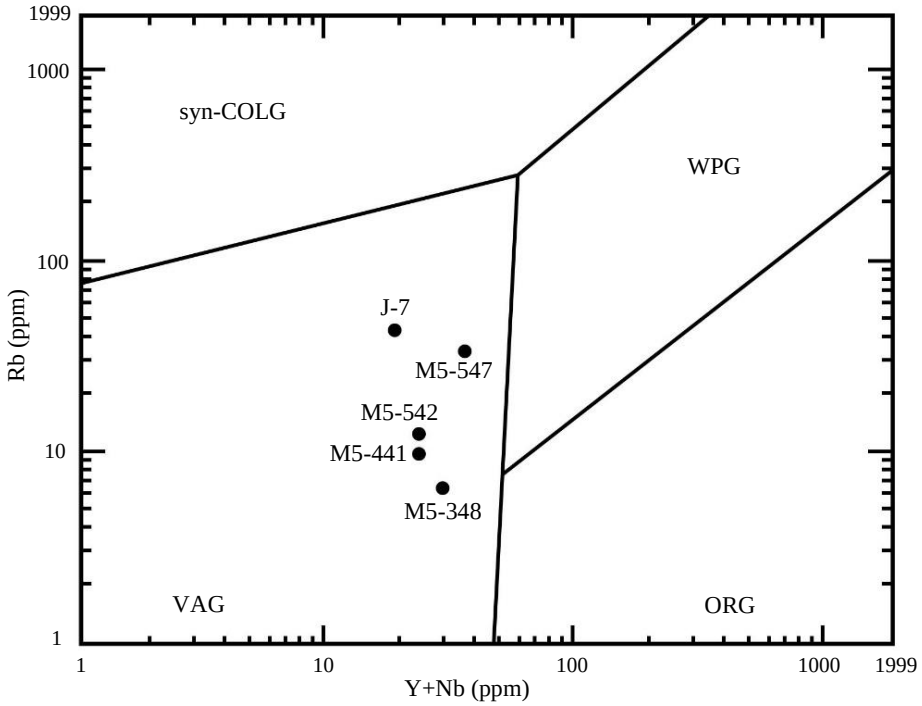

Figure 27. Plot of analyses of Santiago and Apuela granitoids on the tectonic environment discrimination diagram of Pearce et al. (1984)

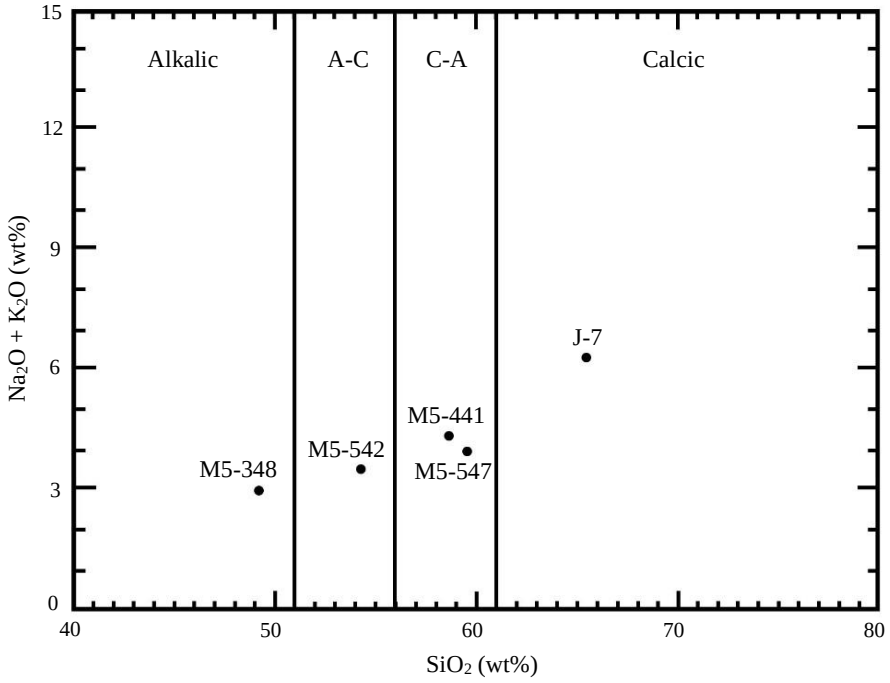

Figure 28. Plot of analyses of Santiago and Apuela granitoids on the granite discrimination diagram of Peacock (1931)

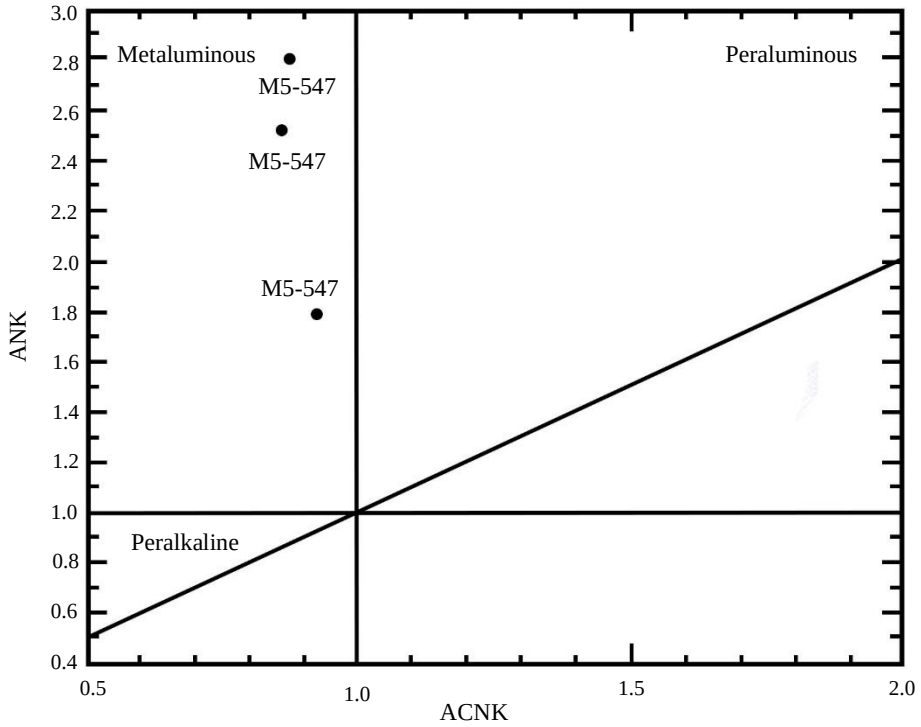

Figure 29. Plot of analyses of Santiago and Apuela granitoids on the granite discrimination diagram of Maniar and Piccoli (1989)

4.2 Apuela Batholith

The Apuela Batholith is a large N-S elongated intrusion, 50 km in length and 10-20 km wide, which crosscuts the Toachi, faults and intrudes the Mulaute and Pilatón Units in the east and the Naranjal Unit in the west. A number of smaller, probably associated intrusive bodies were also mapped, the largest of which is the La Merced intrusion. The Apuela Batholith is seen to contact metamorphose the Pilatón and Mulaute Units, with metamorphic biotites overgrowing shear-related cleavages in both units.

The main Apuela Batholith is a coarse to medium grained hornblende-biotite tonalite/quartz diorite. Augite and sphene are also reported from the intrusive. A sample from the main batholith yielded an age of 16.5 ± 1.1 Ma (Early Miocene) while the La Merced intrusive was dated at 15.6 ± 1.1 Ma (Middle Miocene). Similar ages have been reported from I-type granitoids further south in the Cordillera, for example the Río Quindigua intrusion dated at 14.8 ± 0.14 Ma (McCourt et al., 1997).

On the various discrimination diagrams plotted in Figures 27 to 29 the Apuela Batholith plots as a calcic, meta-aluminous, volcanic arc granitoid. On the arc maturity discrimination diagram of Brown et al. (1984) the sample plots towards the normal continental arc field.

4.3 Other intrusions

Two gabbroic intrusions were mapped within the Naranjal Unit; a small body exposed in the Río Naranjal [7277-00328] and a larger intrusion mapped to the southeast of the Río Canandé [7191-00523]. The former was dated by K-Ar at 47.2 ± 2.4 Ma (Appendix 4).

A weakly deformed hornblende diorite is exposed to the north of the Río Blanco, just south of San Miguel de Los Bancos. On petrographic grounds the intrusion appears to be similar to the foliated intrusion mapped immediately to the south of the present map area at Dos Ríos, the age of which has been used to determine the age of the Mulaute shear zone (Hughes and Bermúdez, 1997). However, the Río Blanco intrusion yielded a K-Ar age of 28.7 ± 3.2 Ma (Appendix 4), considerably younger than the 48.28 ± 0.55 Ma age of the foliated Dos Ríos body. The Río Blanco intrusion is epidotised and thus the age determined for the intrusion may be reset.

Along the Colombian border a porphyritic, biotite rich intrusive is exposed on the road between Chical and Maldonado [8147-01037]. The intrusive is heavily weathered and Van Thournout (1991) interpreted much of the alteration as representing a late-stage magmatic hydrothermal effect. K-Ar dating of the biotite and plagioclase phases yielded a Late Miocene age of 7.5 ± 0.4 Ma (Appendix 4).

5. STRUCTURE

5.1 Faulting

The boundaries between the main units are largely faulted with only those of the younger Eocene to Miocene units such as the San Juan de Lachas, Zapallo and Chota retaining original sedimentary contacts with the underlying units. The outcrop pattern of the main units is controlled by a series of major NE-SW striking faults. The faulted nature of contacts is often indicated by the broad zones of largely brittle deformation [e.g. at 7832-00286] where intense fracturing, in places associated with calcite veining, occurs within the Silante Unit up to 200 m from its contact with the Pallatanga. Cataclastic deformation results in the development of fault gouges and fault breccias along these contacts. A conjugate set of E-W trending faults occur which are marked in the field by highly tectonised zones cross-cutting the regional strike is also present.

Several of the regional fault systems identified further south in the cordillera, such as the Pallatanga Fault which marks the eastern structural limit of Western Cordillera (McCourt et al., 1997) can be traced onto the current map area. The Pallatanga Fault system which represents the southern extension of the Cali-Cauca-Patía Fault of Colombia (McCourt et al., 1984) occurs as the series of NE-SW trending faults exposed on the roads to Nanegalito and Yunguilla, west of Calacalí.

Further to the west boundary between the Mulaute Unit and the more westerly Cordilleran sequences is interpreted as reflecting the northward continuation of the Toachi-Toacazo Fault mapped to the south (Hughes and Bermúdez, 1997). The interpretation of a NE-SW trending fault along this contact is based largely on the existence of such a structure to the south, which marks the western limit of both the Mulaute Unit and the broad zone of ductile deformation within the Mulaute and Pilatón Units.

An E-W brittle fault lies along the Río Canandé marking the contact between the sediments of the Río Desgracia unit to the north and the igneous rocks of the Naranjal Unit. The fault is shown as part of the Sabaleta Fault on the 1:1000000 scale national tectonic map, and terminates to the east against the Esmeraldas Fault. The significance of this structure is still unclear, the igneous rocks seen to the north of the fault being interpreted in this study as being part of the Naranjal Unit. However, further geochemical investigations are needed to determine whether these igneous rocks are related to the sequences of supposed Piñón exposed at Tabuga on the Manabí coast (BGS-CODIGEM, 1993).

5.2 Shear zones

Two principal zones of ductile deformation have been identified in the current map area. The first represents the northern continuation of the Mulaute shear zone first identified by Hughes and Bermúdez (1997) from the area immediately to the south of the current map sheet. This zone, which strikes NE-SW, comprises a western “slate” belt up to 8 km wide of continuous penetrative cleavage development in generally fine-grained mudstones and siltstones of the Mulaute Unit. Stretching lineations are subhorizontal and kinematic indicators show a dominant dextral displacement sense. Further east in the coarser grained sediments of the eastern half of the Mulaute and Pilatón Units ductile deformation tends to be concentrated in discrete zones which are separated by undeformed country rock. Nevertheless, penetrative cleavages, which are in places mylonitic, are present throughout the Pilatón Unit and in the extreme east adjacent to the contact with the Silante Unit a 1 km wide zone is exposed to the north of the Río Guayllabamba [7688-00192]. Assuming that this shear zone relates to the same deformational episode that produced the Mulaute shear zone then penetrative cleavage development occurs over a cross strike width of 25 km.

Hughes and Bermúdez (1997) report a 48.28 ± 0.55 Ma K-Ar age for a hornblende mineral separate from a syntectonic foliated diorite, the Dos Ríos intrusion, which intrudes into the Mulaute shear zone to the south. This age is thus interpreted as representing the age of deformation. No deformed intrusives were seen in the current map area, however the shear zone fabric is overgrown by biotites, which are interpreted as being related to contact metamorphism by the Apuela Batholith, which was intruded at 16.5 ± 1.1 Ma.

North of the Río Guayllabamba the Mulaute shear zone is cut by the Apuela Batholith, and the main "slate belt" zone cannot be traced north of this. Only a few restricted outcrops of the Mulaute Unit occur north of the batholith, with the units seen to the west of the Toachi Fault further south being in contact with Pilatón Unit rather than Mulaute north of the Apuela intrusion. Penetrative shear fabrics are seen within the Pilatón Unit and in places weak dextral S-C fabrics are developed [8111-00794].

The absence, north of the Apuela Batholith, of both the Mulaute Unit and the broad zone of deformation associated with its contact with the terrane to the west is problematic. The position of the boundary between the Pilatón Unit and western terrane seen to the north of the Apuela intrusion corresponds to the contact between the Pilatón and Mulaute units further south. The eastward step in this contact could reflect either an original feature of the terrane collision or a subsequent modification. The absence of major ductile deformation at the terrane contact to the north suggests that this may not be the original collision zone and that the Mulaute Unit and related deformation may have been cut out by subsequent strike-slip movement.

The Naranjal shear zone [7370-00443] is a previously unknown structure, which deforms the igneous rocks of the Naranjal unit. The type section of the shear zone is seen in the northeastern reaches of the Río Naranjal and the zone was also traversed to the north in the rivers Bravo [7463-00545] and Barbudo [7562-00614]. The zone is associated with the occurrence of amphibole rich lithologies within the Naranjal Unit and these rocks can be traced as far north as the Río Conejales [7708-00605] where they are undeformed. A penetrative, in places "slaty" cleavage is developed within these igneous rocks indicating high levels of strain. The strike of the Naranjal shear zone, which is up to 2 km wide, changes strike from NE-SW along the Río Naranjal to E-W north of the Apuela Batholith. The zone was not seen within the rocks of the Naranjal Unit exposed in the Salinas-Lita road, however a penetrative cleavage defined by amphibole laths is present within samples collected from a raft/roof pendant within the undeformed Santiago Batholith. These rocks may represent a deeper level in the shear zone preserved within the batholith but clearly show that the shear zone predates the emplacement of the Santiago Batholith, the oldest radiometric age for which is 44 Ma.

In the Río Naranjal cleavage development is not pervasive throughout the sequence but rather occurs in discrete zones up to tens of metres wide which pass laterally into undeformed country rock. Cleavage strike varies from N-S to NE-SW suggesting an anastomosing set of zones and cleavage rotation from the margins to the highest strain parts of the zones indicates a dextral movement sense. Stretching lineations were not seen within the fabric. In thin section the protolith consists of euhedral amphibole grains, up to 3 mm in size, within a matrix of finer grained amphibole laths. The amphiboles are actinolites but whether these are replacements after original amphiboles or other is unclear. Deformation results in this mineralogy being progressively replaced by chlorite and calcite, with the strongest cleavage being defined by chlorite layers, with anastomosing iron-rich seams, and augening elongate calcite lenses.

The northward continuation of the zone can be seen in the rivers Bravo and Barbudo, the zone of deformation having a cross zone width of 2 km in the Río Bravo. In both sections the zone is seen to be bounded by undeformed lavas interpreted as being part of the Naranjal Unit and thus the shear zone does not appear to represent a terrane boundary. A sample collected from the Río Barbudo (M5-908a) [7575-00609] displays the most penetrative cleavage seen from the zone, with secondary extensional crenulation cleavages offsetting the slaty cleavage, and mica and chlorite fish being developed within the cleavage.

The shear zone strike swings to an E-W orientation north of the Apuela Batholith, but although the distinctive amphibole-rich lavas associated with the zone were seen further east in the Río Conejales [7698-00608], these rocks were undeformed. However, a penetrative cleavage was seen in lavas within a raft of the Santiago Batholith, exposures which lie northeast along strike from the zone seen in the Río Naranjal. The cleavage in the roof pendant is defined by fresh, acicular amphiboles of actinolite-hornblende composition and brown biotites, the cleavage augening euhedral feldspars. The fabric reflects deformation under higher P-T conditions than seen elsewhere and may represent a deeper level of the shear zone, which has been brought up with the intrusion. Whether the shear zone consists of a single zone or splays into E-W and NW-SE striking zones north of the Apuela Batholith is unclear.

5.3 Folding

Mesoscopic folds are conspicuous by their absence but at outcrop-scale the Yunguilla is folded by chevron folds with upright axial planes and shallowly inclined axes [8184-00656] (Plate 6). Variations in bedding dip suggest the presence of larger scale folds, however the lack of consistent broad scale dip patterns, together with the probable local influence of fault drag means that large scale fold axes were not defined in the current study area.

6. MINERALISATION

Mineral exploitation in the current map area is largely limited to working of alluvial gold and platinum in the rivers, which drain the western margin of the Cordillera del Toisán and into the coastal plain. These placer deposits were first described by Wolf (1879) and in the current map area workings have been reported from the Santiago, Cayapas, Bravo and Tigre rivers. Currently alluvial deposits are being worked commercially near Playa de Oro [7460-00970] on the Río Santiago.

Mosquero (1949) reported metal contents from the Río Santiago of gold at 0.8-3.31 g/m^3 and platinum at 0.06 g/m^3 and from the Río Mira of gold 0.89-4.15 g/m^3 and platinum 0.02-0.17 g/m^3. Beddoe-Stephens (1987) analysed platinoids collected from the Río Camumbi which lies just to the west of the current map area, and concluded that their composition indicated source rocks of a mafic-ultramafic composition belonging to an ophiolitic suite. Based on the gold-silver ratios of the alluvial gold Van Thournout (1991) concluded that the detrital gold was derived from two different sources; silver-rich gold being indicative of a low temperature, epithermal environment while the silver-poor, copper-rich gold is indicative of higher temperature deposition, possibly associated with intrusion related metasomatism in an oceanic environment.

Alluvial gold has also been worked in the Río Chirapi, near to Pacto [7480-00158]. Gold, hosted in quartz veins cutting the Pilatón Unit, has also until recently been worked in the Pacto area and a number of adits into this vein system remain [7471-00131].

A number of mineral prospects were identified during the 1980's by a Belgian Mission working in conjunction with INEMIN, and these are described in the project report (INEMIN, 1990). Two of these prospects, Junín and Río Verde, have subsequently been further investigated by mining companies though neither have reached production.

The Junín prospects [7610-00360] is a porphyry copper-molybdenum system hosted within the Apuela Batholith. Boreholes drilled into the main part of the system intersected four principal alteration zones, with a potassic zone at the centre passing outwards through a silicic and propylitic zone to an argillic zone at the margins (JICA, 1998). Primary mineral assemblages include pyrite, chalcopyrite, bornite, molybdenite, sulphosalts and hematite, while secondary minerals include chalcocite, covellite, cuprite, native copper, chrysocolla and limonite. A borehole in the most intensely mineralised zone has proven mineralisation to a depth of more than 150 m. Grades range up to 3.84% Cu and average 1.3% Cu over an intersection of 140.8 m which is open at depth. Another mineralised zone yielded grades of up to 2.1% and averaged 0.46% between depths of 6 m and 233.5 m.

At the El Corazón prospect [7410-00285] two zones of sheeted vein gold mineralisation have been identified. These are hosted in andesitic and pyroclastic rocks, which were mapped in the current project as part of the Naranjal Unit. The first zone occurs along the Río Verde Chico and is characterised by a series of northeast trending parallel structures which can be traced over 1 km along strike. Boreholes in this zone have yielded intercepts of up to 52.5 metres of 1.3 g/t gold. The second zone, termed Tres X, occurs 1.2 km north of the Río Verde Chico and is a sheeted vein gold mineralisation system identified over an area of 1100 m × 600 m. Drill intercepts of 67.0 m at 2.7 g/t gold have been reported. The owners of the prospect report a proven resource of 350000 ounces of gold for the two zones.

Of the other mineral occurrences identified by the Belgian Mission only that at Parambas [7980-00850] was considered to have possible economic potential. Parambas is an epithermal deposit of Cu-Pb-Zn-Ag-Au, consisting of sporadic veins within a zone of propylitic, and locally silicic, alteration. The mineralisation is possibly related to the volcanic activity associated with the San Juan de Lachas Unit.

7. NON-METALLIC MINERALS

Non-metallic minerals are worked throughout the area, mainly to supply local demand for construction materials. Of the larger scale operations, the most important is at Selva Alegre [7741-00313], where limestone present towards the top of the El Laurel Unit is worked to supply the cement industry. There are numerous large quarries within the Quaternary volcanics north of San Antonio de Pichincha, which supply building materials to the Quito construction industry. The limestones of the El Laurel Unit are worked on a smaller scale at Hualchán [8092-00856], the material from here being used as ornamental stone. Quarries for roadstone are seen within the Pilatón and Naranjal Units along the Salinas-Lita road and also in the La Cubera Unit to the west of Diez de Agosto [7080-00125].

8. GEOLOGICAL HISTORY

The oldest rocks in the study are the oceanic basalts of the Pallatanga Unit of Santonian (or possibly older) age and which are interpreted as representing part of a fragmented ocean floor or ocean plateau, and may correlate with the similar age ocean plateau basalts in Colombia (Kerr et al., 1997). The accretion of the Pallatanga Unit to the continental margin of South America occurred in the Late Cretaceous, probably in the Campanian. Aspden et al. (1992) reported widespread resetting of isotopic ages in the Cordillera Real between 85-65 Ma, and a similar event was also reported from the Central Cordillera or Colombia by McCourt et al. (1984). Both authors related this event to the accretion of the Western Cordillera terrane, which corresponds to the Pallatanga Unit in Ecuador, the Grupo Diabásico in Colombia and related oceanic rocks in Panama. Further evidence of the probable Campanian-age of the accretion is the unconformity that exists between the Albian-Santonian (?Early Campanian) age Napo Formation in the Ecuadorian Oriente and the overlying Maastrichtian-age Tena Formation (Baldock, 1982). It was proposed that the unconformity related to a period of uplift in the Campanian (83-74 Ma) caused by accretion of the Western Cordillera terrane to the Cordillera Real along a suture now represented by the regional Cali-Patía-Calacalí-Pallatanga Fault system (Aspden et al., 1992). During the Late Campanian-Maastrichtian deposition of the Tena Formation and Yunguilla Unit occurred in contrasting continental and marine environments on either side of the Cordillera Real, the marine Yunguilla Unit in the west being floored by the accreted Pallatanga oceanic terrane.

The Senonian-age volcanosedimentary rocks of the Mulaute and Pilatón Units, which are interpreted as being floored, by rocks of the Pallatanga Unit, were also probably accreted during the same event. The source of both these units remains problematic and further investigation, including more precise palaeontological data, is required. Foraminifera ages determined during the present study suggest that the Mulaute and Pilatón Units are contemporaneous with the continental volcanic arc of the Río Cala Unit, which also sourced the Campanian age sediments of the Natividad Unit. The present structural configuration however of these units has the coarse grained breccias of the Mulaute and Pilatón Units lying to the west of, and thus further from the Río Cala unit, than the fine-grained distal turbidites of the Natividad Unit.

Contemporaneous with the accretion of the Pallatanga Unit, the intraoceanic Naranjal arc developed to the west and the related marine sedimentary sequences of the Colorado and Río Desgracia units were deposited. Initiation of the arc may reflect changes in plate movement related to accretion of the Pallatanga Unit and thus provides further support for a Campanian age of this event.

The accretion of the Naranjal arc and its associated sedimentary sequences onto the continental edge probably took place in the Eocene. The upper limit for the age of accretion of the "Naranjal terrane" is constrained by the presence of a suite of undeformed I-type granitoids, which intrude the Naranjal Unit. One of these intrusions, the Santiago Batholith, also contains a raft/roof pendant of deformed Naranjal Unit. The K-Ar mineral ages obtained from these granitoids range from 44-35 Ma and therefore indicate a minimum age for the accretion of late Middle Eocene.

The lower limit for the accretion of the Naranjal Unit is less well-constrained. However, the cherts of the La Cubera Unit suggest that a sediment starved basin existed between the Naranjal arc and the continental margin during the Late Paleocene-age (60.5-56.5 Ma), with the accretion of the Naranjal terrane being marked by a change in the Middle-Late Eocene to deposition of the Tortugo Unit with its input of volcanic material. Thus, an Early Eocene age (55-50 Ma) for the accretion of the Naranjal terrane seems probable. The accretion resulted in the ductile, generally dextral, deformation seen in the Mulaute and Pilatón Units.

The accretion of the Naranjal Unit, and of the Macuchi Unit further to the south, probably occurred in the same event, an interpretation supported by the fact that the Mulaute shear zone separates the "Pallatanga terrane" in the east from both the Macuchi and Naranjal arcs to the west. An early Middle Eocene age for accretion of the Macuchi is supported by a single K-Ar hornblende age of 48 Ma from a foliated diorite intrusion in the Mulaute shear zone (Hughes and Bermúdez, 1997) however Dunkley and Gaibor (1997) favour a latest Eocene, 40-38 Ma, age for this event.

Sedimentation on the continental edge during the Eocene was represented by the Rumi Cruz and Silante Units and their probable lateral equivalent, the marine deposits of the El Laurel Unit. Further west the Eocene marine sequences of the Tortugo and Zapallo Units were deposited in the area floored by the Naranjal terrane.

The occurrence of calc-alkaline lavas towards the top of the Silante Unit, the "Tandapi beds" of Egüez (1986), and the presence of a high volcanic input within the sedimentary succession suggest that deposition within the Silante basin was contemporaneous with continental margin volcanism. This volcanism activity probably relates to the calc-alkaline arc which developed along the continental margin following the accretion of the "Naranjal terrane", the deeper levels of which are seen in the I-type intrusions of the Santiago Batholith and related bodies which range in age from 44-35 Ma. The Oligocene to Early Miocene lavas of the San Juan de Lachas Unit may represent the extrusive component of this arc. In regional terms this arc appears to correspond in part to the 42-22 Ma (Late Eocene-Middle Miocene) Saraguro event seen south of 2°S in the Western Cordillera (Dunkley and Gaibor, 1997; Steinmann, 1997). The increasingly older ages of the I-type granitoids northwards within the cordillera suggest an earlier initiation of plutonism in the north.

The breakup of the Farallón plate into the Nazca and Cocos plates occurred around 22 Ma (Pilger, 1983), this reorientation of plate movements was marked in the south of the cordillera by a break in volcanic activity and major uplift and deformation of the Saraguro Group (Pratt et al., 1997). However, events related to this change are not clear in the present study area. During the Miocene-Pliocene the Western Cordillera was the site of extensive sub-aerial, acid-intermediate volcanism, the products of which have been mapped in the cordillera as the Zumbagua Group. In the present study area, the intrusion of the I-type Apuela Batholith and related bodies occurred in the Early to Mid-Miocene, the main intrusive being dated at 16.5 ± 1.1 Ma, while Mio-Pliocene volcanics have been mapped as the Angochagua and Pugarán volcanics; extensive Pliocene to Holocene acid volcanism is reflected in the numerous volcanic centres seen in the cordillera.

9. BIBLIOGRAPHY

AGUIRRE L. and ATHERTON M. P. (1987) Low-grade metamorphism and geotectonic setting of the Macuchi Formation, Western Cordillera of Ecuador. *Journal of Metamorphic Geology*, 5, 473-494.

ASPDEN J. A., HARRISON S. M. and RUNDLE C. C. (1992) New geochronological control for the tectono-magmatic evolution of the metamorphic basement. Cordillera Real and El Oro Province of Ecuador. *Journal of South American Earth Sciences,* Vol. 6, 77-96.

BALDOCK J. W. (1982) Geología del Ecuador. Boletín de la Explicación del Mapa Geológico (1:1000000) de la República del Ecuador. Ministerio de Recursos Naturales y Energéticos. Quito, 54 pp.

BALDOCK J. W. y LONGO R. (1982) Mapa Geológico Nacional de la República del Ecuador, escala 1:1000000. Dirección General de Geología y Minas (DGGM). Quito-Institute of Geological Sciences (IGS) London.

BEDDOE-STEPHENS B. (1987) A pilot examination of alluvial and in situ gold and platinum from Ecuador. *British Geological Survey Mineralogy and Petrology Research Group, Report No.* 87/3.

BOLAND M. P., PILATASIG L. F., IBADANGO C. E., McCOURT W. J., ASPDEN J. A., HUGHES R. A. and BEATE B. (2000) Informe No. 10, Proyecto de Desarrollo Minero y Control Ambiental, Programa de Información Cartográfica y Geológica: Geology of the Western Cordillera between 0°-1°N. CODIGEM-BGS, Quito.

BRISTOW C. R. (1981) An annotated bibliography of Ecuadorian geology. *Overseas Geology and Mineral Resources, Institute of Geological Sciences,* No. 58, London.

BRISTOW C. R. and HOFFSTETTER R. (1977) *Lexique Stratigraphique International.* (2nd Edition). Centre National de la Recherche Scientifique, Paris.

BRITISH GEOLOGICAL SURVEY and CORPORACIÓN DE DESARROLLO E INVESTIGACIÓN GEOLÓGICO MINERO Y METALÚRGICA (1993) National geological map of Ecuador, scale 1:1000000. (Keyworth, Nottingham; BGS, and Quito; CODIGEM).

BRITISH GEOLOGICAL SURVEY and CORPORACIÓN DE DESARROLLO E INVESTIGACIÓN GEOLÓGICO MINERO Y METALÚRGICA (1994a, b) Geological and metal occurrence maps of the Cordillera Real and El Oro metamorphic belt Ecuador. 1:500000 scale.

BROWN G. C., THORPE R. S. and WEBB P. C. (1984) The geochemical characteristics of granitoids in contrasting arcs and comments on magma sources. *Journal Geological Society London,* 141, 413-426.

COSMA L., LAPIERRE H., JAILLARD E., LAUBACHER G., BOSCH D., DESMET A., MAMBERTI M. et GABRIELE P. (1998) Pétrographie et géochimie de la Cordillère Occidentale du Nord de l'Equateur (0°30'S): implications tectoniques. *Bull. Soc. Geol. Fr.* 169, 739-751.

COX K. G., BELL J. D. and PANKHURST R. J. (1979) The interpretation of igneous rocks, London. Allen and Unwin, 450 pp.

DIRECCIÓN GENERAL DE GEOLOGÍA Y MINAS (1978) Mapa geológico del Ecuador, Machachi, Hoja 66 (1:100000). (Quito).

DIRECCIÓN GENERAL DE GEOLOGÍA Y MINAS (1980) Mapa metalogénico del Ecuador, escala 1:1000000 (Paladines A. and Sanmartín H.) Quito, Ecuador.

EGÜEZ A. (1986) Evolution Cénozoïque de la Cordillère Occidentale Septentrionale d'Equateur (0°15'S o 1°10'S). Les minéralisations associées. Unpublished Ph.D. Thesis ; Université Pierre et Marie Curie, Paris. 116p.

EGÜEZ A. y BOURGOIS J. (1986) La Formación Apagua, edad y posición estructural en la Cordillera Occidental del Ecuador. Memoria Cuarto Congreso Ecuatoriano de Geología, Minas y Petróleos. **Tomo 1,** 161-178, Quito.

FAUCHER B., JOYES R., MAGNE F., SIGAL J., VERNET R., GRANJA V. J., GRANJA B. J. C., CASTRO R. y GUEVARA G. (1968) Informe geológico sobre las posibilidades petroleras de las provincias costeras de la República del Ecuador. Institut Français du Pétrole (IFP) y Servicio Nacional de Geología y Minas; Quito.

FAUCHER B., VERNET R., BIZON G., BIZON J. J., GREKOFF N., LYS M. and SIGAL J. (1971) Sedimentary formations in Ecuador. A stratigraphic and micropaleontological survey. *Bureau d'études industrielles et de coopération de l'Institut Français du Pétrole. Paris.*

FAUCHER B. y SAVOYAT E. (1973) Esquema Geológico de los Andes Ecuatorianos. *Revue de Géographie et de Géologie Dynamique* (2). **XV Fase 1-2,** 115-142. Paris.

FEININGER T. (1977) Simple Bouguer gravity anomaly map of Ecuador (1:1000000). Escuela Politécnica Nacional, Quito, Ecuador.

FEININGER T. (1978) Geologic map of the western part of the El Oro Province (1:50000). Escuela Politécnica Nacional, Quito, Ecuador.

FEININGER T. and BRISTOW C. R. (1980) Cretaceous and Paleogene geologic history of coastal Ecuador. *Geologische Rundschau*, Vol. **69**, 849-874.

GANSSER A. (1973) Facts and theories on the Andes. Journal of the Geological Society of London, Vol. 129, 93-131.

GILL J. B. (1981) Orogenic andesites and plate tectonics. Springer-Verlag, Berlin, 389pp.

GOOSSENS P. J. (1972) Metallogeny in the Ecuadorian Andes. *Economic Geology*. 67, 458-468.

GOOSSENS P. J. and ROSE W. I. (1973) Chemical composition and age determination of tholeiitic rocks in the Basic Igneous Complex, Ecuador. *Bulletin geological Society of America*, 84, 1043-1052.

HALL M. L. y MOTHES P. A. (1994) Tefroestratigrafía holocénica de los volcanes principales del valle interandino, Ecuador. p. 47-68. In: El Contexto Geológico del Espacio Físico Ecuatoriano (ed. R. Marocco). Colegio de Geógrafos del Ecuador, Quito, Ecuador. 113p.

HENDERSON W. G. (1977) Geology of the Cordillera Occidental of Northern Ecuador. Internal report IGS/DGGM, Quito, 79p.

HENDERSON W. G. (1979) Cretaceous to Eocene volcanic arc activity in the Andes of northern Ecuador. *Journal of the Geological Society of London,* Vol. 136, 367-378.

HENDERSON W. G. (1981) The Volcanic Macuchi Formation, Andes of Northern Ecuador. *Newsl. Stratigr.,* 9, 157-168.

HOLLIS C. J. (1999) Report (1) on radiolarian age determinations for Misión Británica Geológica. Report Number CJH9904. Institute of Geological and Nuclear Sciences, New Zealand.

HOLLIS C. J. (2000) Report (2) on radiolarian age determinations for Misión Británica Geológica. Report Number CJH0001. Institute of Geological and Nuclear Sciences, New Zealand.

HUGHES R. A. and BERMÚDEZ R. A. (1997) Proyecto de Desarrollo Minero y Control Ambiental, Programa de Información Cartográfica y Geológica. Report Number 4. Geology of the area between 0°00' and 1°00'S, Western Cordillera, Ecuador.

INEMIN (1990) Inventario de los recursos minerales metálicos en el noroccidente del Ecuador.

IRVINE T. N. and BARAGAR W. R. A. (1971) A guide to the chemical classification of the common volcanic rocks. *American Journal of Earth Sciences*, **8**, 523-548.

JAPAN INTERNATIONAL COOPERATION AGENCY (JICA) (1998) Informe final sobre la exploración mineral de cooperación técnica en el área de Imbaoeste, República del Ecuador.

KEHRER W. and VAN DER KAADEN G. (1979) Notes on the geology of Ecuador, with special reference to the Western Cordillera. *Geol. Jahrbuch,* **35**, 5-57.

KENNERLEY J. B. (1980) Outline of the geology of Ecuador. Institute of Geological Sciences. *Overseas Geology and Mineral Resources,* No. 55, 20 pp.

KERR A. C., TARNEY J., MARRINER G. F., NIVIA A., KLAVER G. T. and SAUNDERS A. D. (1996) The geochemistry and tectonic setting of late Cretaceous Caribbean and Colombian volcanism. *Journal of South American Earth Sciences,* **9**, 111-120.

KERR A. C., MARRINER G. F., TARNEY J., NIVIA A., SAUNDERS A. D., THIRWALL M. F. and SINTON C.W. (1997) Cretaceous basaltic terranes in Western Colombia: Elemental, chronological and Sr-Nd isotopic constraints on petrogenesis. *Journal of Petrology,* 38, 677-702.

LE MAITRE R. W. (1989) A classification of Igneous Rocks and glossary of terms. Blackwell Publications London, 193p.

LEBRAT M. (1985) Caractérisation géochimique du volcanisme ante-orogénique de l'Occident Equatorien: implications géodynamiques. Unpubl. PhD Thésis Centre Géologique and Géophysique de Montpellier, 119p.

LEBRAT M., MEGARD F., JUTEAU T. and CALLE J. (1985) Pre-orogenic volcanic assemblage and structure in the western cordillera of Ecuador, between 1°40'S and 2°20'S. *Geologische Rundschau*, 74, 343-351.

LEBRAT M., MEGARD F., DUPUY C. and DOSTAL J. (1987) Geochemistry and tectonic setting of pre-collision Cretaceous and Paleogene volcanic rocks of Ecuador. *Bulletin of the Geological Society of America*, Vol. 99, 569-578.

LITHERLAND M. and ASPDEN J. A. (1992) Terrane-boundary reactivation: a control on the evolution of the Northern Andes. *Journal of South American Earth Sciences*, 5, 71-76.

LITHERLAND M., ZAMORA A. and EGÜEZ A. (1993a) National Geological Map of the Republic of Ecuador, scale 1:1000000. British Geological Survey (Nottingham) and CODIGEM (Quito).

LITHERLAND M., ZAMORA A. and EGÜEZ A. (1993b) National Metallogenic Map of the Republic of Ecuador, scale 1:1000000. British Geological Survey (Nottingham) and CODIGEM (Quito).

LITHERLAND M., ASPDEN J. A. and JEMIELITA R. A. (1994) The metamorphic belts of Ecuador. *Overseas Memoir of the British Geological Survey*, No. 11.

LONSDALE P. (1978) Ecuadorian Subduction System. *Bulletin American Association of Petroleum Geologists*, 62, 2454-2477.

MANIAR P. D. and PICCOLI P. M. (1989) Tectonic discrimination of granitoids. *Geological Society of America Bulletin*, 101, 635-643.

McCOURT W., ASPDEN J. A. and BROOK M. (1984) New geological and geochronological data from the Colombian Andes: Continental growth by multiple accretion. Journal of the Geological Society of London, 141, 831-845.

McCOURT W., MUÑOZ C. A. and VILLEGAS H. (1991) Regional geology and gold potential of the Guapi-Napi drainage basin and the upper Timbiqui river, Department of Cauca SW Colombia. BGS Overseas Geology Series, Technical Report WC/90/34, 62p.

McCOURT W., DUQUE P. and PILATASIG L. (1997) Geology of the Cordillera Occidental of Ecuador between 1° and 2°S. Geological Information Mapping Programme (GIMP) Report No. 3. World Bank Mining Development and Environmental Control Project (PRODEMINCA). Misión Geológica Británica, CODIGEM, Quito, Ecuador.

MESCHEDE M. (1986) A Method of discriminating different types of mid-ocean ridge basalt and continental tholeiites with the Nb-Zr-Y diagram. Chem. Geol., 56, 207-218.

MEGARD F. and LEBRAT M. (1987) Los terrenos exóticos del occidente ecuatoriano y sus relaciones con Sudamérica. Coloquio Ecuador 86, Quito, *Casa Cultura*, 240, 161-172.

MIDDLEMOST E. A. K. (1975) The basalt clan. *Earth. Sci. Rev.*, 11, 337-364.

MIYASHIRO A. (1974) Volcanic rock series in island arcs and active continental margins. *American Journal of Science*, 274, 321-355.

MOSQUERA C. F. (1949) Viaje de reconocimiento y estudio por el Río Santiago (Prov. de Esmeraldas). *Bol. Inf. Cient. Nac.*, 2, 15-24.

MULLEN E. D. (1983) $MnO/TiO_2/P_2O_5$: a minor element discriminant for basaltic rocks of oceanic environments and its implications for petrogenesis. *Earth and Planetary Science Letters*, 62, 53-62.

OLSSON A. A. (1942) Tertiary deposits of northwestern South America and Panamá. *Proceedings of the American Scientific Congress,* Washington, 231-287.

PEACOCK M. A. (1931) Classification of igneous rock series. *Journal of Geology,* 39, 54-67.

PEARCE J. A. (1975) Basalt geochemistry used to investigate past tectonic environments on Cyprus. *Tectonophysics,* 25, 41-77.

PEARCE J. A. and NORRY M. J. (1979) Petrogenic implications of Ti, Zr, Y and Nb, variations in volcanic rocks. *Contributions to Mineralogy and Petrology,* 69, 33-47.

PEARCE J. A., HARRIS N. B. W. and TINDLE A. G. (1984) Trace element discrimination diagrams for the tectonic interpretation of granitic rocks. *Journal of Petrology*, **25**, 956-983.

PILGER R. H. (1983) Kinematics of the Southern American subduction zone from global reconstructions. Geodynamics of the Eastern Pacific Region, Caribbean and Scotia arcs. *American Geophysical Union Geodynamics Service,* 9, 113-126.

PRATT W. T., FIGUEROA J. F. and FLORES B. G. (1997) Report No. 1, Mining Development and Environmental Control Project, Geological Information Mapping Programme: Geology of the Western Cordillera between 3°-4°S. CODIGEM-BGS, Quito.

REA D. K. and MALFAIT B. T. (1974) Geologic evolution of the Northern Nazca Plate. *Geology*, **2**, 317-320.

READING H. G. (1986) Sedimentary Environments and Facies (2nd Edition). Blackwell Scientific Publication, London, 615p.

REYNAUD C., JAILLARD E., LAPIERRE H., MAMBERTI M. and MASCLE G. H. (1999) Oceanic plateau and island arcs of southwestern Ecuador, their place in the geodynamic evolution of northwestern South America. *Tectonophysics,* 307, 235-254.

SALAZAR E. (1981) Informe de comisión realizada a Hualchán del 24 de Noviembre al 4 de Diciembre de 1981. *DGGM, Quito, Informe 5873*. Unpubl. Report.

SANTOS M. and RAMÍREZ F. (1986) La Formación Apagua, una nueva ciudad eocénica en la cordillera occidental ecuatoriana. *Memorias Cuarto Congreso Ecuatoriano de Geología, Minas y Petróleos*, Tomo 1, 179-189.

SAUER W. (1957) El mapa geológico del Ecuador. Memoria explicativa. (Universidad Central; Quito).

SAUER W. (1965) Geología del Ecuador. Edit. Ministerio de Educación Pública, Quito, 383p. (Quito).

SAVOYAT E., VERNET R., SIGAL J., MOSQUERA C., GRANJA J. and GUEVARA G. (1970) Formaciones sedimentarias de la Sierra tectónica andina en el Ecuador. Informe Instituto Francés de Petróleo y Servicio Nacional de Geología y Minería, Quito.

SERVICIO NACIONAL DE GEOLOGÍA Y MINERÍA (1969) Mapa geológico de la República del Ecuador. (1:1000000). (Quito).

SHERVAIS J. W. (1982) Ti vs V plots and the petrogenesis of modern and ophiolitic lavas. *Earth and Planetary Science Letters*, **59**, 101-118.

SIGAL J. (1968) Estratigrafía micropaleontológica del Ecuador, datos anteriores y nuevos. Informe Instituto Francés de Petróleo y Servicio Nacional de Geología y Minería, Quito.

SILLITOE R. H. (1974) Tectonic segmentation of the Andes: implication for magmatism and metallogeny. Nature, London, Vol. 250.

STEINMANN M. (1977) Fission-track age determinations on Zircons. Consultants Report, GIMP mapping project Ecuador, Geological Institute, ETH, Zürich, Switzerland, 59p.

THALMANN H. E. (1946) Micropalaeontology of Upper Cretaceous and Paleocene in Western Ecuador. *Bulletin of the American Association of Petroleum Geologists,* Vol. 30, 337-347.

TSCHOPP H. J. (1948) Geologische Skizze von Ekuador. *Bull. Assoc. Suisse Géol. Ing. Pét.*, Vol. 15, 14-45.

TSCHOPP H. J. (1953) Oil explorations in the Oriente of Ecuador. 1938-1950. *Bulletin of the American Association of Petroleum Geologists,* Vol. 37, 2303-2347.

VAN THOURNOUT F. (1991) Stratigraphy, magmatism and tectonism in the Ecuadorian Northwestern Cordillera: metallogenic and geodynamic implications. PhD Thesis Katholieke Universiteit Leuven.

VAN THOURNOUT F., HERTOGEN J. and QUEVEDO L. (1992) Allochthonous terranes in northern Ecuador. In: Andean Geodynamics, Special Volume. *Tectonophysics*, 205, 205-222.

WALLRABE-ADAMS H. J. (1991) Petrology and Geotectonic development of the Western Ecuadorian Andes: the Basic Igneous Complex. *Tectonophysics*, 185, 163-182.

WILKINSON I. P. (1998a) Calcareous microfossils from Cretaceous and Tertiary deposits in Ecuador. Technical Report WH/98/45R. Biostratigraphy and Sedimentology Research Group, BGS, Nottingham, UK.

WILKINSON I. P. (1998b) Foraminifera from a suite of Late Cretaceous to Paleocene samples of the Cordillera Occidental, Ecuador. Technical Report WH/98/56R. Biostratigraphy and Sedimentology Research Group, BGS, Nottingham, UK.

WILKINSON I. P. (1998c) Calcareous microfossils from a suite of samples from the Western Cordillera, Ecuador. Technical Report WH/98/163R. Biostratigraphy and Sedimentology Research Group, BGS, Nottingham, UK.

WILKINSON I. P. (1999) Calcareous microfauna from a suite of samples from the Cordillera Occidental, Ecuador. Technical Report WH/99/87R. Biostratigraphy and Sedimentology Research Group, BGS, Nottingham, UK.

WINCHESTER J. A. and FLOYD P. A. (1977) Geochemical discrimination of different magma series and their differentiation products using immobile elements. *Chemical Geology*, 20, 325-343.

WOOD D. A. (1980) The application of a Th-Hf-Ta diagram to problems of tectonic magmatic classification and to establishing the nature of crustal contamination of basaltic lavas of the British Tertiary volcanic province. *Earth and Planetary Scientific Letters*, 50, 11-30.

WOLF T. (1892) Geografía y Geología del Ecuador. Leipzig; Brockhaus.

APPENDIX 1 OF REPORT:

GEOLOGY OF THE WESTERN CORDILLERA
OF ECUADOR
BETWEEN 0°00' AND 1°00' N

DESCRIPTION OF THE MIOCENE-HOLOCENE VOLCANIC SEQUENCES

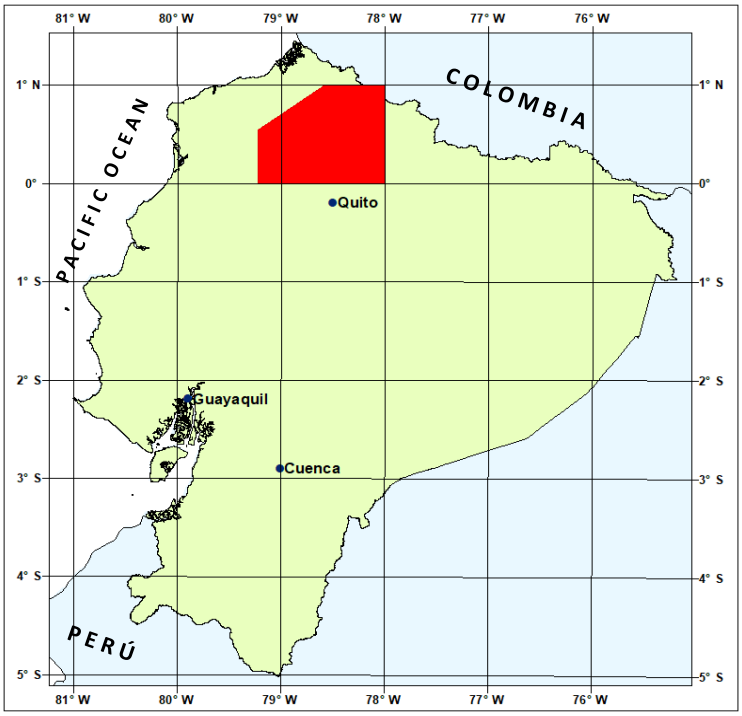

GEOLOGICAL INFORMATION MAPPING PROGRAMME
(LOCATION OF MAP 5 AREA)

M. BOLAND
L. PILATASIG
E. IBADANGO
W. MCCOURT
J. ASPDEN
R. HUGHES
B. BEATE

QUITO, 2000

Summary of Mio-Plio-Quaternary Volcanic Rocks
on Map #5 at a scale of 1:200000. BGS/PRODEMINCA 3.3

Prepared by: *Eng. Bernardo Beate, PRODEMINCA Consultant, Dec. 1998, for Dr. Martin Boland, coordinator of map #5/Subcomponent 3.3 of PRODEMINCA (revised version as of March, 2000).*

This work summarizes the main characteristics of Mio-Plio-Quaternary volcanic rocks and volcanoclastic deposits present in map #5 of BGS/PRODEMINCA, covering the E and SE sides, encompassing an area of 3353 km^2. This area has been surveyed and studied by the author during previous works since the 1980s. Preferably, a chronological order is followed, from oldest to most recent, to describe the different lithological units and groups. The ages are mostly estimated and based on morphological criteria; however, some published radiometric data available at the time of writing this summary are included.

Therefore, the sequence of volcanic stratigraphy is inferred and subject to change according to new data.

1. Metamorphic Rocks

Metamorphic rocks outcrop on the eastern edge of the study area, mainly in the Chota Valley. These rocks have not been studied by PRODEMINCA, but based on previous studies (Baldock, 1982 and Van Thournout, 1990), they consist mainly of sericitic schists and graphite-rich green schists. Structural details are found in Litherland et al. (1994) (page 55).

2. Angochagua Volcanics (M-Pl_{Ang})

These outcrop towards the eastern limit of the map, in the foothills of the Cordillera Real (CR). They cover a vast area from the Chota River valley in the north to the Cayambe volcano in the south. They overlie pre-Cretaceous basement metamorphic rocks of the Cordillera Real and Miocene sedimentary rocks of the Chota basin. Locally, they are overlain by glacial deposits and cangahua, which are not generally represented on the map due to scale reasons. Pleistocene glacial erosion has affected these volcanics, forming deep U-shaped valleys that drain towards the Inter-Andean Valley.

These consist of an undifferentiated volcanic rock package ranging from 500 to 1500 meters thick, slightly tilted to the west. Proximal and medial facies predominate, such as lava flows, dikes, vent breccias, and subvolcanic stocks of andesitic to dacitic compositions. To a lesser extent, epiclastic sediments, breccias, tuffs, and associated volcanoclasts of intermediate to acidic compositions are also found. Emission centers such as stratovolcanoes or volcanic cones are not distinguished due to intense erosion.

The age of these rocks falls within the Late Miocene to Pliocene, according to K/Ar radiometric ages obtained by Barberi (1988), which yielded 3.65 ± 0.07 Ma, 6.30 ± 0.06 Ma, and 6.31 ± 0.10 Ma, supporting a correlation with the Pisayambo Formation (Hall and Beate, 1991).

3. Pugarán Volcanics (M-Pl_{Pn})

These rocks cover the crest of the Western Cordillera (CO) between Cahuasquí and La Merced de Buenos Aires, north of the Yanaurco volcanic area up to almost the Mira River in the north. They show intense glacial erosion and consist of andesitic lava flows and hornblende dacite stocks, with associated breccias and tuffs. The age of these rocks is Pliocene, as indicated by the Fission Track result of 5.0 ± 2.9 Ma (BGS, 1999). Their thickness is unknown. They are partially correlated with the Angochagua volcanics. They overlie sediments of the Silante Unit and are partially covered by glacial moraines. Hydrothermal alteration zones are observed on the flanks and crest. The La Florida stock and dikes outcropping at the Amarillo River bridge near the Mira River may belong to this magmatic pulse. Together with the Angochagua Volcanics, they may represent part of the sediment source for the Chota Basin during its infilling phase and for the initial stages of the Inter-Andean Valley fill (?).

4. Inter-Andean Valley Fill (Pl-P_D)

This includes a series of undifferentiated packages of distal epiclastic and volcanoclastic sediments, primary and reworked, with a predominantly volcanic source, and of inferred Plio-Quaternary age. It also includes fluvial and lacustrine sediments, local colluvium, mudflows, a few lava flows, pyroclastic flows, large debris avalanche deposits, and cangahua. The packages are generally horizontal in the upper parts and tilted or folded (by slumping and/or tectonism) in the lower sequences.

They constitute the fill along the Inter-Andean Valley, preferably in its central part, and outcrop in the deep canyons of the Guayllabamba, Ambi, and Chota-Mira rivers. They are overlain by Quaternary volcanic products, generally interbedded with them towards the top.

5. Andesitic Volcanic Edifices (A^A)

This group includes the Quaternary andesitic volcanic edifices present in map #5, represented by the extent of their proximal facies, especially lava flows. Below is a brief description of these edifices in ascending chronological order.

5.1 Cushnirrumi Volcano (A^A Csh)

It is located 10 km south of the Cuicocha lagoon and represents the ancient remains of an elongated andesitic structure (15 km) from SE to NW, with a width of 10 km. It is probably of Lower Quaternary age. Its highest points reach 3713 meters above sea level at Cerro Cushnirrumi [981-215] and 3514 meters above sea level at Cerro Pirulo [924-241]. The dominant lithology consists of pyroxene andesites, although more differentiated facies are present, such as the amphibole dacite dome (R^D Csh) of Cerro Blanco [966-236]. Its lavas overlie pre-Neogene rocks of the Western Cordillera basement and are covered by more recent products from Mojanda and Cuicocha. On the southern flank towards San José de Minas, there is an avalanche caldera open to the south, with some zones of hydrothermal alteration with pyrite in tuffs observed on its interior walls.

5.2 Cusín volcano (A^A Cus)

This is an ancient, inactive, and eroded andesitic stratovolcano with an avalanche caldera open to the NW. Its highest point is 3989 meters above sea level [177-179], and its extent covers a basal diameter of about 10 km. It is composed of thick and abundant lava flows, predominantly pyroxene andesites. No pyroclastic deposits or zones of hydrothermal alteration are known from this volcano. On the SE flank is the Muyurco dome - R^A Cus [220-128, 3344 meters above sea level], of andesitic nature. The age of Cusín Volcano is unknown, possibly Lower to Middle Pleistocene (?).

5.3 Cayambe volcano (A^A Ca) – ancient

The northwestern flank of this large stratovolcano occupies the southeast corner of the map and consists of ancient lava flows, radiating from the summit, which are intensely glaciated and show topographic inversion. The dominant lithology is pyroxene andesitic rocks. They overlie metamorphic rocks of the Cordillera Real and are covered by cangahua and Holocene tephras. The age of this initial lava phase of Cayambe Volcano is unknown but is inferred to be Early Pleistocene.

5.4 Mojanda volcano (A^A Moj)

This includes an extensive volcanic edifice located in the southern part of the map, where it overlies non-outcropping pre-Tertiary basement rocks. The oldest parts (Early Pleistocene?) are composed of andesitic lava flows (A^A Moj) distributed radially to summit caldera structures (Cerro Negro sector, 053-137, 4260 meters above sea level). Basic andesite breccias (A^B Moj) are associated with summit phreatomagmatic events (Robin et al., 1998).

5.5 Fuya Fuya volcano (A^A FF)

Fuya Fuya Volcano [019-153, 4263 meters above sea level] is adjacent and contemporary to Mojanda Volcano, according to Robin et al. (1998). The latter predominantly features andesitic lava products, while the former has dacitic products, including domes (R^D FF) and pyroclastic flows (T^D FF). Both exhibit effusive phases (A^A Moj and A^A FF) and explosive phases, with the formation of respective avalanche calderas open to the west and extensive pyroclastic flow deposits (T^D FF/T^D Moj) and debris avalanche deposits (Avl FF). The datable youngest products have yielded ages greater than 40 ky BP, and apparently, most of this complex's activity belongs to the Early to Middle Pleistocene. It is covered by a thick layer of cangahua and is highly eroded.

5.6 Cotacachi volcano (A^A Cot)

This large stratovolcano, standing at 4939 meters above sea level, is located on the crest of the Western Cordillera, 26 km west of Ibarra [954-403]. Its base extends about 20 km (N-S) and 26 km (E-W). It is intensely affected by glacial erosion, with its summit still having small patches of ice that are currently on the verge of disappearing. The volcano is primarily composed of pyroxene andesites dating from the early to middle Pleistocene (a dike on the SE flank yielded a K/Ar radiometric age of 0.63 ± 0.06 Ma, OLADE, 1980). It overlies pre-Neogene basement rocks of the Western Cordillera and is covered by thick layers of cangahua. Its southern flank is completely covered by explosive products from Cuicocha volcano (T^D Cui, 3000 years BP). Apparently, the most recent activity, aside from that of Cuicocha, is from dacitic domes at its summit and on its NE flank, the Piribuela dome (R^D Prb, Holocene?). An avalanche caldera is open to the west, and partial reworking of its products has led to lahar deposits (Avl Cot) along the Intag River to its confluence with the Guayllabamba. On its SW flank, there is a small set of three andesitic domes, the main one being Muyurco [896-362, 3572 meters above sea level], whose age is unknown. Another intermediate composition dome, Catzopamba (R^D Cz, 024-392, 3055 meters above sea level), is located at the eastern foot of Cotacachi volcano.

5.7 Chiltazón volcano (A^A Cz)

This is a modest-sized andesitic stratovolcano located on the NE boundary of the map. It reaches a height of 3967 meters above sea level. Its base extends 4 km (E-W) and 3 km (N-S). It has a conical shape, with its summit [317-759] showing an accumulation of breccias in a poorly preserved central crater. It overlies pre-Tertiary basement rocks, and its dominant lithology is andesitic rocks. Its age is unknown, but a middle Pleistocene age is inferred from its preserved morphology.

5.8 Iguán volcano (A^A Ig)

It is located immediately south of Chiltazón volcano, on the eastern boundary of the map. Its summit reaches 3819 meters above sea level [332-688], and its base has a diameter of about 6 km. It has a truncated conical shape, with a 1.5 km wide avalanche caldera open to the west. An associated debris deposit (Avl Ig) extends from the volcano to the W and SW, along the El Alumbral ravine and the Santiaguillo River, for a stretch of about 10 km. The dominant lithology consists of pyroxene andesites in lava flows and dacites in tephras (T^D Ig) distributed to the south in the Mira fan. The age of this volcano is unknown, though a middle Pleistocene age is inferred. The fragmentary products show evidence of hydrothermal activity prior to explosive events.

5.9 Imbabura volcano (A^A Imb)

This stratovolcano is located in the Inter-Andean Valley, about 12 km SSW of Ibarra. It has a conical shape with a base diameter of 14 km and a summit elevation of 4560 meters above sea level [139-271]. It consists of andesitic lavas, partly porphyritic, probably from the Middle to Upper Pleistocene, intensely dissected by erosion and covered by younger dacitic fragmentary products such as pyroclastic flows (T^D Imb, 15 ky BP in charcoals from a pyroclastic flow deposit in the Tahuando River, north of Ibarra, E. Salazar, 1980). The summit is composed of andesitic breccias, with the crater open to the east, and appears to be a blasted dome, which would be the center of emission for the last pyroclastic flows deposited around the flanks and base of the cone. The cone does not exhibit features of an avalanche caldera, but an extensive deposit (Avl Imb) of this type originates from the northern flank of the volcano and extends to the Ambi River canyon, following it to the Chota River. Late eruptive phases (Upper Pleistocene?) involve the construction of dacitic domes with hornblende (R^D Imb).

5.10 Cubilche volcano (A^A Cb)

Located adjacent to the SE foot of Imbabura volcano, it has a basal diameter of about 6 km, and its highest point reaches 3802 meters above sea level [196-259]. It mainly consists of olivine andesitic (A^{AB} Cb) to pyroxene andesitic (A^A Cb) lava flows, with subordinated tephras. The lava flows have emanated from a central vent, which reactivated within an avalanche caldera open to the north. Satellite vents on the E and S flanks, Plancha Ladera and Pucará Loma, produced lava flows and a dome, Cunro [234-256, 3304 meters above sea level], of andesitic composition. The age of this volcano is unknown, but the preserved morphology of its flanks and lava flows suggests an Upper Pleistocene age. Some recent lavas from the SE flank of Imbabura collide with the Cubilche edifice. The base of this volcano is not observed.

5.11 Chachimbiro Volcanic Complex

This complex ranges from basic andesitic rocks to rhyodacites, spanning from the early Pleistocene (Pliocene?) to the Holocene. It is located along the axis of the Western Cordillera in a SE-NW elongated direction, about 25 km NW of Ibarra. The following volcanic structures comprise the complex in ascending chronological order.

5.11.1 Yanaurco volcano (A^A Ya) is located on the crest of the Western Cordillera, overlying pre-Neogene rocks of the Silante Unit. Its highest point is 4535 meters above sea level [974-538], and its base extends 5 km (E-W) by 8 km (SW-NE). It is composed of thick pyroxene andesitic lava flows towards the base and more evolved products, such as rhyodacites (R^D Ya), towards the top. Morphologically, it shows intense erosion, mainly by glaciers, and does not have a defined volcanic shape or distinguishable emission centers. An age from the Lower Pleistocene to possibly Pliocene (?) is inferred. It is possible that the andesitic massif of Pulumbura is an older prolongation towards the SW of Yanaurco volcano.

5.11.2 Huanguillaro volcano (A^A Hll), is located on the eastern edge of the CO. Its highest point is at 3960 meters above sea level [008-526]. It has the approximate shape of a truncated cone, with a large avalanche caldera 3 km in diameter open towards the ESE. It is composed of lava flows ranging from basic andesite to very porphyritic pyroxene andesite, distributed radially along the caldera rim. The age of this edifice appears to be Middle Pleistocene, based on a dating of 0.46 Ma with K/Ar (Barberi, 1988) on fragments of porphyritic pyroxene andesites taken from the debris avalanche of this volcano on the Ibarra-Chota road, which overlies the volcanic rocks of Angochagua. This avalanche deposit does not appear on the map because it is covered by younger products.

The post-avalanche eruptive phases of Huanguillaro are characterized by being highly explosive, resulting in extensive deposits of Plinian tephra, non-welded ignimbrites, and block & ash deposits (dome collapse flows) marked as T^D Ch on the map and located in the Urcuquí, Tumbabiro, Cahuasquí, and Salinas valleys [195-550]. Additionally, there are intracaldera rhyodacitic domes with biotite (R^D Hg, Hugá, 020-059) and dacitic domes (R^D Ch) with hornblende (e.g., El Churo, 049-355) located on the open eastern edge of the caldera. The initial explosive phases appear to belong to the Middle Pleistocene, and dome activity extended into the Upper Pleistocene. There is evidence from post-glacial tephra layers of moderate explosive activity in this volcanic complex (5690 ± 50 years BP, Ego et al., 1996).

5.11.3 Pilavo volcano (A^A Pil) is located west of Yanaurco [993-582], reaches 4254 meters above sea level and has a very well-preserved conical shape with a base of 6 km (E-W) by 10 km (SW-NE). The boundaries of each lava flow are clearly visible in a radial arrangement. To the east, its lavas collide with Yanaurco and to the south with Pulumbura. It overlies rocks of the Silante and Pilatón Units. It is entirely composed of lavas of pyroxene and mainly hornblende andesites; related pyroclastic deposits have not been found. Its age should be Upper Pleistocene, given its high degree of preservation and almost complete absence of glacial erosion. A satellite cone, named Parulo, with a basal diameter of 1.5 km (SE-NW) and 3285 meters above sea level [863-573], is located west of Pilavo Volcano, and its lavas have the same characteristics as those of Pilavo. It is responsible for blocking drainage to form Laguna Donoso [850-570] to the west.

6. Rhyodacitic Volcanic Rocks (R^{RD})

These are the petrographically most differentiated volcanic rocks present on the map and the rarest. They are found near the summit of Yanaurco Volcano (see section 4.11.1) and their extent is limited. They are flow deposits with a tuffaceous appearance, rich in biotite and hornblende, with free quartz and a glassy matrix (R^D Ya).

Another outcrop of rhyodacite occurs in the Huanguillaro caldera (4.11.1) and consists of the Hugá dome (R^D Hg). This dome measures 3.5 km in diameter and rises about 400m above its base. Its age would be Middle to Upper Pleistocene (?).

It is possible that more rocks of this composition exist in the mapped area, but they are currently unknown.

7. Dacitic Domes (R^D)

These monogenetic volcanic edifices of rather modest extent are quite common on the map and are generally associated with younger eruptive phases of andesitic complexes. Petrographically, they are light to dark gray rocks with a high degree of porphyritic texture, containing phenocrysts of plagioclase, hornblende, scarce biotite, and quartz, in a non-vesicular, highly felsic, sometimes glassy matrix.

Their age ranges from Middle Pleistocene (?) to Holocene, with the youngest domes being Cuicocha (2900 years BP, von Hillebrandt, 1989) and Pululahua (2305 years BP, Hall and von Hillebrandt, 1988). The Piribuela dome on the NE flank of Cotacachi also appears to have a Holocene age, similar to the Pitzantzi dome in the Chachimbiro dome complex, as evidenced by a radiocarbon dating obtained from the paleosol of a post-glacial tephra (5690 ± 50 years BP, Ego et al., 1996). The presence of high enthalpy thermal springs in Chachimbiro attests to the existence of a heat anomaly in the subsurface due to young magmatic bodies (Beate, 1991). The other domes in the complex, nearly a dozen, have estimated ages ranging from Middle to Upper Pleistocene.

Pululahua Volcano is a complex of more than a dozen dacitic domes (R^D Pul) located over pre-Tertiary basement greenstones (Natividad Unit). Its age ranges from the Upper Pleistocene to Holocene. It also presents an explosion and/or avalanche (?) caldera open to the west, with the most recent domes inside it. Papale and Rossi (1993) obtained an age of 2400 years BP for the Plinian tephra, apparently related to the formation of the caldera. Its explosive activity has formed extensive dacitic pyroclastic deposits (T^D Pul).

In the Mojanda complex, the explosive facies of Fuya Fuya are characterized by the formation in the Middle Pleistocene (?) of the domes (R^D FF): Fuya Fuya, Colangal, and Panecillo, with their respective pyroclastic deposits (T^D FF). Older dacitic lavas, related to Mojanda (R^D Moj), have reached almost to Otavalo.

Imbabura Volcano presents a large dacitic dome on its SW flank, Huarmi Imbabura [122-262, 3845 masl], of Upper Pleistocene age (?). Another exploded dome appears in the summit sector, associated with radial deposits (T^D Imb) around the volcano.

Cotacachi Volcano has two dacitic domes: the poorly defined and heavily glaciated summit dome of unknown age and the Piribuela dome (R^D Prb) mentioned above.

On the SW flank of Cotacachi is Cuicocha Lake, representing a collapse caldera of 4 km (SE-NW) by 2.5 km (N-S). It formed from the explosion of the Cuicocha dome [955-343, 3377 masl] about 3000 years BP (von Hillebrandt, 1989), with the consequent formation of extensive pyroclastic deposits (T^D Cui). Late dacitic domes occupy the central part of the caldera (R^D Cui).

The El Artezón dome [131-554, 2200 masl], in Pablo Arenas, is composed of hornblende-rich dacites. The dome's basement rocks are pre-Tertiary CO rocks, and their age is unknown. It might belong to an early phase of Chachimbiro (R^D Ch?) or, given its ancient appearance, could be part of the Pugarán volcanics (?) (see section 2).

8. Basic Volcanic Rocks - Basaltic Andesites (A^B)

These are a type of rock that is uncommon in this part of the map, and their presence is limited to moderate lava flows at Mojanda (A^B Moj) and Cubilche (A^B Cb), and breccias at the former, as mentioned earlier. The flows at Cubilche appear to be younger than those at Mojanda.

9. Dacitic Pyroclastic Deposits (T^D)

These deposits are grouped under this acronym, for scale reasons, and mainly consist of block & ash pyroclastic flows (dome collapse flows), although they also contain other types of pyroclastic flows, tephra, ignimbrites, and debris flow deposits (lahars), both primary and reworked. The deposits (T^D) represent distal facies of explosive events, generally associated with dome extrusions. Their distribution tends to be radial from the emission center, whether stratovolcano and/or dome, although topography, especially valleys, can mask this trend, as gravity-driven pyroclastic flows fill valleys and depressions. For example, at Huanguillaro, the T^D have formed a fan towards the east, covering the Salinas valley, or at Fuya Fuya, where all flows have gone westward. At Imbabura, they are distributed more radially, although they predominate towards the east, north, and west. The same occurs at Cuicocha, but the main trend is towards the southeast, towards the Ambi River valley. In Pululahua, the distribution is radial towards the east and west, little to the north, and almost none towards the south. In Mojanda, the radial distribution is more uniform and is only interrupted by the Cushnirrumi edifice.

The composition of T^D is predominantly dacitic with crystals of plagioclase and hornblende, scarce biotite and quartz. There are also andesitic compositions and rarely rhyodacitic or rhyolitic compositions. The age of each T^D corresponds to that of its emission center, as discussed earlier.

10. Debris Avalanche Deposits (Avl)

In all major andesitic features on the map, except for Pilavo, Yanaurco, Chiltazón, and Imbabura, typical caldera avalanche features – more or less preserved – have been found. In some cases, such as Cusín, Cubilche, Huanguillaro, and Cushnirrumi, the caldera edges are distinguishable, but the corresponding deposit does not outcrop due to being covered by younger products. The debris avalanche deposits represented on the map correspond to Mojanda, Cotacachi, Imbabura, and Iguán volcanoes. The dominant composition of the deposits is andesitic, reflecting that of the source stratovolcano. Sometimes there is hydrothermally altered material and/or more felsic rocks. The deposit is dry gravitational and has the appearance of a matrix-supported breccia with unsorted angular clasts, and jigsaw textures, where the matrix is the rock powder itself. The extent of these deposits can reach tens of kilometers and tend to follow river channels and fill depressions. The age varies according to the event that formed them, although almost all are from Middle to Upper Pleistocene. A young avalanche (Upper Pleistocene) is that of Imbabura, whose deposit in the Tahuando River is covered by lacustrine sediments, which are in turn covered by a pyroclastic flow from about 15000 years BP. The Pululahua avalanche is perhaps the youngest (Holocene?), but very eroded. It consists of fragmented materials from dacitic domes that have filled the drainage towards the Guayllabamba River. The largest avalanches are those of Cotacachi, Huanguillaro, and Mojanda, the Imbabura avalanche is regular, and the Iguán avalanche is modest in size.

11. Quaternary Alluvial Deposits (Q_A)

Under this denomination, all mappable deposits – apart from those described above – of alluvial, epiclastic, and distal volcanoclastic sedimentary type, both primary and reworked, that have accumulated in local depressions between volcanoes and along river channels and their tributaries, have been grouped. Their age is considered Quaternary, and the main source are the volcanic complexes in the surrounding area.

12. Colluvial Deposits

These are gravitational type deposits, mass movements caused by terrain instability due to tectonic activity, slope instability, hydrothermal alteration, surface and groundwater, and other factors. They are numerous in the mapped area, but smaller-sized deposits have been omitted for scale reasons.

Eng. Bernardo Beate

Quito, March 27, 2000

References

BARBERI F., COLTELLI M., FERRARA G., INNOCENTI F., NAVARRO J. M. and SANTACROCE F. (1988) Plio-Quaternary volcanism in Ecuador. Geol. Mag. 125 (1). G. Britain, pp. 1-14.

BEATE B. (1991) La Geotermia: conceptos generales, aplicaciones y estado actual en el Ecuador. Est. Geogr. #4, Coorp. Edit. Nac., Quito, pp. 71-84.

EGO F., SEBRIER M., CAREY-GAILHARDIS E. and BEATE B. (1996) Do the Billecocha normal faults (Ecuador) reveal extension due to lithospheric body forces in the Northern Andes? Tectonophysics 265, pp. 255-273.

HALL M. and BEATE B. (1991) El volcanismo Plio-Cuaternario en los Andes del Ecuador. Est. Geogr. #4, Coorp. Edit. Nac, Quito, pp. 5-17.

HALL M. and HILLEBRANDT CH. V. (1988) Mapa de los Peligros Volcánicos potenciales asociados con el Volcán Pululahua, Prov. de Pichincha. Escala 1:50000. Proyecto EPN-UNDRO. Instituto Geofísico-EPN, Quito.

HILLEBRANDT CH. V. (1989) Estudio Geovolcanológico del complejo Volcánico Cuicocha-Cotacachi y sus aplicaciones, Provincia de Imbabura. Tesis de magister, EPN, Quito.

OLADE (1980) Informe geo-vulcanológico: proyecto de investigación geotérmica de la República del Ecuador, Quito.

PAPALE P. and ROSSI M. (1993) A case of no-wind plinian fallout at Pululahua caldera (Ecuador): implications for models of clast dispersal. Bull. Volcanol. 55, Springer Verlag, pp. 523-535.

ROBIN C., HALL M., JIMÉNEZ M., MONZIER M. and ESCOBAR P. (1998) Mojanda volcanic complex (Ecuador): development of two adjacent contemporaneous volcanoes with contrasting eruptive styles and magmatic suites. Jour. South. Amer. Earth Sciences. V. 10, Nos. 5-6, pp. 345-359. Pergamon, G. Britain.

SALAZAR E. (1980) Com Pers., DGGM, Quito.

APPENDIX 2 OF REPORT:

GEOLOGY OF THE WESTERN CORDILLERA
OF ECUADOR
BETWEEN 0°00' AND 1°00' N

FOSSIL AGES

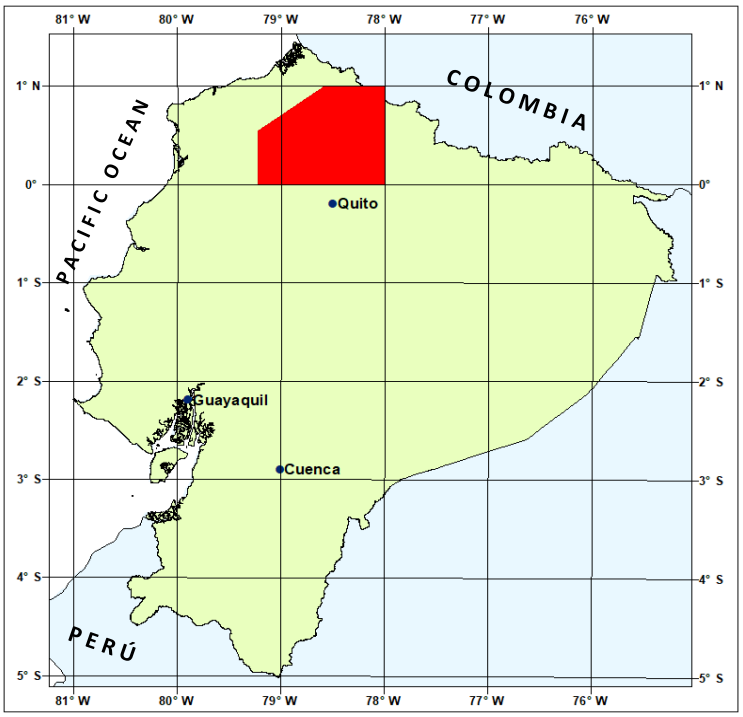

GEOLOGICAL INFORMATION MAPPING PROGRAMME
(LOCATION OF MAP 5 AREA)

M. BOLAND
L. PILATASIG
E. IBADANGO
W. MCCOURT
J. ASPDEN
R. HUGHES
B. BEATE

QUITO, 2000

PALAEONTOLOGICAL SAMPLES

SAMPLES	TOPOGRAPHIC SHEET	COORDINATES		AGE		UNIT
		UTMX	UTMY	RANGE	PROBABLE	
M5-113	Guayllabamba	7472	265		Campanian	Mulaute
M5-127	Otavalo	7845	286	Santonian-Early Campanian		Pallatanga
M5-128	Otavalo	7845	286		Late Cretaceous	Natividad
M5-173	Calacalí	7754	059	Campanian-Maastrichtian		Yunguilla
M5-191	Calacalí	7731	115		Early Oligocene	Silante
M5-196	Calacalí	7723	089		Eocene	Silante
M5-212	Mira	8188	645		Eocene	Rumi Cruz
M5-236	Carolina	8107	801	Campanian-Eocene		Pilatón
M5-184	Calacalí	7765	144	Late Campanian-Early Maastrichtian	Campanian	Yunguilla
M5-245	Otavalo	7832	269	Campanian-Maastrichtian		Natividad
M5-274	Vacas Galindo	7783	207		Campanian	Yunguilla
M5-372	Guadalupe	8046	869	Late Cretaceous-Late Eocene		Pilatón
M5-432A	Maldonado	8280	925		Oligocene	El Laurel
M5-JX4 (233)	Carolina	8112	787		Maastrichtian	Pilatón
M5-JX6 (213)	Mira	8184	655		Late Campanian	Yunguilla
M5-JX11 (127)	Otavalo	7845	287	Santonian-Early Campanian		Pallatanga
M5-JX12 (127)	Otavalo	7845	287	Santonian-Early Campanian		Pallatanga
M5-JX14 (127)	Otavalo	7845	287		Maastrichtian	Natividad
M5-JX15 (128)	Otavalo	7845	287	Late Campanian-Early Maastrichtian		Natividad
M5-JX17 (191)	Calacalí	7730	115	Late Eocene-Middle Oligocene		Silante
M5-268A	Calacalí	7770	120	Late Campanian-Early Maastrichtian	Campanian	Yunguilla
M5-268B	Calacalí	7770	120	Eocene		Rumi Cruz
M5-635	La Merced B. A.	7893	668	Paleocene		Pilatón
M5-746	Guayllabamba	7275	236	Middle Eocene-Late Eocene		Tortugo
M5-794	Guayllabamba	7239	252	Eocene?		La Cubera
M5-795	Guayllabamba	7227	293		Campanian	Naranjal
M5-797X	P. V. Maldonado	7080	125		Paleocene	La Cubera
M5-797Y	P. V. Maldonado	7080	125		Paleocene	La Cubera
M5-874	Gualpi	7164	556	Late Campanian-Maastrichtian		Río Desgracia
M5-911	R. Las Piedras	7558	626	Late Cretaceous	Campanian	Colorado
M5-1010	Gualpi	6983	560	Late Campanian-Middle Campanian		Río Desgracia

APPENDIX 3 OF REPORT:

GEOLOGY OF THE WESTERN CORDILLERA
OF ECUADOR
BETWEEN 0°00' AND 1°00' N

GEOCHEMICAL DATA

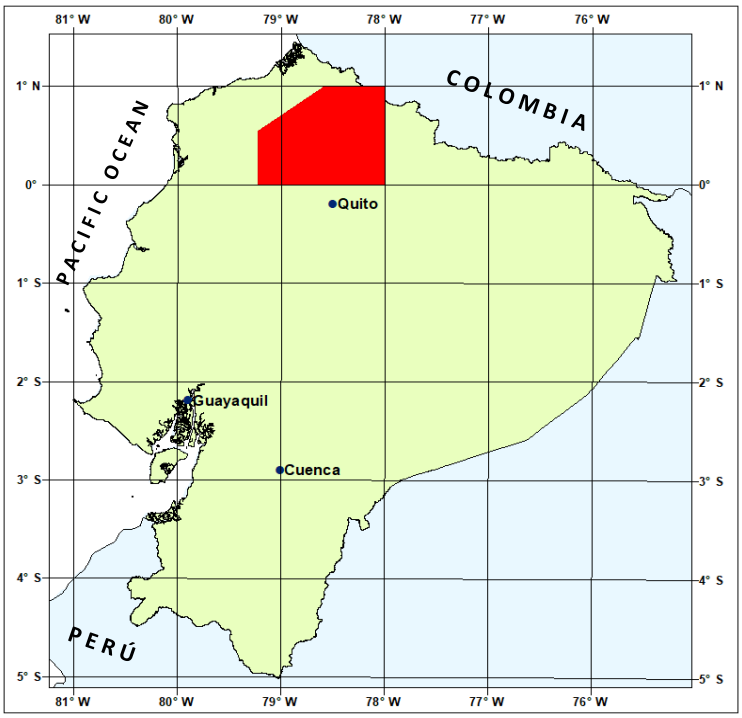

GEOLOGICAL INFORMATION MAPPING PROGRAMME
(LOCATION OF MAP 5 AREA)

M. BOLAND
L. PILATASIG
E. IBADANGO
W. MCCOURT
J. ASPDEN
R. HUGHES
B. BEATE

QUITO, 2000

SAMPLE	J-7	JX-24	M5-1	M5-82	M5-124	M5-125	M5-158	M5-205a	M5-211a
UTMX	7748	7331	7897	7877	7844	7839	7879	7858	8197
UTMY	429	015	353	277	287	288	272	190	616
UNIT	Intrusive	Intrusive	Río Cala	Río Cala	Pallatanga	Pallatanga	Río Cala	Pallatanga	Pallatanga
LITHOLOGY	Granodiorite	Gabbro	Breccia	Tuff	Pillow	Basalt	Breccias	Basalt	Pillow
LOCALITY	Apuela	Río Blanco	Chaupichupa	Urcutambo	Q. Pumamaque	Q. Pumamaque	Quinllachupa	Río Cala	Palacara
SiO_2	65.42	51.31	49.09	50.03	44.72	44.07	52.06	45.07	49.79
TiO_2	0.37	0.74	0.63	0.76	0.31	0.27	0.72	1.66	1.02
Al_2O_3	16.40	17.99	15.47	16.21	15.18	13.24	16.63	11.64	13.97
Fe_2O_3	4.52	10.81	9.44	9.97	9.98	8.38	8.98	13.75	12.21
MnO	0.08	0.16	0.13	0.15	0.13	0.13	0.15	0.25	0.18
MgO	1.89	4.98	8.11	5.60	9.67	7.55	6.24	5.11	7.34
CaO	4.71	7.67	10.85	7.60	9.88	13.11	6.49	11.54	9.97
Na_2O	4.11	3.10	2.31	3.82	2.61	2.38	3.27	3.79	2.92
K_2O	2.19	1.96	1.31	2.35	1.04	2.31	2.34	0.13	0.31
P_2O_5	0.12	0.10	0.23	0.37	0.05	0.05	0.43	0.17	0.09
LOI	0.24	1.24	2.28	3.18	6.50	8.64	2.73	7.01	1.75
Total	**100.05**	**100.06**	**99.85**	**100.04**	**100.07**	**100.13**	**100.04**	**100.12**	**99.55**
Ba	563	325	216	437	62	97	500	35	145
Ce	0	0	9	29	0	0	36	8	0
Co	9	36	39	35	45	35	32	52	50
Cr	7	33	318	81	522	403	89	31	198
Cs	0	0	0	0	1	0	7	0	8
Cu									
Hf	0	0	0	0	0	0	3	0	0
La	9	5	5	17	0	0	20	5	0
Nb	4	2	3	5	2	1	4	8	4
Nd	10	5	7	21	4	3	24	12	4
Ni	7	20	105	32	138	96	28	47	91
Pb	8	5	2	2	4	2	8	1	1
Rb	46	52	47	52	17	35	49	1	3
Sc	16	43	40	27	37	35	29	38	42
Sm	2	1	4	3	2	0	4	7	0
Sr	385	266	442	378	102	107	565	36	129
Th	4	0	1	2	0	2	2	2	0
U	2	0	0	2	2	0	1	2	0
V	75	337	247	272	198	163	247	375	311
Y	16	19	17	19	13	11	18	35	20
Zr	88	70	53	89	22	22	106	104	62
Ga									
S									
Zn									
Ta									

SAMPLE	M5-297	M5-299	M5-300	M5-303	M5-334	M5-348	M5-394	M5-441	M5-445
UTMX	8188	8194	8178	8147	8065	7912	8120	7768	7784
UTMY	635	633	655	738	836	920	1060	981	982
UNIT	Río Cala	Río Cala	Pallatanga	Pallatanga	S. J. L	Intrusive	Naranjal	Intrusive	Colorado
LITHOLOGY	Greenstone	Greenstone	Pillow	Pillow	Andesite	Tonalite	Lava	Tonalite	Dyke
LOCALITY	Cuambo	Cuambo	Río Amarillo	Tercer Paso	Guallupe	Cachaco	Chical	Auchayacu	Guadual
SiO_2	50.53	56.05	43.22	49.87	54.87	49.28	52.22	58.62	65.61
TiO_2	0.56	0.46	0.21	0.61	0.53	0.72	0.90	0.56	0.65
Al_2O_3	13.51	18.32	10.76	14.69	18.16	19.26	15.86	16.98	15.44
Fe_2O_3	8.08	7.71	10.37	11.95	8.01	10.71	12.75	8.67	6.17
MnO	0.12	0.15	0.19	0.17	0.16	0.17	0.35	0.21	0.19
MgO	8.47	4.08	11.64	2.75	3.38	5.10	4.48	2.96	1.72
CaO	8.77	3.96	16.30	6.27	7.49	10.83	8.31	7.10	5.70
Na_2O	1.94	4.93	0.31	3.88	4.03	2.59	3.21	3.58	3.27
K_2O	0.18	2.11	0.10	2.33	1.70	0.38	1.00	0.75	1.08
P_2O_5	0.11	0.16	0.03	0.15	0.24	0.16	0.16	0.14	0.21
LOI	7.84	2.05	6.93	7.22	1.61	0.74	0.60	0.38	0.52
Total	**100.11**	**99.98**	**100.06**	**99.89**	**100.18**	**99.94**	**99.84**	**99.95**	**100.56**
Ba	198	1911	18	152	421	116	218	192	182
Ce	0	0	0	0	0	10	15	0	20
Co	34	27	50	47	23	35	45	27	13
Cr	639	99	1915	753	0	0	0	0	28
Cs	4	2	0	6	0	6	2	0	<2
Cu									13
Hf	0	0	0	0	0	0	0	0	3.7
La	5	10	0	0	0	0	0	5	10.1
Nb	3	2	1	4	2	2	2	2	3.4
Nd	6	3	0	2	10	9	13	9	18.0
Ni	192	33	365	120	13	17	19	4	<2
Pb	5	5	3	4	5	3	4	4	<1.4
Rb	1	35	1	46	25	7	25	10	14
Sc	34	30	39	42	21	38	39	26	20
Sm	0	4	0	4	1	8	4	3	
Sr	454	250	37	72	591	357	256	360	342.5
Th	2	1	4	0	1	3	2	0	2.8
U	1	1	0	2	0	2	1	1	<1.6
V	174	190	205	221	207	336	372	123	
Y	0	14	6	24	19	28	22	22	36.6
Zr	61	47	17	59	67	33	68	48	119
Ga									16
S									26
Zn									101
Ta									<2

SAMPLE	M5-448	M5-448a	M5-448b	M5-456b	M5-456c	M5-456d	M5-461a	M5-542	M5-547
UTMX	7794	7794	7794	7837	7837	7838	7944	7753	7839
UTMY	970	970	970	964	964	964	871	987	984
UNIT	Naranjal	Naranjal	Naranjal	Naranjal	Naranjal	Naranjal	S.J.L.	Intrusive	Intrusive
LITHOLOGY	Breccia	Breccia	Breccia	Lava	Breccia (clast)	Lava	Breccia (clast)	Tonalite	Tonalite
LOCALITY	Río Piguambi	Río Piguambi	Río Piguambi	Río Lita	Río Lita	Río Lita	Río Cachaco	Anchayacu	Río Baboso
SiO_2	54.98	59.25	59.42	53.96	60.67	62.08	48.15	54.25	59.53
TiO_2	0.68	0.48	0.48	0.85	0.75	0.82	0.42	0.65	0.54
Al_2O_3	16.36	17.46	17.04	16.53	13.87	14.82	12.86	17.56	16.94
Fe_2O_3	9.46	7.25	7.09	10.53	9.34	8.05	8.09	10.43	7.69
MnO	0.17	0.15	0.15	0.21	0.20	0.14	0.13	0.24	0.16
MgO	4.59	2.52	2.54	3.05	2.88	1.77	8.97	3.96	2.99
CaO	8.91	6.38	6.11	5.98	5.10	4.42	14.77	8.19	7.26
Na_2O	2.55	3.58	4.00	6.67	4.99	6.18	2.50	2.90	3.13
K_2O	0.76	1.23	1.09	0.20	0.74	0.68	0.30	0.59	0.80
P_2O_5	0.15	0.20	0.20	0.27	0.24	0.38	0.12	0.09	0.11
LOI	1.51	1.02	1.91	1.81	1.16	0.68	3.65	0.83	0.67
Total	**100.12**	**99.52**	**100.03**	**100.06**	**99.94**	**100.02**	**99.96**	**99.69**	**99.82**
Ba	110	201	200	57	122	53	209	214	63
Ce	12.9	0	0	13	0	0	0	0	0
Co	30	21	20	34	24	38	28	22	39
Cr	23	0	5	0	8	553	0	0	548
Cs	<2	5	3	9	5	9	0	6	0
Cu	91								
Hf	<2	0	0	0	0	0	0	0	0
La	4.1	7	4	10	11	4	5	7	6
Nb	1.4	1	2	2	3	2	1	2	4
Nd	11.5	8	5	15	14	7	5	6	3
Ni	14	5	4	5	4	104	5	6	78
Pb	<1.4	4	4	5	4	4	3	3	2
Rb	9.5	16	14	1	11	6	10	13	36
Sc	29	17	15	32	28	45	36	26	38
Sm		0	1	4	0	3	1	0	5
Sr	320.8	446	387	192	318	255	347	318	167
Th	2.0	0	0	2	2	2	4	3	2
U	<1.6	1	0	1	1	1	0	1	1
V		70	62	218	200	292	171	147	163
Y	22.9	19	18	26	31	11	20	22	33
Zr	67.1	44	44	71	69	30	49	51	64
Ga	17								
S	118								
Zn	70								
Ta	<2								

SAMPLE	M5-552	M5-556	M5-658b	M5-680b	M5-682	M5-684	M5-687	M5-689	M5-740a
UTMX	8145	8142	7840	7587	7948	7953	7662	8123	7213
UTMY	738	623	973	954	945	953	1034	1080	260
UNIT	Pallatanga	Intrusive	Naranjal	Naranjal	Naranjal	Naranjal	Naranjal	Naranjal	Naranjal
LITHOLOGY	Pillow	Rhyodacite	Breccias	Basalt	Breccias	Pillow	Breccia	Lava	Pillow
LOCALITY	Tercer Paso	Río Amarillo	Río Mira	Río Negro	Río Verde	Río Verde	Río Cachaví	Peñas Blancas	Salto del Tigre
SiO_2	44.21	75.20	52.13	45.92	56.15	51.73	63.22	53.40	68.43
TiO_2	0.52	0.50	0.72	0.67	0.61	1.00	0.56	0.87	0.67
Al_2O_3	12.07	17.03	17.69	17.86	15.09	15.98	14.88	15.83	12.81
Fe_2O_3	10.17	0.81	10.77	12.09	8.55	12.25	6.13	11.85	5.97
MnO	0.13	0.01	0.20	0.19	0.13	0.18	0.18	0.20	0.15
MgO	4.27	0.43	4.02	7.14	5.05	5.10	2.85	4.83	1.06
CaO	13.95	0.04	8.20	9.80	7.14	4.30	4.33	6.24	2.04
Na_2O	1.90	0.44	4.27	2.85	4.85	5.05	2.41	6.04	5.62
K_2O	1.66	1.57	0.53	0.52	0.38	1.78	2.00	0.28	1.88
P_2O_5	0.21	0.06	0.31	0.13	0.16	0.18	0.17	0.16	0.32
LOI	10.60	3.69	1.26	2.75	1.86	2.46	3.21	0.31	0.81
Total	**99.69**	**99.78**	**100.10**	**99.92**	**99.97**	**100.01**	**99.94**	**100.01**	**99.76**
Ba	787	167	200	57	379	561	69	181	174
Ce	0	13	10	0	0	0	0	17	18
Co	0	39	49	31	46	16	41	19	23
Cr	86	26	14	416	55	0	23	0	7
Cs	4	0	0	7	5	3	7	3	0
Cu									
Hf	0	0	0	0	0	3	0	3	4
La	7	11	4	7	4	9	7	12	15
Nb	4	1	2	3	2	3	2	4	2
Nd	6	16	9	9	13	16	7	17	22
Ni	2	17	30	120	27	5	23	0	7
Pb	21	3	1	0	1	3	4	4	5
Rb	28	9	5	7	26	32	2	8	14
Sc	15	27	34	29	33	24	36	20	21
Sm	5	9	2	0	0	7	7	4	6
Sr	310	373	413	182	145	487	93	353	343
Th	4	1	4	1	3	5	3	2	4
U	1	1	0	0	1	0	1	1	2
V	106	214	286	192	278	83	317	65	66
Y	5	29	15	24	26	34	21	35	40
Zr	85	80	40	56	86	110	75	114	144
Ga									
S									
Zn									
Ta									

SAMPLE	M5-740b	M5-740c	M5-773	M5-786	M5-787	M5-791A	M5-791B	M5-792	M5-792A
UTMX	7213	7213	7413	7277	7267	7055	7055	7162	7162
UTMY	260	260	276	328	227	522	522	343	343
UNIT	Naranjal	Naranjal	Naranjal	Intrusive	Naranjal	Naranjal	Naranjal	Naranjal	Naranjal
LITHOLOGY	Pillow	Pillow	Lava	Diorite	Pillow	Basalt	Basalt	Pillow	Pillow
LOCALITY	Salto del Tigre	Salto del Tigre	Río Verde	Río Naranjal	Río Naranjal	C. Colón	C. Colón	R. Guayllabamba	R. Guayllabamba
SiO_2	60.50	50.59	48.39	52.33	52.84	49.80	49.19	52.93	56.53
TiO_2	0.76	0.68	0.53	0.53	0.86	1.19	1.16	0.71	0.69
Al_2O_3	15.84	15.33	16.62	15.21	16.66	14.99	14.27	14.57	13.77
Fe_2O_3	8.02	11.89	9.54	10.31	11.77	12.14	12.50	12.76	11.62
MnO	0.22	0.21	0.13	0.16	0.19	0.19	0.19	0.16	0.17
MgO	2.25	3.33	8.28	6.22	3.61	8.26	8.19	4.56	4.07
CaO	2.99	8.46	10.39	0.79	7.37	11.95	11.89	6.41	6.26
Na_2O	6.39	4.42	2.24	4.76	3.73	1.98	2.00	3.87	3.99
K_2O	0.83	1.37	0.16	1.30	0.32	0.13	0.14	1.87	1.04
P_2O_5	0.33	0.35	0.07	0.12	0.24	0.10	0.10	0.14	0.13
LOI	1.78	3.29	3.32	2.10	2.02	0.53	0.64	2.17	2.10
Total	**99.91**	**99.92**	**99.67**	**99.83**	**99.58**	**101.26**	**100.27**	**100.15**	**100.37**
Ba	80	105	63	157	201	38	24	223	172
Ce	0	13	12	15	27.4	26	22.8	15.1	17.7
Co	42	31	42	39	38	49	51	45	41
Cr	71	0	274	29	<2	251	216	<2	<2
Cs	0	1			<2	<2.0	<2.0	<2.0	<2.0
Cu			128	66	1267	153	150	29	31
Hf	0	0			2.9	<2.0	<2.0	<2.0	<2.0
La	6	9	4	4	7.9	5.7	4.5	<2.0	4.4
Nb	1	2	<2	<2	1.3	5.1	4.9	<0.8	1.7
Nd	11	14	4	13	16.3	11.0	11.0	9.0	9.0
Ni	16	5	46	26	6	106	118	15	13
Pb	3	1	<2	<2	<1.4	<1.4	<1.4	<1.4	<1.4
Rb	30	13	2	28	3.6	<1.0	1.7	44.4	18.2
Sc	29	24	57	43	30	46	41	35	37
Sm	0	3							
Sr	364	272	259	328	616.6	112.7	110.1	216.2	102.2
Th	3	4	2	3	4.1	<1.4	1.9	<1.4	3.0
U	1	0	<2	3	<1.6	<1.6	<1.6	<1.6	<1.6
V	352	191	303	260					
Y	20	28	11	21	23.5	23.8	24.8	21.1	20.0
Zr	53	68	27	83	87.3	71.5	67.7	58.9	57.4
Ga			15	14	19	18	17	15	15
S					177	319	834	<20	<20
Zn			78	41	97	84	78	73	63
Ta					5.2	2.3	<2.0	<2.0	<2.0

SAMPLE	M5-792B	M5-805	M5-820	M5-835B	M5-870	M5-871	M5-873	M5-936	M5-1014	M5-1043
UTMX	7162	7191	7233	7432	7205	7210	7165	7464	6973	7324
UTMY	343	523	290	744	512	521	557	564	544	662
UNIT	Naranjal	Intrusive	Naranjal	Naranjal	Naranjal	Naranjal	Naranjal	Naranjal	Naranjal	Naranjal
LITHOLOGY	Pillow	Gabbro	Pillow	Basalt	Igneous rock	Lava	Igneous rock	Basalt	Basalt	Lava
LOCALITY	R. Guayllabamba	R. Canandé	Naranjito	R. S. Miguel	R. Canandé	R. Salvador	W. R. Silencio	Río Bravo	R. Desgracia	Río Tigre
SiO_2	52.48	49.80	51.42	51.75	50.72	49.87	57.22	48.22	47.84	51.80
TiO_2	0.71	1.43	0.80	0.82	2.44	1.73	2.16	0.90	1.22	0.95
Al_2O_3	14.59	12.99	15.88	16.99	11.75	12.69	10.98	14.19	14.34	16.36
Fe_2O_3	12.99	14.71	12.74	11.11	18.13	16.54	14.94	10.94	13.30	11.23
MnO	0.16	0.22	0.18	0.16	0.21	0.22	0.20	0.16	0.24	0.17
MgO	4.72	5.90	4.83	6.22	3.56	5.52	1.54	9.29	7.48	4.54
CaO	6.26	9.28	7.04	9.65	7.70	6.75	6.99	11.78	9.64	6.02
Na_2O	3.80	2.85	4.08	2.42	3.63	4.36	4.54	1.83	3.77	5.71
K_2O	2.01	0.23	0.47	0.16	0.29	0.11	0.04	0.17	0.23	0.80
P_2O_5	0.14	0.12	0.22	0.14	0.21	0.14	0.30	0.08	0.10	0.13
LOI	2.14	1.38	1.55	1.10	1.57	1.68	1.17	2.43	1.85	2.17
Total	**100.00**	**98.91**	**99.21**	**100.52**	**100.21**	**99.61**	**100.08**	**99.99**	**100.01**	**99.88**
Ba	224	42	224	82	107	42	25	41	98	258
Ce	20.2	13	27.0	20.6	38	29	46	24	20	9
Co	46	57	44	41	65	61	47	49	54	41
Cr	<2	17	27	15	<2	28	18	417	166	16
Cs	<2.0		<2.0	<2.0						
Cu	23	195	124	150	196	159	18	132	143	115
Hf	<2.0		<2.0	<2.0						
La	<2.0	5	9.2	7.0	9	4	18	<4	6	<4
Nb	1.5	5	1.5	1.4	9	7	12	4	4	<2
Nd	9.6	8	14.8	9.3	20	11	29	10	<4	7
Ni	14	55	14	17	33	57	<2	135	93	23
Pb	<1.4	<2	<1.4	2.3	<2	<2	<2	<2	<2	<2
Rb	47.2	3	3.9	1.8	4	<2	<2	3	3	10
Sc	42	51	41	33	41	48	35	42	40	35
Sm										
Sr	229.7	118	555.6	286.0	143	84	55	124	121	264
Th	2.1	3	2.8	3.8	4	2	2	3	2	2
U	<1.6	<2	<1.6	<1.6	2	2	<2	<2	<2	<2
V		375			564	480	33	271	340	390
Y	21.0	31	22.4	19.9	54	37	80	25	26	26
Zr	60.8	85	84.2	68.0	147	100	194	45	73	79
Ga	16	20	21	18	20	18	21	16	19	18
S	<20		88	94						
Zn	75	81	120	72	101	126	92	73	74	84
Ta	<2.0		2.0	3.1						

SAMPLE	M5-82	M5-124	M5-125	M5-158	M5-205A	M5-211A	M5-299	M5-300	M5-303	M5-394	M5-448	M5-658	M5-680B	M5-740C
La	17.01	2.85	2.36	22.86	8.59	4.02	7.87	1.38	5.38	6.35	6.98	10.33	6.26	6.22
Ce	38.59	5.49	6.46	48.11	22.85	11.21	17.58	2.69	11.1	15.4	15.54	23.98	14.76	14.62
Pr	4.6	0.76	0.94	5.78	3.32	1.72	2.01	0.43	1.49	2.23	2.1	3.35	1.96	2.14
Nd	18.96	3.72	4.53	25.33	16.15	8.73	9.06	2.28	7.11	11.79	10.43	16.51	9.48	11.17
Sm	4.9	1.27	1.4	6.24	5.27	3.01	2.7	0.78	2.41	3.77	2.95	4.92	3.1	3.49
Eu	1.55	0.53	0.5	1.74	2.11	1.26	0.92	0.32	1	1.18	0.97	1.45	1.23	1.11
Gd	4.71	1.94	2.02	4.86	7.41	4.65	3.18	1.5	4.23	4.08	3.18	5.09	3.93	3.52
Dy	4.68	2.8	2.48	4.25	9.09	5.48	3.62	2.1	5.43	4.63	3.3	5.07	4.15	3.47
Er	2.43	1.91	1.79	2.23	5.73	3.55	1.96	1.45	3.37	2.68	1.89	2.87	2.46	2.03
Yb	2.19	2.14	1.72	1.8	5.29	3.2	1.52	1.37	3.35	2.46	1.74	2.33	2.18	1.82
Lu	0.31	0.36	0.3	0.28	0.79	0.5	0.26	0.25	0.51	0.33	0.25	0.37	0.3	0.27

SAMPLE	M5-773	M5-786	M5-787	M5-791A	M5-792	M5-805	M5-820	M5-835	M5-870	M5-871	M5-873	M5-936	M5-1014	M5-1043
La	2.06	7.53	8.18	3.28	4.33	4.97	7.47	5.48	8.34	6.16	16.97	4.49	3.93	4.94
Ce	5.91	19.28	19.84	8.92	10.78	14.69	18.24	15.70	26.52	15.86	40.86	11.14	12.97	14.98
Pr	0.97	2.86	2.84	1.36	1.51	2.21	2.35	2.30	3.81	2.39	5.65	1.62	2.16	2.57
Nd	5.13	13.06	14.51	7.80	7.50	11.61	10.96	10.95	18.72	11.42	24.36	8.28	11.53	12.87
Sm	1.7	3.73	4.44	2.71	2.20	3.73	3.40	3.28	5.76	3.58	7.89	2.54	3.75	3.59
Eu	0.61	1.00	1.3	1.04	0.89	1.23	1.22	1.25	1.82	1.25	2.34	0.82	1.03	1.08
Gd	2.39	3.30	4.6	3.56	3.00	3.99	4.01	4.33	6.65	4.75	8.83	2.81	3.42	3.46
Dy	2.49	3.05	4.94	4.25	3.20	4.52	3.95	4.91	7.42	5.27	9.75	3.14	3.91	3.08
Er	1.73	1.86	2.75	2.57	199.00	3.00	2.31	3.08	5.10	3.33	5.65	2.24	2.37	2.07
Yb	1.61	1.66	2.54	2.53	1.89	3.24	2.25	2.70	5.29	3.74	6.12	2.03	2.42	2.23
Lu	0.24	0.25	0.38	0.39	0.29	0.51	0.35	0.42	0.78	0.56	0.90	0.30	0.37	0.35

APPENDIX 4 OF REPORT:

GEOLOGY OF THE WESTERN CORDILLERA
OF ECUADOR
BETWEEN 0°00’ AND 1°00’ N

RADIOMETRIC AGES

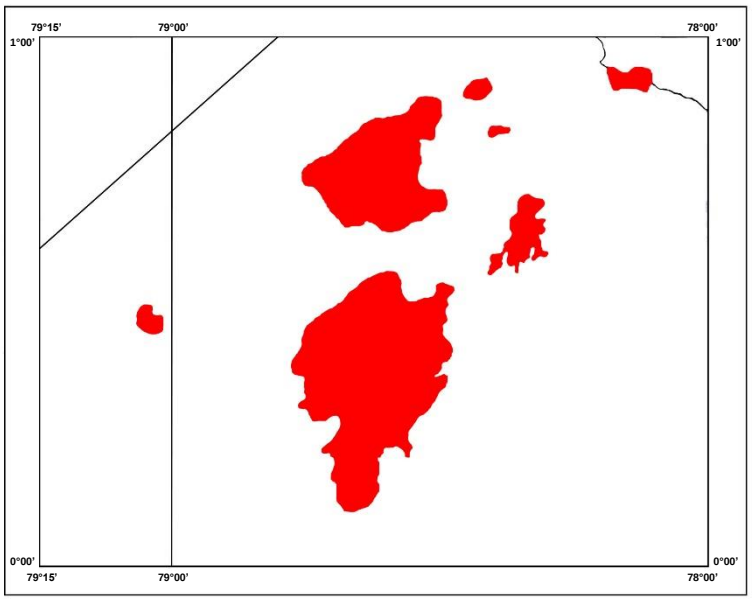

GEOLOGICAL INFORMATION MAPPING PROGRAMME
(LOCATION OF MAP 5 AREA)

M. BOLAND
L. PILATASIG
E. IBADANGO
W. MCCOURT
J. ASPDEN
R. HUGHES
B. BEATE

QUITO, 2000

K/Ar GEOCHRONOLOGY

Sample #	Topographic sheet	Unit/Intrusive	UTMX	UTMY	Mineral	Age (Ma)	%K
JA-7	Apuela	Apuela	7748	429	Hornblende Biotite	16.5 ± 1.1 16.0 ± 0.8	0.91-0.89 6.80-6.85
JX-24	S. M. Bancos	Nameless	7331	015	Hornblende	28.7 ± 3.2	0.2
M5-348	Guadalupe	Cachaco	7912	915	Hornblende	34.7 ± 1.7	0.18
M5-351	Guadalupe	Hornblendic dyke	7948	905	Hornblende	36.3 ± 2.0	0.2
M5-441	Anchayacu	Río Santiago	7768	981	Hornblende	44.6 ± 2.2	0.45
M5-520	L. M. Buenos Aires	La Merced	7977	707	Hornblende	15.6 ± 1.1	0.55
M5-542	Anchayacu	Río Santiago	7753	987	Hornblende	38.2 ± 1.9	
M5-542	Anchayacu	Río Santiago	7753	987	Hornblende	38.2 ± 1.9	0.38
M5-547	Lita	Río Baboso	7839	984	Hornblende Biotite	42.4 ± 2.1 42.2 ± 2.1	0.13 5.67
M5-547	Lita	Río Baboso	7839	984	Hornblende	42.4 ± 2.1	0.78
M5-550	Guadalupe	Hornblendic dyke	8023	875	Hornblende	19.8 ± 3.1	0.007
M5-550	Guadalupe	Hornblendic dyke	8023	875	Hornblende	19.8 ± 3.1	0.1
M5-786C	Río Guayllabamba	Nameless	7277	328	Hornblende	47.2 ± 2.4	0.14
M5-1526	Río Santiago	Río Santiago	7743	752	Biotite	41.9 ± 2.1	5.45
M5-1535	Río Santiago	Río Santiago	7621	771	Hornblende	35.8 ± 1.8	0.27

FISSION TRACK GEOCHRONOLOGY

Sample #	Topographic sheet	Unit/Intrusive	UTMX	UTMY	Age (Ma)
M5-RH	Río Guayllabamba	S. Juan de Lachas	7319	241	23.5 ± 1.5
M5-076	Río Guayllabamba	S. Juan de Lachas	7338	253	24.5 ± 3.1
M5-108	Otavalo	Subvolcanic	7800	326	0.9 ± 0.1
M5-398	Maldonado	Maldonado	8147	1037	7.5 ± 0.4
CHI-329	L. M. Buenos Aires	Subvolcanic	8050	623	5.0 ± 2.9

APPENDIX 5 OF REPORT:

GEOLOGY OF THE WESTERN CORDILLERA
OF ECUADOR
BETWEEN 0°00' AND 1°00' N

PETROGRAPHY

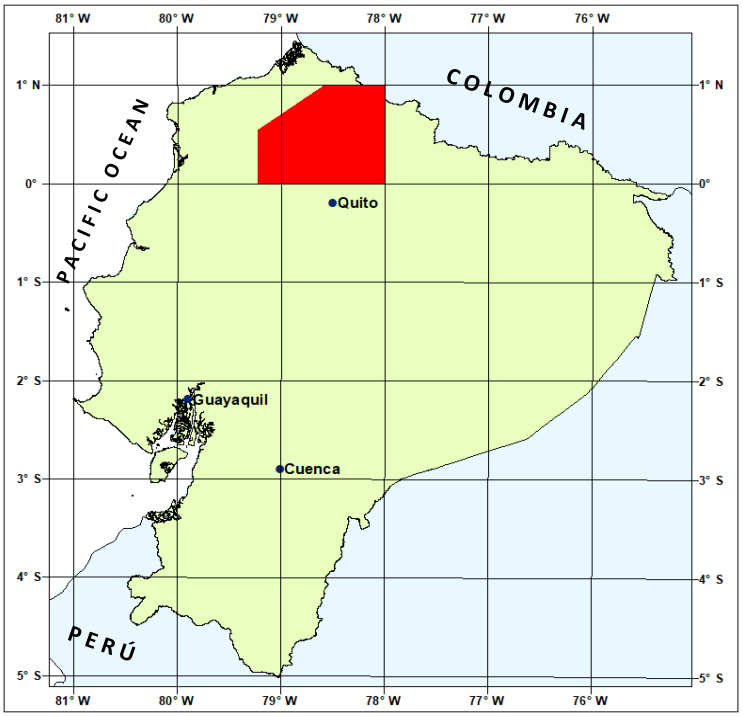

GEOLOGICAL INFORMATION MAPPING PROGRAMME
(LOCATION OF MAP 5 AREA)

M. BOLAND
L. PILATASIG
E. IBADANGO
W. MCCOURT
J. ASPDEN
R. HUGHES
B. BEATE

QUITO, 2000

Sample#	Topographic sheet	Coordinates		Unit	Mineralogy	Description
		UTMX	UTMY			
M5-1	Otavalo	7897	00353	Río Cala	Altered mafic minerals to chlorite. Altered feldspars to sericite.	Strongly altered lava
M5-24	S. M. B.	7423	00179	Mulaute	Sericite and opaque matrix, fine rounded quartz grains.	Deformed quartzite
M5-25	S. M. B.	7421	00177	Mulaute	Fine quartz and opaque minerals matrix. Quartz and calcite veins.	Silicified siltstone
M5-34	Calacalí	7524	00173	Pilatón	Quartz grains, elongated fine feldspars. Chlorite and epidote patches.	Fine sedimentary rock with quartz veins and opaque minerals
M5-42	Calacalí	7530	00026	Pilatón	Euhedral feldspar fragments and opaque minerals. Chlorite and epidote feldspar matrix.	Sedimentary rock
M5-50	S. M. B.	7504	00170	Pilatón	Feldspar, pyroxene (augite) clasts. Fine feldspar, chlorite, and epidote matrix.	Deformed volcanic breccia with quartz veins
M5-58	Vacas Galindo	7687	00192	Pilatón	Subangular fine feldspars, pyroxene, and quartz, chlorite and calcite fragments.	Silicified and tectonized igneous rock, cleavage development
M5-65	Vacas Galindo	7539	00252	Mulaute	Zoned plagioclase, elongated grains. Quartz, epidote, and opaque matrix.	Deformed sedimentary rock (slate)
M5-75	Guayllabamba	7319	00241	S. J. Lachas	Altered sedimentary rock fragments. Fine quartz, opaque matrix.	Medium-grained sandstone with slight alteration
M5-79	Guayllabamba	7406	00270		Basaltic hornblende, euhedral pyroxenes. Zoned plagioclase and glass.	Andesite (dyke)
M5-82	Otavalo	7877	00277	Río Cala	Feldspar and pyroxene phenocrysts. Chloritic vesicular matrix.	Autobreccia
M5-83	Otavalo	7858	00287	Natividad	Feldspar, chlorite, and epidote matrix. Chlorite, sericite, and lime vesicles.	Fine-grained igneous rock
M5-84	Otavalo	7868	00292	Río Cala	Pyroxene phenocrysts. Fine feldspar and pyroxene matrix.	Igneous rock
M5-85	Otavalo	7865	00295	Río Cala	Chlorite and Fe and Ti oxides matrix. Quartz and chlorite vesicles.	Igneous rock
M5-86	Otavalo	7866	00302	Río Cala	Subrounded clasts, quartz and chlorite vesicles. Fine feldspar and chlorite matrix.	Deformed volcanic breccia
M5-97	Vacas Galindo	7758	00315	Pilatón	Quartz crystals and grains.	Recrystallized fine-grained sandstone
M5-104	Vacas Galindo	7778	00238		Pyroxene (augite) phenocrysts, opaque. Fine chlorite and epidote matrix.	Intrusive rock
M5-106	Vacas Galindo	7782	00336		Sericite, feldspar, chlorite, and epidote matrix. Amphibole phenocrysts.	Fine-grained igneous rock
M5-111A	Otavalo	7805	00323	Silante	Fine sandstone and igneous rock clasts; feldspar and pyroxene matrix.	Sedimentary rock
M5-124A	Otavalo	7844	00287	Pallatanga	Calcite and epidote clasts.	Rock with spherulitic texture
M5-125	Otavalo	7839	00288	Pallatanga	Calcite in fractures, also chlorite and epidote.	Highly altered igneous rock
M5-133	Otavalo	7853	00298	Pallatanga	Fine quartz, sericite, and opaque matrix, large calcite and quartz vesicles.	Sedimentary rock
M5-137	Otavalo	7844	00268	Natividad	Feldspar and pyroxene phenocrysts. Fine feldspar, epidote, and chlorite matrix.	Vesicular igneous rock
M5-139	Otavalo	7840	00266	Natividad	Feldspar and pyroxene phenocrysts. Fine feldspar matrix.	Igneous rock
M5-144	Vacas Galindo	7729	00263	Pilatón	Fine quartz and chlorite matrix. Deformed clasts.	Deformed sedimentary rock
M5-157	Vacas Galindo	7754	00321	Pilatón	Quartz-rich layers and opaque-rich layers. Quartz veins.	Fine-grained sedimentary rock
M5-158	Otavalo	7879	00279	Río Cala	Augite pyroxene phenocrysts in a chloritized fine matrix.	Altered igneous rock
M5-159	Otavalo	7864	00265	Río Cala	Altered and broken pyroxene phenocrysts, quartz vesicles. Chlorite, epidote, and opaque matrix.	Altered vesicular igneous rock

Sample#	Topographic sheet	Coordinates		Unit	Mineralogy	Description
		UTMX	UTMY			
M5-165	Mojanda	7820	00146	Natividad	Feldspar and lava clasts. Amorphous matrix.	Breccia
M5-166	Mojanda	7816	00149	Natividad	Altered feldspars and epidote. Recrystallized matrix of quartz, chlorite, and epidote.	Deformed breccia with volcanic clasts
M5-174	Calacalí	7769	00069	Natividad	Rounded clasts of altered feldspars. Fine matrix of quartz and epidote.	Sedimentary rock
M5-177	Calacalí	7774	00032	Natividad	Large calcite crystals. Matrix of chlorite and acicular calcite.	Sedimentary rock with a degree of metamorphism
M5-181	Mojanda	7792	00122	Yunguilla	Fine quartz grains, calcite veins, and clasts.	Fine-grained sandstone
M5-185	Calacalí	7765	00149	Yunguilla	Feldspar and pyroxene crystals. Fine matrix with chlorite replacement.	Tuff or volcanogenic sediment
M5-189	Mojanda	7801	00131	Natividad	Feldspar phenocrysts, quartz vesicles. Fine feldspar matrix.	Vesicular igneous rock
M5-190	Mojanda	7823	00176	Natividad	Small quartz grains, clayey matrix.	Sedimentary rock with cleavage
M5-197	Calacalí	7714	00039	Pallatanga	Euhedral feldspar clasts. Matrix of calcite, quartz, and feldspar.	Breccia with clasts of porphyritic volcanic rocks
M5-205	Otavalo	7858	00190	Pallatanga	Deformed feldspars. Matrix of chlorite and epidote.	Altered igneous rock
M5-205A	Otavalo	7858	00190	Pallatanga	Feldspar phenocrysts, pyroxene fragments. Fine matrix of feldspar, quartz, opaques, and chlorite.	Altered and tectonized igneous rock
M5-209	Mira	8078	00579	Silante	Euhedral feldspars and opaques. Fine matrix of quartz and feldspars.	Altered igneous rock
M5-211A	Mira	8197	00616	Pallatanga	Minerals with high relief and low birefringence.	Spherulitic texture. Cleavage in some places
M5-212A	Mira	8188	00645	Rumi Cruz	Quartz grains within a fine-grained matrix.	Sedimentary rock with angular pyroxene clasts
M5-213A	Mira	8184	00655	Yunguilla	Fine matrix, uniformly sized grains, quartz and calcite veins.	Sedimentary rock, shales with slight cleavage development
M5-217	Mira	8185	00668	Yunguilla	Crystalline quartz matrix. Actinolite grains and some calcite.	Rock with igneous texture
M5-229A	Mira	8141	00737	Pilatón	Fine rounded grains of different compositions, chlorite and calcite.	Altered fine-grained sandstone
M5-229B	Mira	8141	00737	Pilatón	Fine rounded grains of different compositions, chlorite and calcite.	Altered fine-grained sandstone
M5-231	La Carolina	8117	00776	Pilatón	Subrounded feldspars, grains resembling epidote.	Recrystallized sedimentary rock
M5-231A	La Carolina	8117	00776	Pilatón	Feldspar-phyric and olivines. Matrix of chlorite and epidote with feldspars.	Breccia with subangular clasts
M5-231B	La Carolina	8117	00776	Pilatón	2 feldspar-phyric and pyroxene clasts. Fine green matrix.	Breccia with angular to subrounded clasts of black rocks
M5-233	La Carolina	8112	00787	Pilatón	Fine matrix of chlorite, sericite, and quartz, feldspar grains, quartz, and other lithics.	Reworked sedimentary rock
M5-236	La Carolina	8107	00801	Pilatón	Quartz and chlorite matrix with deformed quartz grains and feldspars.	Green sandstone, medium to coarse-grained
M5-247	Otavalo	7838	00265	Pilatón	Fine matrix of feldspar, sericite, and chlorite. Phenocrysts of pyroxene and euhedral feldspars.	Vesicular igneous rock with recrystallized minerals
M5-250	Otavalo	7829	00201	Río Cala	Pyroxene fragments, calcite vesicles. Matrix of fine feldspars.	Altered lava with quartz and calcite veins
M5-254	Otavalo	7821	00191	Río Cala	Fine pyroxene fragments, altered igneous rock clasts.	Tectonized breccia
M5-254A	Otavalo	7821	00191	Río Cala	Altered lava clasts, pyroxene fragments. Matrix of chlorite and quartz veins.	Tectonized tuff
M5-258	Mojanda	7832	00151		Pyroxene phenocrysts, altered feldspars, opaques, chlorite patches.	Intrusive rock (gabbro)

Sample#	Topographic sheet	Coordinates		Unit	Mineralogy	Description
		UTMX	UTMY			
M5-260	Mojanda	7812	00154	Natividad	Pyroxene and feldspar fragments. Feldspar matrix.	Volcanosedimentary rock
M5-263	Mojanda	7793	00137	Rumi Cruz	Quartz fragments. Sedimentary rocks, opaques in a fine clayey matrix.	Altered medium-grained sandstone
M5-267	Calacalí	7770	00118	Rumi Cruz	Rounded and subrounded quartz grains, calcite in fractures.	Very coarse-grained sandstone
M5-267A	Calacalí	7770	00118	Rumi Cruz	Quartz and plagioclase fragments, clasts of siliceous sedimentary rocks.	Medium-grained sandstones. Fine matrix of quartz, opaques, chlorite, and epidote
M5-280	Vacas Galindo	7518	00206	Mulaute	Amphibole clasts being replaced by biotite.	Dyke. Fine matrix of quartz and small grains of biotite
M5-287	S. M. B.	7410	00176	Mulaute	Vesicular and porphyritic material clasts; feldspar crystals.	Lava or autobreccia; the chloritic matrix appears to be vesicular
M5-288	S. M. B.	7423	00180	Mulaute	Rounded quartz grains in fine quartz and feldspar matrix with epidote and chlorite.	Fine sandstone
M5-291	S. M. B.	7495	00184	Pilatón	Rounded and fractured grains; fractures contain calcite.	Quartz-rich sandstone
M5-298	Mira	8196	00626	Río Cala	Euhedral augites and feldspars. Some chlorite in the interstices.	Fine to medium-grained green igneous rock
M5-300	Mira	8178	00655	Pallatanga	Fibrous minerals with a high amount of calcite.	Altered igneous rock
M5-301A	Mira	8118	00655	Pallatanga	Euhedral feldspar and pyroxene clasts. Sericitized feldspar and pyroxene matrix.	Breccia with rounded clasts
M5-303	La Carolina	8147	00783	Pallatanga	Fine matrix of elongated feldspars, epidote grains, quartz and calcite veins.	Deformed and altered lavas
M5-311	La Carolina	8171	00802	Pilatón	Numerous opaques in the section. Chlorite and epidote in the fractures.	Silicified igneous rock
M5-317	La Carolina	8150	00783	Pilatón	Subangular feldspars and volcanic clasts in a fine matrix.	Volcanic sandstone
M5-326	La Carolina	8097	00796	Pilatón	Clasts of volcanic material and feldspars. Fine matrix of quartz, chlorite, and epidote.	Volcanic sandstone
M5-332A	Mira	8073	00729	S. J. de Lachas	Zoned plagioclase phenocrysts, amphibole (hornblende). Fine matrix of feldspars and glass.	Igneous rock, possible hornblendic dyke
M5-334	La Carolina	8065	00836	S. J. de Lachas	Amphibole and euhedral feldspars. Matrix of quartz and feldspars with epidote and calcite.	Igneous rock
M5-336	La Carolina	8075	00854	S. J. de Lachas	Feldspar phenocrysts and fragments of pyroxene. Fine matrix of feldspar and opaques.	Igneous breccia
M5-338	La Carolina	8088	00856	El Laurel	Fine calcareous matrix with large foraminifera.	Limestone with macroscopic gastropod and bivalve corals
M5-348	Guadalupe	7912	00915		Feldspar phenocrysts, quartz, zoned plagioclase, amphibole, and pyroxene.	Intrusive rock (granodiorite)
M5-350	Guadalupe	7939	00909	Tortugo	Euhedral feldspars, aggregates of feldspars and amphibole in a feldspar matrix.	Volcanic rock
M5-351	Guadalupe	7948	00905		Euhedral feldspar phenocrysts and amphibole. Fine matrix of feldspars and amphibole.	Lava
M5-358	Guadalupe	8036	00807	Pilatón	Clasts of igneous rocks with euhedral pyroxenes (augite).	Clastic rock with subrounded feldspar fragments
M5-364	La Carolina	8064	00831	S. J. de Lachas	Euhedral feldspars and vesicles with calcite and chlorite.	Volcanic rock
M5-368	Guadalupe	7987	00908	S. J. de Lachas	Feldspar-phyric and amphibole clasts. Matrix with patches of chlorite.	Breccia with angular clasts
M5-393	Maldonado	8116	01061	Naranjal	Feldspar phenocrysts, actinolite, opaques, some fibrous grains, quartz, and biotite.	Basalt
M5-394	Maldonado	8120	01060	Naranjal	Pyroxene and feldspar phenocrysts, aggregates of amphibole in the fractures.	Altered volcanic rock, recrystallized chlorite and quartz, biotite and epidote
M5-395	Maldonado	8120	01052	S. J. de Lachas	Polysynthetic feldspars and amphibole, green biotite and amphibole intergrowths.	Igneous rock

Sample#	Topographic sheet	Coordinates		Unit	Mineralogy	Description
		UTMX	UTMY			
M5-404	Maldonado	8215	01032	S. J. de Lachas	Fragments of quartz and fine sedimentary rocks	Medium-grained sandstone
M5-426	Maldonado	8269	00964	El Laurel	Euhedral grains of pyroxene, feldspar, and amphibole, lava clasts	Sandstone
M5-439A	Anchayacu	7761	00994	Colorado	Small grains of amphibole, vesicular material clasts	Sedimentary rock, feldspar grains in a matrix of epidote and chlorite
M5-439C	Anchayacu	7761	00994	Colorado	Angular feldspars, vesicular clasts, actinolite grains	Autobreccia with feldspars in a vesicular and chloritic matrix
M5-441	Anchayacu	7768	00981		Phenocrysts of feldspar, pyroxene, quartz, hornblende, biotite	Intrusive rock (tonalite)
M5-443A	Anchayacu	7751	00997	Colorado	Rounded clasts of fine feldspars, opaque and chlorite. Plagioclase phenocrysts	Crystallized tuff
M5-445	Lita	7784	00982	Naranjal	Angular feldspars, patches of amphibole. Fine matrix of amphibole and chlorite	Volcanic rock, possible dyke
M5-446	Lita	7788	00982	Naranjal	Euhedral feldspars and angular grains of amphibole	Breccia
M5-448	Lita	7794	00970	Naranjal	Pyroxene and feldspar clasts. Vesicular matrix with chlorite	Breccia; matrix with chloritic alteration, felsic grains, and pyroxene
M5-449	Lita	7801	00975	Naranjal	3 mm feldspars and 1 mm pyroxene. Matrix of feldspars and opaques	Igneous rock; chloritic alteration
M5-456A	Lita	7837	00964	Naranjal	Clasts with vesicles filled with chlorite, phenocrysts of feldspars and clinopyroxenes	Sedimentary rock. Reworked clasts of angular feldspars
M5-456B	Lita	7387	00964	Naranjal	Phenocrysts of feldspar and pyroxene, quartz grains. Fine matrix of feldspars and chlorite	Altered porphyritic-textured lava
M5-456D	Lita	7387	00964	Naranjal	Phenocrysts of feldspar and pyroxene. Fine matrix of fine feldspars, chlorite, and epidote	Altered porphyritic-textured lava
M5-520	L. M. B. A.	7978	00707		Phenocrysts of feldspar, quartz, plagioclase, amphibole, and opaques	Intrusive rock (granodiorite)
M5-542	Anchayacu	7753	00987		Phenocrysts of plagioclase, amphibole, quartz, opaques, replaced by chlorite	Intrusive rock (altered granodiorite)
M5-547	Lita	7839	00984		Phenocrysts of feldspar, quartz, opaques, and altered pyroxene	Intrusive rock (tonalite)
M5-549	Guadalupe	8010	00878	S. J. de Lachas	Rounded feldspars and amphiboles. Amphiboles replaced by chlorite	Sedimentary rock with volcanic clasts and reworked sediments
M5-550	Guadalupe	8023	00875	S. J. de Lachas	Phenocrysts of feldspar and pyroxene. Fine matrix of feldspars, glass, opaques, quartz grains	Igneous rock with porphyritic texture
M5-577	Guadalupe	7907	00774	Tortugo	Fragments of sedimentary rocks, plagioclase and quartz, spots of chlorite	Slightly altered medium-grained sandstone
M5-581	Guadalupe	7888	00791	S. J. de Lachas	Broken amphibole and pyroxene in a fine matrix of feldspars, glass, and opaques	Aphanitic-textured lava
M5-585	Guadalupe	7830	00841	Tortugo	Phenocrysts of feldspars and pyroxenes. Cryptocrystalline matrix	Autobreccia; vesicular chloritic matrix and clinopyroxene fragments
M5-592B	Guadalupe	7830	00841	Naranjal	Phenocrysts of feldspar and pyroxene, vesicles filled with quartz, chlorite, and epidote	Fine-grained matrix of opaques, feldspars, and chlorite
M5-593	Guadalupe	7441	00838	Naranjal	Aligned 5 mm feldspars, chlorite and epidote in the interstices	Igneous rock with quartz vesicles in a fine-grained green matrix
M5-605	Guadalupe	7851	00900	Naranjal	Euhedral feldspars, some vesicles, quite a bit of epidote	Igneous rock
M5-610	Lita	7840	00984	Naranjal	Euhedral feldspars in a fine matrix of actinolite and pyroxene grains	Altered volcanic rock
M5-615	Lita	7840	00984	Naranjal	Phenocrysts of feldspars, fragments of pyroxene. Fine matrix of feldspars, chlorite, epidote, opaques	Altered porphyritic igneous rock
M5-619	Lita	7871	00982	Naranjal	Dominant chlorite and epidote, remnants of amphibole	Highly altered rock
M5-621	Lita	7857	00970	Naranjal	Subrounded clasts. Feldspars in a matrix of chlorite and angular feldspars	Breccia with subangular clasts and medium-grained green matrix

Sample#	Topographic sheet	Coordinates		Unit	Mineralogy	Description
		UTMX	UTMY			
M5-623A	Guadalupe	7839	00916	Naranjal	Subrounded clasts of vesicular lavas with phenocrysts of feldspar	Breccia with feldspar and pyroxene fragments, chlorite replacement
M5-630	Lita	7875	00941	Naranjal	Pyroxene cores and amphibole rims, patches of chlorite and epidote	Recrystallized green igneous rock
M5-634	La Merced	7911	00673	Pilatón	Clasts of igneous and sedimentary rocks; matrix of feldspar and quartz	Volcanic sandstone
M5-643	Guadalupe	7846	00743	Tortugo	Clasts of vesicular rocks. Matrix with subrounded grains	Highly altered rock to calcite, sericite, and chlorite
M5-644	Guadalupe	7842	00748	Tortugo	Fragments of igneous rocks, feldspars and pyroxene. Fine matrix of feldspars, quartz and chlorite	Altered igneous breccia
M5-646	Guadalupe	7840	00973	S. J. de Lachas	Subrounded clasts of vesicular material. Mafic and some augites.	Medium-grained green sandstone. Fine feldspathic matrix
M5-651	Guadalupe	7817	00798	S. J. de Lachas	Large fragments of feldspars, quartz, subangular pyroxenes. Fine matrix of feldspars	Igneous breccia
M5-658	Lita	7840	00975	Naranjal	Clasts of felsic feldspar-phyric and chloritized and epidotized lavas	Subangular to rounded feldspar clasts in a fine green matrix
M5-662	La Carolina	8065	00823		Large plagioclases, pyroxenes, opaques, chlorite in the interstices	Intrusive rock (diorite)
M5-663	Guadalupe	7928	00844	S. J. de Lachas	Subangular feldspars, hornblende, pyroxene, amphibole (actinolite), opaques. Altered matrix	Lava
M5-666	Guadalupe	7883	00860	Naranjal	Pyroxene and feldspar crystals in a fine-grained opaque matrix	Breccias. Numerous amygdules filled with chlorite, calcite, and quartz
M5-667	Guadalupe	7880	00861	Naranjal	Euhedral feldspars, chlorite vesicles. Pyroxene grains. Fine matrix	Altered lava
M5-668	Guadalupe	7902	00899	Tortugo	Feldspars, actinolite, clasts of fine-grained rocks	Clastic rock with fabric defined by actinolite fragments
M5-676	La Carolina	8191	00811		Large altered plagioclases, biotite, altered mafics with chlorite and epidote	Intrusive rock (gabbro)
M5-680	Anchayacu	7587	00954	Naranjal	Augite phenocrysts, feldspars and spherical vesicles with chlorite	Vesicular igneous rock. Fine matrix of feldspars, epidote, and chlorite
M5-680A	Anchayacu	7587	00954	Naranjal	Phenocrysts of feldspar and pyroxene, quartz and chlorite vesicles. Fine matrix of feldspars and opaques	Vesicular igneous rock with chlorite and epidote
M5-680B	Anchayacu	7587	00954	Naranjal	Fine crystals of feldspar and opaques, large amounts of chlorite and epidote	Altered aphanitic-textured lava
M5-683	Lita	7953	00948	Tortugo	Fragments of feldspars, pyroxene and opaques. Fine matrix of feldspars, quartz, chlorite and epidote	Altered medium-grained sandstone
M5-687	Anchayacu	7662	01034	Naranjal	Chloritized fine-grained matrix. Euhedral feldspars and augites	Breccia with feldspar-phyric tuff clasts
M5-689	Maldonado	8123	01080	Naranjal	Phenocrysts of feldspar, broken and altered pyroxenes. Fine matrix of elongated feldspars, chlorite	Altered igneous rock
M5-690	S. M. B.	7302	00182	S. J. de Lachas	Fragments of pyroxene and feldspar in altered fine matrix	Volcanic sandstone
M5-690A	S. M. B.	7302	00182	S. J. de Lachas	Feldspar phenocrysts, fragments of pyroxenes, opaques, spots of chlorite	Igneous rock
M5-693	Guayllabamba	7403	00270		Altered and deformed minerals, chlorite in cleavage planes, garnet?	Metamorphic rock (schist)
M5-696	La Carolina	8266	00872		Matrix of fine feldspars, fragments of igneous rocks, spots of chlorite	Lava (possible dyke). Quartz monzonite
M5-704	La Carolina	8327	00884	Río Cala	Deformed clasts and minerals. Epidote and chlorite matrix	Possible tuff or tectonized breccia
M5-706	La Carolina	8329	00904	Natividad	Fragments of feldspar, pyroxene and quartz. Fine matrix of quartz, opaques, chlorite and epidote	Fine-grained sandstone
M5-710	Guadalupe	7895	00741	Mulaute	Angular feldspars in a fine matrix of quartz and feldspar	Clastic rock, contains chlorite and some epidote
M5-712	Guadalupe	7893	00750	Tortugo	Fragments of quartz, pyroxene and opaques in a fine matrix of the same composition	Medium-grained sandstone

Sample#	Topographic sheet	Coordinates		Unit	Mineralogy	Description
		UTMX	UTMY			
M5-713	Guadalupe	7892	00750	S. J. de Lachas	Subhedral feldspar fragments, altered pyroxenes. Fine matrix of feldspars	Tuff
M5-714	Guadalupe	7891	00753	S. J. de Lachas	Feldspar phenocrysts, fragments of rocks of different composition and opaques	Slightly altered tuff
M5-722A	Imantag	7996	00450	Río Cala	Calcite in vesicles and fractures. Matrix of chlorite and epidote	Vesicular igneous rock, with a degree of metamorphism
M5-729	La Merced	7815	00652	Mulaute	Pyroxene and volcanic rock clasts. Phenocrysts of pyroxene and feldspar	Clastic rock, difficult to identify the fine-grained matrix
M5-732	La Merced	7832	00673	El Laurel	Fragments of feldspar, quartz, and opaques in a very fine matrix	Clayey sandstone
M5-734	La Merced	7822	00682	Tortugo	Crystals of feldspar and pyroxene in a matrix of quartz and feldspar	Altered green igneous rock
M5-735	La Merced	7823	00682	Tortugo	Sericitized euhedral feldspars, pyroxene, some olivine grains	Medium-grained clastic rock, pyroxenes replaced by chlorite
M5-740A	Golondrinas	7213	00260	Naranjal	Feldspar phenocrysts, quartz and calcite vesicles. Fine matrix of feldspars, quartz, chlorite	Altered lava with quartz and calcite vesicles
M5-740B	Golondrinas	7213	00260	Naranjal	Feldspar phenocrysts, fragments of pyroxene. Fine matrix of feldspars, chlorite, epidote, and quartz	Altered lava
M5-740C	Golondrinas	7213	00260	Naranjal	Feldspar phenocrysts, fragments of pyroxene. Fine matrix of feldspars, chlorite, epidote, and quartz	Altered lava with quartz and calcite vesicles
M5-741	Guayllabamba	7366	00260	Naranjal	Subhedral feldspars and augites, vesicles filled with quartz and calcite	Medium-grained lava, 3 mm grains, euhedral pyroxenes and vesicles
M5-743	Guayllabamba	7305	00243	Naranjal	Euhedral feldspars, some mafics, vesicles filled with chlorite	Fine-grained gray-green rock
M5-744	Guayllabamba	7305	00263	Naranjal	Subhedral augites and euhedral feldspars. Fine-grained matrix	Lava with quartz-filled vesicles
M5-745	Guayllabamba	7275	00236	Tortugo	Felsic feldspars-phyric clasts. Matrix of feldspars and amphibole fragments	Breccias. Fine-grained matrix, 2 cm clasts of rhyolitic rocks
M5-763B	Guayllabamba	7499	00332	Tortugo	Clasts of fine-grained lava. Saussuritized euhedral feldspars	Green sandstone, medium-grained matrix, chloritized mafics
M5-765	Guayllabamba	7496	00318	Tortugo	Angular feldspars in a fine matrix of feldspars, epidote, and chlorite	Fine-grained sedimentary rock with 2 mm euhedral feldspars
M5-773	Guayllabamba	7413	00276	Naranjal	Clasts of igneous rocks with pyroxene	Breccia with subrounded volcanic clasts
M5-776	Guayllabamba	7456	00287	Tortugo	Saussuritized feldspar grains, subrounded quartz and augite, some amphibole	Hydrothermally altered breccia
M5-783	Guayllabamba	7350	00241	S. J. de Lachas	Angular fragments of feldspar, amphibole, and pyroxene in a fine matrix of feldspars	Conglomerate
M5-784	Guayllabamba	7343	00236	S. J. de Lachas	Subrounded grains of quartz and sediments. No mafics present	Coarse-grained sedimentary rock, 2 mm grains
M5-786	Guayllabamba	7277	00328		Phenocrysts of feldspars, broken and altered pyroxenes, chlorite and epidote in the interstices	Intrusive rock (diorite)
M5-786A	Guayllabamba	7277	00328		Phenocrysts of feldspars, fragments of pyroxene, chlorite and epidote in the interstices	Intrusive rock (diorite)
M5-787	Guayllabamba	7267	00327	Naranjal	Fine matrix of elongated feldspars, opaques, chlorite, and epidote, fragments of pyroxene	Altered aphanitic-textured lava
M5-788	Guayllabamba	7252	00315	Naranjal	Fine matrix of elongated feldspars, opaques, chlorite, epidote, fragments of pyroxene	Altered aphanitic-textured lava
M5-791A	Zapallo	7055	00522	Naranjal	Fine crystals of elongated feldspar, fragments of pyroxene, chlorite spots	Tectonized and altered basalt
M5-791B	Zapallo	7055	00522	Naranjal	Fine crystals of elongated feldspar, fragments of pyroxene, chlorite spots	Tectonized and altered basalt
M5-791C	Zapallo	7055	00522	Naranjal	Chlorite matrix, quartz vesicles, few feldspar crystals	Completely altered basalt
M5-792	Golondrinas	7162	00343	Naranjal	Elongated feldspars, fragments of clinopyroxene, chlorite, epidote, and opaques	Altered aphanitic-textured lava, possible presence of spinel

Sample#	Topographic sheet	Coordinates		Unit	Mineralogy	Description
		UTMX	UTMY			
M5-792A	Golondrinas	7162	00343	Naranjal	Elongated feldspars, fragments of pyroxene, spots of chlorite, epidote, and opaques	Altered aphanitic-textured lava
M5-793	Golondrinas	7191	00337	Colorado	Fine grains of quartz, subangular feldspars, and fragments of amphibole	Fine-grained sandstone
M5-799	Zapallo	7156	00545		Deformed plagioclases, altered pyroxenes, opaques, chlorite, and epidote	Intrusive rock (gabbro)
M5-801	Zapallo	7207	00514	Naranjal	Feldspar phenocrysts, fragments of pyroxene, opaques. Fine matrix of feldspars, chlorite, epidote	Altered porphyritic igneous rock
M5-801A	Zapallo	7207	00514	Naranjal	Altered and deformed feldspar phenocrysts, pyroxene, opaques, chlorite, and epidote	Altered porphyritic igneous rock
M5-805	Zapallo	7191	00523		Large altered and deformed plagioclases, altered pyroxene and amphibole	Deformed intrusive rock (gabbro) with a large amount of chlorite and epidote
M5-808	Zapallo	7174	00546		Altered feldspar and pyroxene phenocrysts, opaques, and chlorite spots	Altered intrusive rock (gabbro), broken pyroxenes
M5-809	Zapallo	7168	00551	Naranjal	Acicular feldspar fragments, epidote, and chlorite. Feldspar phenocrysts	Recrystallized lava with aligned crystals
M5-810	Gualpi	7180	00560	R. Desgracia	Fragments of igneous rocks, pyroxene, and quartz. Fine matrix of chlorite and quartz	Altered medium-grained sandstone
M5-811	Gualpi	7184	00561	Naranjal	Fragments of feldspars, epidote, and chlorite	Recrystallized lava with small opaque grains
M5-817A	Zapallo	7188	00375	Naranjal	Feldspar phenocrysts, fragments of pyroxene, quartz grains, and igneous rocks	Altered igneous breccia
M5-820	Guayllabamba	7233	00290	Naranjal	Feldspar phenocrysts, fragments of pyroxene. Fine matrix of feldspars, glass, and chlorite	Altered aphanitic-textured lava
M5-821	Guayllabamba	7272	00255	Tortugo	Subangular feldspar phenocrysts, clasts of igneous and sedimentary rocks	Feldspathic volcanic sandstone, quartz grains, opaques, chlorite, and epidote
M5-823	Imantag	8033	00486	Río Cala	Phenocrysts and fragments of pyroxene. Fine matrix of feldspars, opaques, chlorite, and epidote	Altered and tectonized aphanitic-textured lava
M5-824	Imantag	8033	00486	Río Cala	Altered feldspar phenocrysts and pyroxenes in a fine matrix of feldspars, chlorite, epidote, and opaques	Altered porphyritic-textured lava
M5-824A	Imantag	8033	00486	Río Cala	Phenocrysts and fragments of pyroxene. Fine matrix of feldspars, pyroxene, and opaques	Altered igneous rock
M5-833	Cayapas	7421	00758	Naranjal	Feldspar phenocrysts, fragments of pyroxene. Fine matrix of elongated feldspars, opaques	Altered porphyritic lava
M5-833A	Cayapas	7421	00758	Naranjal	Feldspar phenocrysts, fragments of pyroxene. Fine matrix of elongated feldspars, opaques	Porphyritic lava with a higher degree of alteration than M5-833
M5-834	Cayapas	7413	00757	Naranjal	Feldspar phenocrysts and quartz vesicles. Fine matrix of feldspar, pyroxene, glass, and chlorite	Altered igneous rock
M5-835A	Cayapas	7432	00744	Naranjal	Fragments of feldspars, quartz vesicles, and chlorite. Fine matrix of feldspars and chlorite	Vesicular lava
M5-835B	Cayapas	7432	00744	Naranjal	Fragments of pyroxene (augite), crystals of feldspar, chlorite, and opaques	Altered igneous rock
M5-839A	R. Bravo	7432	00744	Naranjal	Fine elongated feldspars, fragments of pyroxene, opaques, and chlorite spots	Aphanitic-textured lava
M5-842	Cayapas	7363	00761	Zapallo	Fragments of feldspars, clasts of igneous rocks. Matrix of fine feldspars	Tuff
M5-862	R. Naranjal	7239	00506	Naranjal	Crystals of feldspar and equidimensional broken pyroxenes, chlorite spots	Porphyritic igneous rock (dyke)
M5-869	R. Naranjal	7276	00481	Colorado	Subrounded vesicular clasts, one pyroxene. Feldspathic matrix, calcite, and quartz	Medium-grained sandstone, 5 mm grains
M5-870	Zapallo	7205	00512	Naranjal	Intergrowth of feldspars, altered pyroxenes, replacement of chlorite	Altered intrusive rock
M5-873	Gualpi	7165	00557	Naranjal	Subrounded quartz in a fine tectonized matrix, broken plagioclases and mafics	Tectonized igneous rock
M5-873A	Gualpi	7165	00557	Naranjal	Pyroxenes replaced by brown biotite, chlorite	Igneous rock with brittle deformation, grain size reduction

Sample#	Topographic sheet	Coordinates		Unit	Mineralogy	Description
		UTMX	UTMY			
M5-879	R. Naranjal	7340	00533	Naranjal	Pyroxene 1-5 mm, opaques, and euhedral feldspars 1 mm, patches of chlorite	Altered igneous rock
M5-881	R. Naranjal	7340	00545	Naranjal	Pyroxene 1-5 mm, some opaques in a matrix of quartz, feldspars, and chlorite	Fine-grained igneous rock
M5-882	R. Bravo	7252	00585	Naranjal	Euhedral pyroxenes 1-5 mm, euhedral plagioclase and opaques, chlorite in fractures	Igneous rock
M5-883	R. Bravo	7278	00626	Naranjal	Pyroxenes 1-5 mm, opaques, euhedral feldspars, patches of chlorite	Altered igneous rock
M5-883A	R. Bravo	7279	00627	Naranjal	Fragments of feldspars, opaques, and pyroxenes. Fine matrix of feldspars and chlorite	Altered igneous rock
M5-885A	R. Bravo	7276	00629	Naranjal	Euhedral feldspars, fragments of fine-grained material	Altered igneous rock
M5-886A	R. Bravo	7264	00630	Naranjal	Euhedral feldspars, opaques, abundant chlorite in patches and vesicles	Altered igneous rock
M5-888	R. Bravo	7251	00621	Naranjal	Feldspars, broken pyroxenes, and opaques	Tectonized and altered igneous rocks
M5-895	R. Santiago	7684	00893	Colorado	Fragments of feldspars and grains of amphibole	Possible lava with patches of fine-grained material
M5-896	R. Santiago	7683	00887	Colorado	Fragments of feldspars and large grains of amphibole	Possible lava
M5-900	R. Santiago	7624	00933		Intergrowth of feldspars, augites, amphibole (actinolite), and chlorite	Intrusive rock
M5-907	R. Las Piedras	7652	00614	Naranjal	Fine-grained, altered, and oriented minerals	Altered and deformed lava
M5-908	R. Las Piedras	7575	00609	Naranjal	Euhedral and subhedral feldspars. Fine matrix of feldspars, 1 amphibole	Igneous rock, feldspar grains in a fine green matrix
M5-908A	R. Las Piedras	7575	00609	Naranjal	Micas and chlorite developed on cleavage planes	Fine-grained rock with developed cleavage
M5-914	R. Las Piedras	7557	00675	Naranjal	Euhedral feldspars and augites. Fine matrix of feldspars, chlorite, opaques, and epidote	Altered porphyritic-textured lava
M5-924	R. Naranjal	7484	00482	Tortugo	Large grains of amphibole replaced by epidote and chlorite	Possible sedimentary rock
M5-929	R. Naranjal	7460	00523	Naranjal	Altered and deformed feldspars, presence of chlorite	Deformed lava
M5-931	R. Naranjal	7459	00528	Naranjal	Fragments of aligned pyroxene and feldspar	Deformed sedimentary rocks
M5-937A	R. Bravo	7455	00576	Naranjal	Intergrowth of feldspars. Interstices filled with chlorite	Igneous rock. High relief and birefringence of minerals
M5-939	R. Bravo	7456	00602	Naranjal	Fragments of feldspar, epidote, and fine-grained material	Fine-grained igneous rock; texture between M5-929 and M5-937A
M5-1009	Gualpi	6981	00562	R. Desgracia	Intergrowth of euhedral pyroxenes and elongated feldspars, opaques, and chlorite	Fine-grained green crystalline rock
M5-1009B	Gualpi	6981	00562	R. Desgracia	Intergrowth of pyroxenes and finer-grained plagioclases	Fine-grained green crystalline rock, patches of chlorite
M5-1012	Zapallo	6971	00542	Naranjal	Intergrowth of pleochroic augites and plagioclases, fractures with chlorite	Rock with igneous texture
M5-1012A	Zapallo	6971	00542	Naranjal	Pyroxenes and feldspars in an igneous rock clast	Breccia with angular clasts of chloritized rocks
M5-1013	Zapallo	6973	00544	R. Desgracia	Subrounded igneous rocks clasts and fine-grained and sediments	Microconglomerate, matrix rich in pyroxene, feldspar, opaques, and chlorite grains
M5-1014	Zapallo	6973	00544	R. Desgracia	Clasts of pyroxene and feldspar, veinlets of fine-grained material	Hyaloclastites
M5-1014A	Zapallo	6973	00544	R. Desgracia	Clasts of pyroxene and deformed feldspar crystals. Fine matrix of feldspars, quartz	Altered igneous rock with chlorite and epidote
M5-1015	Zapallo	6973	00543	Naranjal	Intergrowth of pyroxene and elongated feldspars	Igneous rock with amygdules filled with chlorite and calcite

Sample#	Topographic sheet	Coordinates		Unit	Mineralogy	Description
		UTMX	UTMY			
M5-1019	Zapallo	7199	00396	Naranjal	Small crystals of feldspar, pyroxene, spots of chlorite, opaques, and epidote	Altered aphanitic-textured lava
M5-1020	Zapallo	7158	00413	Naranjal	Fine matrix of chlorite and feldspars, large amount of quartz veinlets	Chloritized and silicified igneous rock
M5-1020A	Zapallo	7158	00413	Naranjal	Fine matrix of feldspars, chlorite, large amount of quartz veinlets	Chloritized and silicified igneous rock
M5-1021	Zapallo	7149	00420	Naranjal	Small crystals of altered feldspars, many quartz veinlets	Altered aphanitic-textured lava
M5-1022	Zapallo	7151	00428	Naranjal	Feldspars and fragments of pyroxene. Fine matrix of feldspars, chlorite, and opaques	Altered igneous rock
M5-1025	Zapallo	7120	00520	Naranjal	Intergrowth of feldspar and pyroxene, interstices filled with chlorite	Finer-grained gray-green rock than M5-1025A
M5-1025A	Zapallo	7120	00520	Naranjal	Intergrowth of feldspar and pyroxene, interstices filled with chlorite	Fine-grained gray-green rock, recrystallized glass
M5-1026	Zapallo	7122	00518	Naranjal	Elongated plagioclases and pyroxenes	Fine-grained igneous rock with small opaque grains
M5-1032	Otavalo	7870	00246	Río Cala	Fine matrix of elongated and oriented feldspars, spots of chlorite	Tectonized lava, quartz veins
M5-1033	R. Bravo	7314	00678	Zapallo	Phenocrysts of plagioclase and pyroxene, vesicular clasts filled with chlorite	Coarse-grained rock, vesicular matrix, feldspars, and quartz clasts
M5-1037	R. Bravo	7318	00640	Naranjal	Intergrowth of feldspars, opaques, and mafic minerals, chlorite replacement	Intrusive rock with equigranular texture
M5-1038	R. Bravo	7913	00633	Naranjal	Intergrowth of feldspars and pyroxenes, skeletal opaques, chlorite	Crystalline rock with aphanitic texture
M5-1040	R. Bravo	7921	00643	Naranjal	Feldspars, euhedral pyroxenes, small opaques (ilmenite), chlorite	Finer-grained than M5-1037, saussuritized feldspars
M5-1042	R. Bravo	7320	00656	Naranjal	Matrix of feldspar, equigranular pyroxenes, and chlorite	Rock with reworked vesicular rock clasts
M5-1043	R. Bravo	7324	00662	Naranjal	Phenocrysts of feldspar and pyroxene in a fine matrix of feldspar and chlorite	Fine-grained crystalline rock, calcite replacement
M5-1044	R. Bravo	7320	00678	Zapallo	Subrounded volcanic clasts with vesicles, plagioclases, and phenocrysts of pyroxene	Dark green rock with subrounded clasts, interstitial chlorite
M5-1044A	R. Bravo	7320	00678	Zapallo	50% quartz vesicles, phenocrysts and aggregates of feldspars, some pyroxenes	Highly vesicular rock, matrix of dark material
M5-1046	R. Bravo	7309	00708	Naranjal	Elongated feldspars, opaques, and rounded quartz grains	Very fine-grained igneous rock
M5-1048	R. Naranjal	7332	00404	Naranjal	Euhedral crystals of pyroxene and quartz, replacement of chlorite and epidote	Igneous rock, pyroxenes replaced by epidote, spherulitic texture
M5-1052	R. Naranjal	7360	00435	Naranjal	Chlorite and possible serpentine in the matrix	Altered and deformed igneous rock
M5-1052B	R. Naranjal	7360	00435	Naranjal	Altered elongated and oriented feldspars, opaques, and chlorite	Altered aphanitic-textured lava
M5-1053	R. Naranjal	7370	00443	Naranjal	Rock rich in fine grains of chlorite	Dyke
M5-1055	R. Naranjal	7354	00434	Naranjal	Phenocrysts of olivine replaced by chlorite. Fine matrix of feldspars and chlorite	Igneous rock with some degree of metamorphism
M5-1055A	R. Naranjal	7354	00434	Naranjal	Elongated grains of amphibole (actinolite)	Deformed igneous rock
M5-1055B	R. Naranjal	7354	00434	Naranjal	Elongated grains of amphibole (actinolite), replaced by chlorite	Altered rock, abundant sericite and calcite
M5-1058	Guayllabamba	7293	00323	Tortugo	Subangular to subrounded grains of feldspar, some patches of chlorite	Medium-grained sediment, rich in feldspars and some angular mafics
M5-1061	Guayllabamba	7386	00365	Tortugo	Clasts of medium-grained volcanic rocks, oriented feldspars	Sandstone, feldspars replaced by sericite, patches of epidote and chlorite
M5-1061A	Guayllabamba	7386	00365	Tortugo	Subangular grains of vesicular lavas, a lot of sericite, epidote, and chlorite	Altered sandstone, sericite, chlorite, and epidote

Sample#	Topographic sheet	Coordinates		Unit	Mineralogy	Description
		UTMX	UTMY			
M5-1062	Guayllabamba	7345	00322	Tortugo	Fragments of augite, feldspars, and volcanic rocks in a matrix of feldspars	Medium-grained sandstone with a large amount of chlorite and epidote
M5-1064	Anchayacu	7545	00923	Naranjal	Clasts larger than 3 cm of igneous rocks	Breccia with subangular clasts
M5-1066	R. Santiago	7546	00900	Naranjal	Euhedral phenocrysts of pyroxenes in a matrix of feldspars, opaques, and quartz	Igneous rock with chlorite and calcite vesicles
M5-1067	R. Santiago	7536	00875	Naranjal	Euhedral feldspars, chlorite, and epidote in a matrix of feldspars and opaques	Fine to medium-grained weathered igneous rock
M5-1069	R. Santiago	7527	00866	Naranjal	Feldspars, interstitial chlorite, and vesicles filled with epidote and calcite	Altered fine-grained igneous rock
M5-1071	R. Santiago	7548	00857		Altered plagioclases, quartz, altered and broken mafic minerals	Tectonized intrusive rock (granodiorite)
M5-1503	R. Las Piedras	7736	00589	Tortugo	Euhedral phenocrysts of replaced by calcite feldspars, chlorite in the matrix	Lava, fine-grained matrix with rounded vesicles
M5-1504	R. Las Piedras	7725	00611	Tortugo	Subrounded clasts of feldspars. Very fine matrix of feldspars, quartz, and chlorite	Siliceous breccia with subangular clasts
M5-1508	R. Las Piedras	7717	00614	Naranjal	Feldspars, amphibole, and opaques, alignment of the minerals	Igneous rock with a degree of metamorphism
M5-1510	R. Las Piedras	7708	00605	Naranjal	Subrounded quartz; deformation bands in the quartz matrix, opaques, and chlorite	Deformed rock
M5-1511	R. Las Piedras	7698	00608	Naranjal	Amphibole (actinolite), feldspars, chlorite replacement	Medium-grained crystalline igneous rock
M5-1516	R. Las Piedras	7655	00666	Naranjal	Chlorite and epidote in vesicles, fresh pyroxenes in a matrix of chlorite and feldspars	Lava
M5-1516A	R. Las Piedras	7655	00666	Naranjal	Euhedral pyroxenes, chlorite in vesicles. Matrix of fine-grained feldspars	Igneous breccia
M5-1518	R. Las Piedras	7649	00671	Naranjal	Fine-grained feldspars and small grains of pyroxene, some chlorite and epidote	Fine-grained igneous rock
M5-1526	R. Santiago	7604	00792		Hornblende, plagioclase, biotite, quartz	Intrusive rock (granite)
M5-1530	R. Santiago	7677	00749	Naranjal	Quartz grains and clasts of sedimentary rocks, chlorite and epidote	Medium-grained sandstone
M5-1530B	R. Santiago	7677	00749	Naranjal	Amphibole, euhedral feldspars. Matrix of amphibole and biotite	Igneous rock
M5-1531	R. Santiago	7676	00744	Naranjal	Amphibole, free recrystallized feldspars and quartz. Pleochroic amphibole	Medium-grained igneous rock
M5-1532	R. Santiago	7673	00744	Naranjal	Amphibole (actinolite, hornblende, and biotite grains), opaques, and some epidote	Fault zone defined by rock fabric
M5-1535	R. Santiago	7622	00770		Hornblende, plagioclase, quartz, chlorite replacement	Intrusive rock (granite)
M5-1536	R. Santiago	7624	00777	Colorado	Matrix of fibrous chlorite, grains of amphibole, green biotite, and opaques	Igneous rock
14339	R. Naranjal	7320	00387	Tortugo	Clasts of vesicular lavas	Sedimentary breccia
16673	R. Piedras	7753	00673	Naranjal	Clasts of igneous and sedimentary rocks, sandy matrix and spots of chlorite	Breccia
M5- R. Tigre	R. Cayapas	7283	00759		Large plagioclase, quartz, and altered mafics	Intrusive rock (granodiorite)
JA-7	Apuela	7748	00429		Zoned plagioclase, quartz, hornblende, and opaques	Intrusive rock (granodiorite)
JO-16					Fine fragments of pyroxene and altered minerals. Fine matrix of quartz and chlorite	Altered medium-grained sandstone
JX-24	S. M. B.	7332	00015		Altered plagioclases, pyroxene, quartz, chlorite, and opaques	Deformed intrusive rock with cleavage (deformed gabbro)
JX-25	S. M. B.	7332	00015		Altered plagioclases, pyroxene, quartz, chlorite, opaques, quartz veinlets	Deformed intrusive rock with cleavage (deformed gabbro)
M5-837	Cayapas	7446	00739	Naranjal	Elongated feldspars crystals, subhedral pyroxenes and in fragments, chlorite in vesicles	Altered porphyritic lava. Chloritized matrix and opaque minerals
M5-839B	Río Bravo	7461	00734	Naranjal	Clasts of altered lavas and vesicular rocks. Phenocrysts of plagioclase	Altered breccia. Chloritized matrix, quartz and chlorite vesicles
M5-839C	Río Bravo	7461	00734	Naranjal	Large and elongated feldspar crystals, fragments of pyroxene, grains of epidote and opaques	Slightly altered igneous rock